THE DETERMINATION OF THE DEPTHS AND EXTINCTION COEFFICIENTS OF SHALLOW WATER BY AIR PHOTOGRAPHY USING COLOUR FILTERS

By J. GRANGE MOORE, M.A., *Army Photographic Research Unit*

(*Communicated by Sir Thomas Merton, Treas.R.S.—Received* 5 *March* 1946—*Read* 14 *November* 1946)

[Plates 1–15]

CONTENTS

Introduction

The value of air photography for map making and for the study of land detail was appreciated before the war, but the study of under-water detail from air photographs had received little attention. The landing at Tarawa, where the danger of a submerged reef had not been accurately assessed, emphasized the need for a new method of determining depths in shallow water.

Research on the interpretation of air photographs of the sea-bed was therefore started by the Army Photographic Research Unit in September 1944, under the auspices of Professor J. D. Bernal, F.R.S., Scientific Advisor to Combined Operations H.Q., and some 10,000 photographs were taken during extensive trials in Cornwall, the Scilly Isles, Scotland, the Mediterranean and Ceylon. This work was carried out under the orders of the Air Directorate of the War Office, and as the results are of scientific and industrial value the Army Council has agreed to their publication.

The procedure developed has been referred to in the services as the 'Transparency Method', and may briefly be described as follows:

If a sandy beach is photographed vertically from the air through a colour filter, its apparent brightness is found to vary in a simple way with the depth and clarity of the water over it; if the clarity (or the extinction coefficient) of the water is known, the depth of water can be determined by measuring the relative brightness at different points on a single air photograph. If it is not known, the measurements may be made on a pair of photographs taken simultaneously through two special colour filters; since a relationship between the two extinction coefficients can be assumed, depths can be determined from the photographs alone without any other source of information. This is done graphically by means of a special calculator, and from the results the clarity of the water can also be assessed. In average coastal waters depths down to 20 ft. or more may be determined to an accuracy of $\pm 10\,\%$.

It is believed that no previous study of this type has been published, but it is known that similar investigations are in progress in the United States and elsewhere, and there is little doubt that the method described in the present paper can be considerably improved as experience is gained; the uses to which it may eventually be put for such varied purposes as the construction of charts, the study of sandbars, the silting of navigable channels, the control of erosion and pollution, the charting of currents and the study of marine life, remain for others to investigate.

PART I

A THEORETICAL STUDY OF THE METHOD

Part I of this paper is confined to a theoretical study of the procedure outlined in the Introduction, including the choice of suitable filters and the construction of the necessary calculator. This theoretical study is based on the conception of a 'brightness profile', defined below.

Definition of the brightness profile

A brightness profile is defined as the curve produced by plotting, as ordinates, the relative brightnesses of points on the sea-bed against their horizontal distances from the waterline; these brightnesses are measured in a nearly vertical direction from the air.

Analysis of the brightness profile

The brightness of any point on this profile, as observed vertically from the air, is due to:

(*a*) Light from all sources scattered by atmospheric haze in the column of air between the sea surface and the observer.

(*b*) Light reflected vertically upwards by the sea surface.

(*c*) Light scattered vertically upwards by particles within the sea.

(*d*) Light reflected from the sea-bed to emerge vertically from the sea surface.

Considering these components separately:

(*a*) The intensity of the light scattered by atmospheric haze will depend upon a large number of uncontrollable variables, including the sun altitude, the amount of cloud, the height of the observer and the type and density distribution of the haze (Atkins & Poole 1936; Clarke 1938; Hardy 1936; Le Grand 1939; McDermott 1943; Middleton 1941; Subow & Czihirin 1940; Sverdrup, Johnson & Fleming 1942). If $I_{0\lambda}$ is the intensity of light of wave-length λ on a horizontal surface at the level of the observer, and h_λ is the effective diffuse reflectivity of the column of atmospheric haze below the observer, the intensity of the light reflected by the haze will be $I_{0\lambda}h_{0\lambda}$. Both I_0 and h will vary with wave-length, but for any given wave-length at any given instant of time may be taken as constant for adjacent points along the profile.

(*b*) The reflexion from the sea surface has been discussed by various workers (Atkins & Poole 1933; Poole & Atkins 1926; Powell & Clarke 1936; Sverdrup *et al.* 1942) and depends primarily on the sun altitude, the amount of cloud and the size of the waves. If w_λ is the effective diffuse reflectivity of the surface at a given point on the profile, and K'_λ is the fraction of light transmitted by the column of air between the sea surface and the observer (both for light of wave-length λ), the intensity of light reflected at the sea surface will be $I_{0\lambda}K'_\lambda w_\lambda$.

(*c*) Both molecular scattering and scattering by particles of suspended matter will contribute to the intensity of the light scattered upwards from within the sea. Molecular scattering is so small (Le Grand 1939) that it may be neglected, and scattering by suspended matter in coastal waters will generally be in the forward direction, its extent depending on the amount and size of the suspended particles and on the wave-length of the light considered (Atkins & Poole 1933, 1940; Johnson & Liljequist 1938; Jorgenson & Utterback 1939; Kimball & Hand 1930; Le Grand 1939; Utterback 1936; Utterback & Jorgenson 1936). If K''_λ is the fraction of light transmitted by the water surface on the downward journey, $V_\lambda\,dx$ is the effective diffuse reflectivity due to upward scattering from an elementary layer of water of thickness dx, and $(\alpha+\beta)_\lambda$ represents the vertical extinction coefficient of the water (Le Grand 1939), then the intensity of the light reflected by a layer of water of thickness dx at depth x will be $I_{0\lambda}K'_\lambda K''_\lambda V_\lambda 10^{-(\alpha+\beta)_\lambda x}\,dx$.*

(*d*) After passing through the sea water, the light reaching the sea-bed will be partly diffuse and partly parallel (Johnson & Liljequist 1938), the proportions varying over a wide range; the sea-bed will act as a diffuse reflector, the fraction reflected varying from 0·50 to about 0·05, depending on the colour and texture of the bottom and the wave-length of the light considered. Photographic measurements on samples of dry sand from Cornish beaches gave reflectivity factors varying between 0·45 and 0·33 for green light ($\lambda = 5300$ A), and 0·54 to 0·37 for red light ($\lambda = 6200$ A). When the samples were moistened, these reflectivities were reduced by about one-third.

After reflexion from the sea-bed, the light will again be reduced in intensity by absorption and scattering, and on reaching the surface, rays which are at an angle to the vertical greater than about 48° will be internally reflected. The remaining rays will be further reduced in intensity by atmospheric haze before reaching the observer.

If R_λ is the diffuse reflectivity of the sea-bed at a point of depth t below the surface, the light reflected at the sea-bed will be $I_{0\lambda}K'_\lambda K''_\lambda R_\lambda 10^{-(\alpha+\beta)_\lambda t}$.

If the observer is represented by a camera whose optic axis is vertically over a given point on the profile, the intensity of light falling on the film from these four sources can be calculated, as a first approximation, as follows:

Let r be the diffuse reflectivity of any horizontal surface illuminated at intensity I, and let the fraction of I transmitted by any medium placed between this horizontal surface and the lens be K.

Then, if unevenness of illumination due to the lens is neglected, the intensity of the light falling on the film will be given by $B = IJrK$, where J is a constant for the effective f value of a particular lens.

* Throughout this work the extinction coefficient $(\alpha+\beta)$ for a given wave-length of light is defined by the equation

$$I = I_0\,10^{-(\alpha+\beta)t},$$

where t is measured in feet. The use of an extinction coefficient not based on metres and Naperian logarithms may be criticized as introducing unnecessary confusion in the literature. Practical experience, however, showed that this change greatly speeded up subsequent routine work by surveyors and observers. Extinction coefficients based on metres and Naperian logarithms, denoted by a suffix m, may be converted to these units by the relation

$$(\alpha+\beta) = 0{\cdot}132(\alpha+\beta)_m.$$

For convenience, values in both units are given in table 1.

Thus the total intensity B_t of light of any one wave-length reaching the film from any point on the profile of depth t will be the sum of the four components:

(*a*) From haze: $JK'hI_0$.

(*b*) From surface reflexion: $J(K')^2 wI_0$.

(*c*) From scattering by all elementary layers dx within the water:

$$J\frac{(K')^2K''K'''}{\mu^2}VI_0\int_0^t 10^{-2(\alpha+\beta)x}dx = J\frac{(K')^2K''K'''VI_0c}{2\mu^2(\alpha+\beta)}(1-10^{-2(\alpha+\beta)t}),$$

where K''' is the fraction of the light transmitted by the water surface on the upward journey, μ is the refractive index of the sea water, and $c = \log_{10} e$ (e being the base of Naperian logarithms).

(*d*) From the sea-bed: $J\frac{(K')^2K''K'''}{\mu^2}R\,10^{-2(\alpha+\beta)t}I_0$.

Hence
$$B_t = JI_0K'\left[h+K'\left(w+\frac{K''K'''cV}{2(\alpha+\beta)\mu^2}\right)+\frac{K'K''K'''}{\mu^2}\left(R-\frac{cV}{2(\alpha+\beta)}\right)10^{-2(\alpha+\beta)t}\right] \quad (1)$$

for any given wave-length λ. This equation is of the form

$$B_t = I_0(a+b\,10^{-2(\alpha+\beta)t}). \quad (2)$$

Denoting the limiting cases where the point B_t is at the waterline ($t = 0$) or is at infinite depth ($t = \infty$) by B_0 and B_∞ respectively, then it is clear that for light of wave-length λ,

$$\frac{B_0-B_\infty}{B_t-B_\infty} = \frac{I_0 b}{I_0 b\,10^{-2(\alpha+\beta)t}} = 10^{2(\alpha+\beta)t}$$

or
$$\log_{10}\frac{B_0-B_\infty}{B_t-B_\infty} = 2(\alpha+\beta)\,t; \quad (3)$$

similarly,
$$\log_{10}\frac{B_{t_1}-B_\infty}{B_{t_2}-B_\infty} = 2(\alpha+\beta)\,(t_2-t_1), \quad (4)$$

where B_{t_1} and B_{t_2} are points on the profile of depth t_1 and t_2 respectively.

The above equations hold approximately for monochromatic light. If the quantities K', K'', K''', R, V, I_0, $(\alpha+\beta)$, μ, h and w are assumed to be constant over the transmission band of the filter-film combination in use, the equations can be considered to hold for the total light received by the film. This is not strictly true (see later). Although equations (3) and (4) are derived without taking into account the effects of second and higher order scattering, they express very closely the form of the brightness profiles obtained in practice; this will be apparent from consideration of figure 11.

Comments on the above analysis

Certain fundamental assumptions are implicit in the above equations:

(1) It will be understood that for a point B_t, the effective reflectivities R_λ of the sea-bed and w_λ of the sea surface, need not be known, but they must not vary between adjacent points on the profile. This condition can easily be satisfied if care is taken when selecting points for measurements from the photographs (plates 3–4).

(2) It should be noted that the values of $(\alpha+\beta)$ given by equations (3) or (4) will be mean values within the vertical plane through the profile, and for these equations to hold, the

values of $(\alpha+\beta)$ must remain constant throughout the profile. The brightness profile does not permit determinations of extinction coefficients on a vertical line as in the photo-cell method developed by Atkins & Poole (1933, 1936) and others.

Variations in the extinction coefficient, even over the depth ranges of interest (say 0–30 ft.), are certainly possible, whether caused by storms, currents, pollution, diatom outbursts, or the mixing of different water types as at the mouth of estuaries (Clarke 1938; Le Grand 1939; Orr 1933; Poole & Atkins 1926; Sverdrup *et al.* 1942; Utterback & Williams 1935), and such changes may be detected from analysis of brightness profiles. Values remarkably constant with depth have, however, been recorded by many workers (Atkins & Poole 1933; Clarke 1936, 1938; Erikson 1933) under conditions which are in fact most suitable for vertical air photography of the sea-bed; therefore for this analysis the change in extinction coefficient with depth over the range of depths concerned should be small.

The change of extinction coefficient as the distance from the shore increases may be marked. High extinction coefficients may occur in the very shallow water close to the water edge, due to the increased quantity of suspended matter, and possible air bubbles, in the waves breaking on the shore. It has been found that this effect is negligible if the water is calm and a few feet deep; the use of modified forms of equations (3) or (4) will, however, enable depths and extinction coefficients to be determined from this point onwards. The necessary modification is discussed later.

(3) It might be expected that the altitude of the sun, and the presence of clouds in the sky, would determine the mean length of the path travelled by the light in the water and would therefore affect the observed value of the extinction coefficient. Whitney (1941) calculates theoretical mean path lengths, and finds, for instance, that when the sun altitude lies between 30° and 50° the mean path length may be between 110 and 122% of the vertical depth. Careful experimental work (Atkins & Poole 1933; Sverdrup *et al.* 1942) has, however, failed to find, within this range, any corresponding dependence of the extinction coefficient upon sun altitude; corrections for sun altitude or amount of cloud have not therefore been made in the present work, but these quantities have been recorded (part III).

(4) The more oblique diffused rays necessarily travel a longer path in the water than direct rays, and their preferential absorption might therefore be expected to cause a decrease in the observed extinction coefficient with depth. Le Grand (1939) therefore proposes a modification of the simple exponential law defining $(\alpha+\beta)$, but concludes that the modification will be unimportant except in the very clearest ocean water. It is not therefore considered necessary to complicate the calculations in the present paper by abandoning the simple exponential law. For similar reasons the Young-Gordon (1939) modification has not been preferred.

(5) Changes in temperature or salinity of the sea water undoubtedly have no significant effect on the vertical extinction coefficient (Clarke 1938; Clarke & James 1939; Sverdrup *et al.* 1942).

The elimination of B_∞

If the extinction coefficient $(\alpha+\beta)$ changes along the profile, the value of B_∞ in equations (3) and (4) will be affected. It may not, therefore, be possible to determine, by graphical extrapolation of the brightness profile, the value of B_∞ applicable to a given set of points on

the profile. In practice this is found to be a real difficulty, and the following methods have been used to overcome it.

Method 1. Writing equation (4) for points of depth t_1, t_2 and t_3, such that $t_2-t_1 = t_3-t_2$, it can be shown from equation (2) that

$$\log (B_{t_1}-B_\infty) = 2\log (B_{t_2}-B_\infty) - \log (B_{t_3}-B_\infty).$$

This equation may be solved graphically by expressing the values of B_{t_2}, B_{t_3} and B_∞ as percentages of B_{t_1} and calculating possible values of B_{t_3} for sets of values of B_{t_2} and B_∞. Curves of constant B_∞ are then drawn as in figure 1. To determine a value of B_∞ applicable

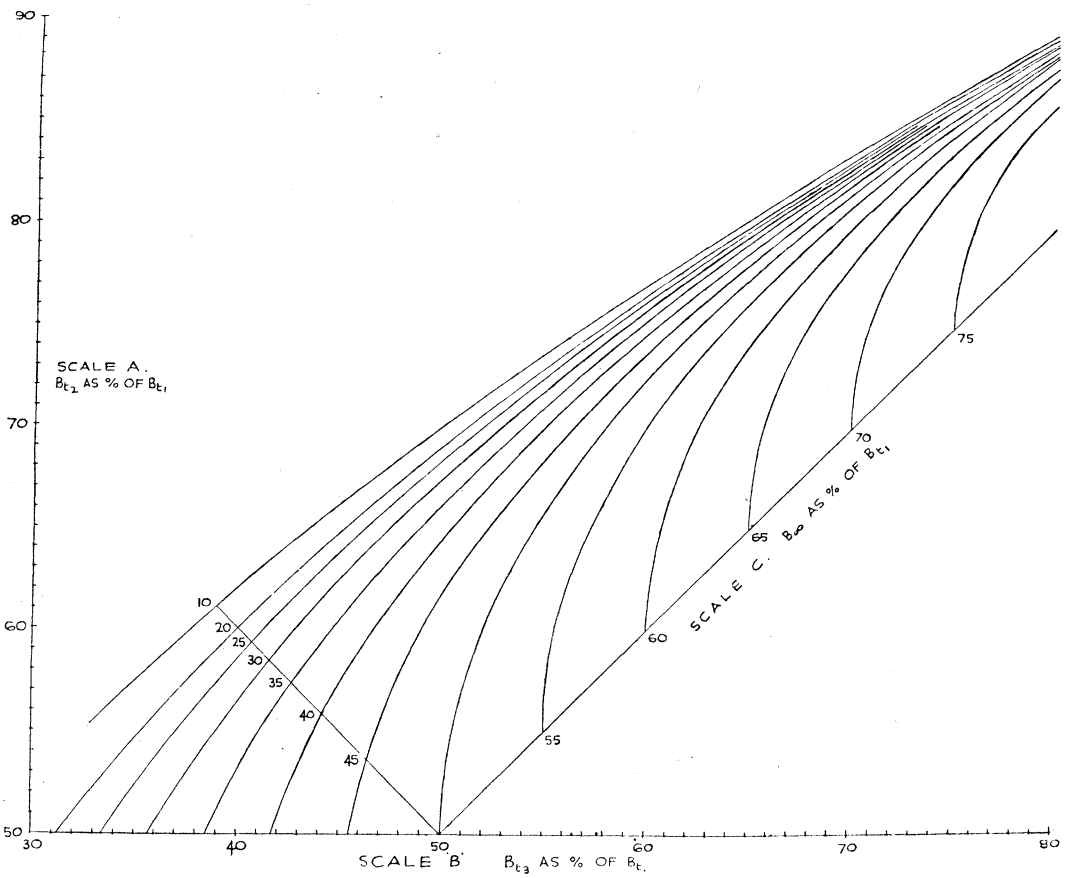

FIGURE 1. Infinity values.

to any short section of a brightness profile, it is therefore only necessary to select three points of depth t_1, t_2 and t_3 such that $t_2-t_1 = t_3-t_2$, express B_{t_2} and B_{t_3} as percentages of B_{t_1}, and interpolate from figure 1 the value of B_∞ as a percentage of B_{t_1}. The three selected points of depth t_1, t_2 and t_3 should be on a portion of the brightness profile having a high rate of curvature in order to obtain maximum sensitivity; assuming depths are not known, the chosen points should be fairly close to, and equidistant from, each other along the profile, the assumption being made that the gradient of the beach from t_1 to t_3 is constant. This assumption can always be checked by comparing the values of B_∞ obtained in this way from another set of three points overlapping the first set.

Method 2. Writing equation (2) for the three points B_{t_1}, B_{t_2} and B_{t_3} and assuming the convention that the values of t_2 and t_3 refer to depth reckoned from the point t_1, it can be shown that

$$\frac{B_{t_1}-B_{t_2}}{B_{t_1}-B_{t_3}}=\frac{1-10^{-2(\alpha+\beta)t_2}}{1-10^{-2(\alpha+\beta)t_3}}. \tag{5}$$

It should be noted that this is true for any values of t_1, t_2 and t_3. Unfortunately, the form of this equation is such that it cannot be used to determine depths unless the value of $(\alpha+\beta)$ is known and the beach gradient is constant, and therefore method 1 is normally preferred.

Equation (5) is, however, useful for the calculation of extinction coefficients if depths are known; for this purpose it is convenient to prepare sets of curves showing theoretical values of the term $2(\alpha+\beta)\,t_2$ for values of the function $(B_{t_1}-B_{t_2})/(B_{t_1}-B_{t_3})$, each curve referring to a particular value of t_2 and t_3. The values of $2(\alpha+\beta)\,t_2$ obtained from such a graph may then be plotted against the known values of t_2; a straight line whose slope is $2(\alpha+\beta)$ should result if the water is homogeneous between B_{t_1} and B_{t_3}. Curvature of this line indicates that the original brightness profile was incorrectly drawn or that the limits of B_{t_1} and B_{t_3} for homogeneity were too wide. This method of analysing a brightness profile in short sections enables mean extinction coefficients to be compared along the profile, but the relative values of B_{t_1}, B_{t_2} and B_{t_3} must be known with a high degree of accuracy if useful results are to be secured.

For the determination of depths, the extinction coefficient being known, the points t_1, t_2 and t_3 should be so chosen that $t_2-t_1=t_3-t_2$; that is, they should be close together and equidistant on the profile. If the convention is again used that t_2 and t_3 are depths below t_1 as zero, it follows that $t_3=2t_2$. Then

$$\log_{10}\left(\frac{B_{t_1}-B_{t_2}}{B_{t_2}-B_{t_3}}\right)=2(\alpha+\beta)\,t_2. \tag{6}$$

With these limitations, therefore, if the extinction coefficient is known, the gradient of a beach below water may be determined from a *single* photograph, even if it is not possible because of waves, dirt or rocks to construct the complete brightness profile.

Summary of uses of a single brightness profile

Provided that the water is calm and optically homogeneous between B_0 (or B_{t_1}) and B_∞, the following information can be obtained by analysis of a single brightness profile:

(*a*) Absolute depths below B_0 (or B_{t_1}), if the extinction coefficient is known. The latter, however, varies with time, season and place over a wide range (Atkins 1932; Atkins & Poole 1933; Atkins, Clarke, Pettersson, Poole, Utterback & Angström 1938; Clarke 1936, 1938; Erikson 1933; Jenkins, Bowen & Rogers 1941; Le Grand 1939; Pettersson 1935; Utterback & Williams 1935; Young & Gordon 1939).

(*b*) The mean extinction coefficients, given a point of known depth.

Determination of depths from a pair of brightness profiles

Because the intensity of light transmitted by a given depth of water varies with wave-length, the shape of a brightness profile will depend on the wave-length of the light used; therefore a comparison of the shapes of a pair of brightness profiles prepared from photo-

graphs taken simultaneously through two contrasting filters enables depths to be determined when absolute values of the extinction coefficients are not known.

The extinction coefficient $(\alpha+\beta)$, defined by the equation $I = I_0 10^{-(\alpha+\beta)t}$, is the sum of the absorption coefficient α and the scattering coefficient β; both α and β vary with the wavelength of the light used for their determination.

The absorption coefficient (α) includes absorption due to the water molecules, and absorption due to foreign matter in solution or suspension in the water.

In sea water the latter is generally small and may often be neglected, although it has been claimed by Kalle (1938) that yellow colouring matter formed by organic processes is in fact responsible for the green hue of coastal water; in lake water there is no doubt that matter in solution contributes to the absorption coefficient (James & Birge 1938), but in normal coastal or oceanic water this effect has not been observed in these trials.

Absorption within the visible spectrum due to the water molecules has been measured by a number of workers, using both distilled water and specially purified sea water (Clarke & James 1939; James & Birge 1938; Le Grand 1939; Sawyer 1931). Their results have been discussed by James & Birge, whose own very exact measurements in a silver-lined tube have been adopted, on the advice of Atkins, for the present work. James & Birge's values for distilled water, smoothed and interpolated graphically by the writer, are given in table 1 and figure 2.

TABLE 1. ABSORPTION COEFFICIENTS OF DISTILLED WATER

wave-length (A)	absorption coefficient $(\alpha)_m$ (m.$^{-1}$ log$_e$)	absorption coefficient (α) (ft.$^{-1}$ log$_{10}$)	wave-length (A)	absorption coefficient $(\alpha)_m$ (m.$^{-1}$ log$_e$)	absorption coefficient (α) (ft.$^{-1}$ log$_{10}$)
3600	0·0424	0·0056	5900	0·1440	0·0190
3700	0·0317	0·0042	6000	0·2150	0·0284
3800	0·0227	0·0030	6100	0·2480	0·0328
3900	0·0159	0·0021	6200	0·2660	0·0352
4000	0·0135	0·0015	6300	0·2870	0·0378
4100	0·0091	0·0012	6400	0·3080	0·0406
4200	0·0091	0·0012	6500	0·3350	0·0442
4300	0·0087	0·0011	6600	0·3680	0·0486
4400	0·0075	0·0010	6700	0·4070	0·0538
4500	0·0061	0·0008	6800	0·4520	0·0596
4600	0·0053	0·0007	6900	0·5090	0·0670
4700	0·0045	0·0006	7000	0·5980	0·0789
4800	0·0053	0·0007	7100	0·7650	0·1010
4900	0·0061	0·0008	7200	1·0400	0·1370
5000	0·0075	0·0010	7300	1·4550	0·1920
5100	0·0106	0·0014	7400	2·1600	0·2850
5200	0·0152	0·0020	7500	2·4900	0·3290
5300	0·0227	0·0030	7600	2·4500	0·3230
5400	0·0340	0·0045	7700	2·3800	0·3150
5500	0·0395	0·0052	7800	2·3200	0·3060
5600	0·0416	0·0055	7900	2·2500	0·2970
5700	0·0477	0·0063	8000	2·2000	0·2900
5800	0·0780	0·0103			

The scattering coefficient (β) will be considered as solely due to particles suspended in the sea water (Le Grand 1939). Work by Mie (1908), Debye (1909) and particularly by Blumer (1926) has demonstrated that the indicatrix of diffusion (Le Grand 1939) for transparent spherical particles of diameter D varies in a complicated way as the ratio D/λ changes.

When D/λ is very small the indicatrix is nearly symmetrical—the same amount of light is scattered forwards as backwards; for a certain type of particle when the ratio D/λ becomes 0·2 there is a great increase in the component scattered forward, and when $D/\lambda = 0{\cdot}6$, the ratio of forward to backward scatter becomes practically constant and at a maximum value.

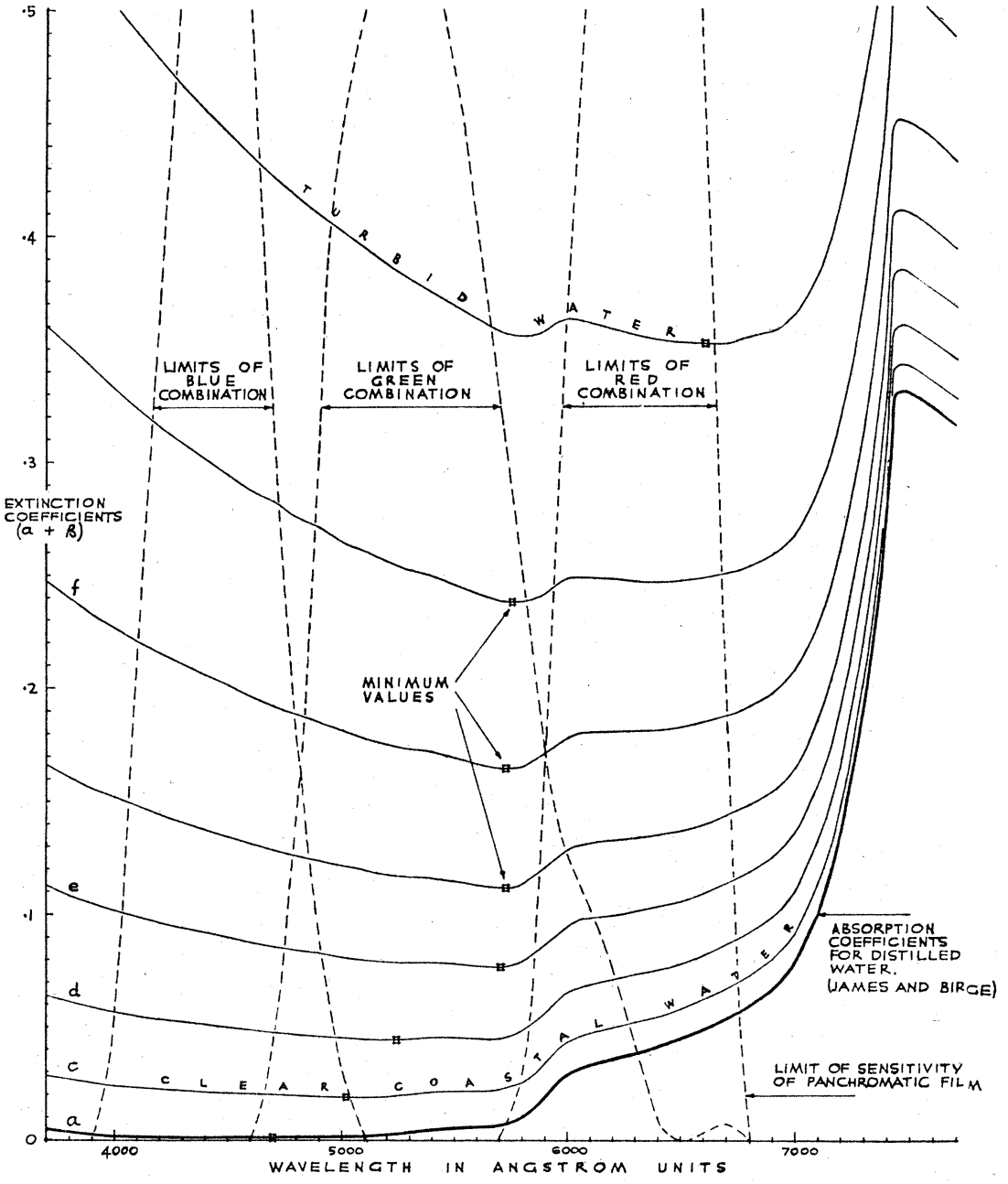

FIGURE 2. Generalized extinction coefficients.

These changes in the indicatrix of diffusion as the diameter of the particle increases are important in the present work because they are accompanied by a reduction in the dependence of β on wave-length (Bhagavantam 1942; Blumer 1926; Cooper & Milne 1938; Jenkins *et al.* 1941; Krishnan 1925; Le Grand 1939; Middleton 1941; Raman 1922; Subow & Czihirin 1940). If these particles are small compared with the wave-length of the light, the scattering coefficient will vary inversely as the fourth power of the wave-length (Rayleigh 1910).

If ρ is defined by the equation $\beta = c'\lambda^{-\rho}$, one example of the variation of ρ with the ratio D/λ is given in table 2. The data for this table was supplied by Le Grand in a private communication based on Blumer's work, and refers to the component scattered forward. The variation of ρ for the component scattered backward is of similar form.

TABLE 2. VARIATION OF ρ WITH THE RATIO D/λ

D/λ	ρ	D/λ	ρ
0·0	4·0	0·7	1·6
0·3	3·8	1·0	1·05
0·4	3·2	1·5	0·75
0·5	2·3	2·0	0·55
0·6	1·9		

From these considerations Le Grand suggests that ρ values near to unity should be assumed for coastal sea water, as a reasonable estimate, and that for turbid estuarine water a value near to zero would be applicable.

It is difficult to calculate ρ values from extinction coefficients determined by various workers, because the filters and instruments used vary widely in their spectral characteristics. There is, however, other evidence that the value of ρ for sea water is about 1:

(*a*) The use of an immersion microscope (Jenkins *et al.* 1941) has established that the particles which cause scattering in sea water are nearly all of diameter less than 25,000 A and not primarily plankton, air bubbles, or grains of sand. They may include very finely dispersed clay (Sverdrup *et al.* 1942). On the other hand, Clarke & James (1939) showed that very efficient filtration of sea water with a Berkfeld filter can reduce the scattering coefficient almost to zero, the filtrate having in the green and red portions of the spectrum the same extinction coefficients as distilled water; values of ρ exceeding about 2 (i.e. D/λ ratios smaller than 0·6) may therefore be uncommon.

(*b*) The ratio of the light scattered upwards to that travelling downwards within the water is in fact small (Atkins & Poole 1940; Sverdrup *et al.* 1942), suggesting an indicatrix of diffusion corresponding to a D/λ ratio exceeding 0·5, that is, a ρ value of less than 2.

(*c*) It will be shown in part III of this paper that measurements of extinction coefficients with narrow band filters in a modified Pulfrich photometer have given ρ values varying between the limits 0·7 and 1·5.

(*d*) Extinction coefficients calculated from brightness profiles agree well with theoretical coefficients based on a ρ of 1.

It will therefore be assumed that in normal coastal water, the scattering coefficient β varies inversely as about the first power of the wave-length over the red and green portions of the spectrum. Because the effective wave-lengths of the filters used in this work are numerically close, variations in the ρ value are not important. There seems to be little justification for assuming that the fourth power law is applicable to sea water (Hulbert 1932; Subow & Czihirin 1940).

Theoretical extinction coefficients

The theoretical variation of the extinction coefficient $(\alpha+\beta)$ with wave-length can now be expressed in graphical form (figure 2), on the assumption that the extinction coefficient is the sum of the absorption coefficient at that wave-length (table 1) and of a scattering

coefficient which itself varies inversely as the wave-length. Theoretical extinction coefficients obtained in this way may be compared with measured values determined by various workers (Atkins 1932; Atkins & Poole 1933; Atkins *et al.* 1938; Clarke 1936; Cooper & Milne 1938; Erikson 1933; Jenkins *et al.* 1941; Le Grand 1939; Young & Gordon 1939). The lack of agreement in some of the latter cases has already been discussed. The shift of the minimum extinction coefficient from the blue to the green and finally into the red as the clarity of the water decreases is of interest, and has actually been observed in measurements in the Tamar Estuary (Cooper & Milne 1938).

It will be apparent from the foregoing, and from figure 2, that the theoretical relationship between the extinction coefficients for any two wave-lengths λ_1 and λ_2 for a given sample of water is of the form

$$(\alpha+\beta)_{\lambda_2} = a(\alpha+\beta)_{\lambda_1}+b, \tag{7}$$

where a and b are constants for any two given values of λ_1 and λ_2.

If it were possible to use monochromatic filters on the air cameras, the value of λ_1 and λ_2 would be known, and thus a and b in equation (7) would be known constants. Depths could then be calculated from a pair of brightness profiles without a knowledge of the extinction coefficients by using a relationship of the form

$$t_2-t_1 = \frac{1}{2b}\log_{10}\left(\frac{B_{t_1}-B_\infty}{B_{t_2}-B_\infty}\right)_{\lambda_2} - \frac{a}{2b}\log_{10}\left(\frac{B_{t_1}-B_\infty}{B_{t_2}-B_\infty}\right)_{\lambda_1}, \tag{7a}$$

which is readily obtained by combining equations (4) and (7). Equations (3) and (7) or (6) and (7) may be used in a similar manner.

Owing to the long exposure required, 'monochromatic' filters cannot be used, except with low-speed aircraft and lenses of exceptionally large aperture. Filters of wide transmission must therefore be used, introducing the complication, apparent from figure 2, that the value of the 'constants' a and b will then vary both with the depth and with the extinction coefficient of the water.

An accurate analysis of a pair of brightness profiles cannot therefore be made by the use of a single relationship such as that based on equations (4) and (7) above. It is necessary to employ a graphical calculator on which all possible variations of $(\alpha+\beta)_{\lambda_1}$ and $(\alpha+\beta)_{\lambda_2}$ with depth and water type are represented. The construction of such a calculator is described in a later section of this paper, and its use is illustrated by examples in part III. The calculator no longer assumes that all the variables remain constant throughout the filter band.

The calculator operates by comparing the rates of curvature of a pair of brightness profiles; errors in the profiles will produce errors in the depths or extinction coefficients recorded by the calculator. It is desirable, therefore, to consider certain additional properties of brightness profiles which become apparent when they are plotted in pairs. Examples of pairs of profiles to illustrate the following points are given in figures 3 and 4.

Comparison of two brightness profiles

The two profiles from simultaneous photographs should be plotted on the same scale for ease of comparison; if the calculator is to be used for their final analysis, the vertical (brightness) scale should be so chosen that the vertical interval between B_0 (or B_{t_1}) and B_∞ does not exceed 20 cm. on any one profile.

(*a*) *Variation of shape with extinction coefficient.* A brightness profile of a uniformly reflecting beach of constant gradient, covered with optically homogeneous water with a calm surface, depends for its shape solely on the extinction coefficient of the water. Consider on such a profile a point of relative brightness B_t at depth t_b, such that the numerical value of the

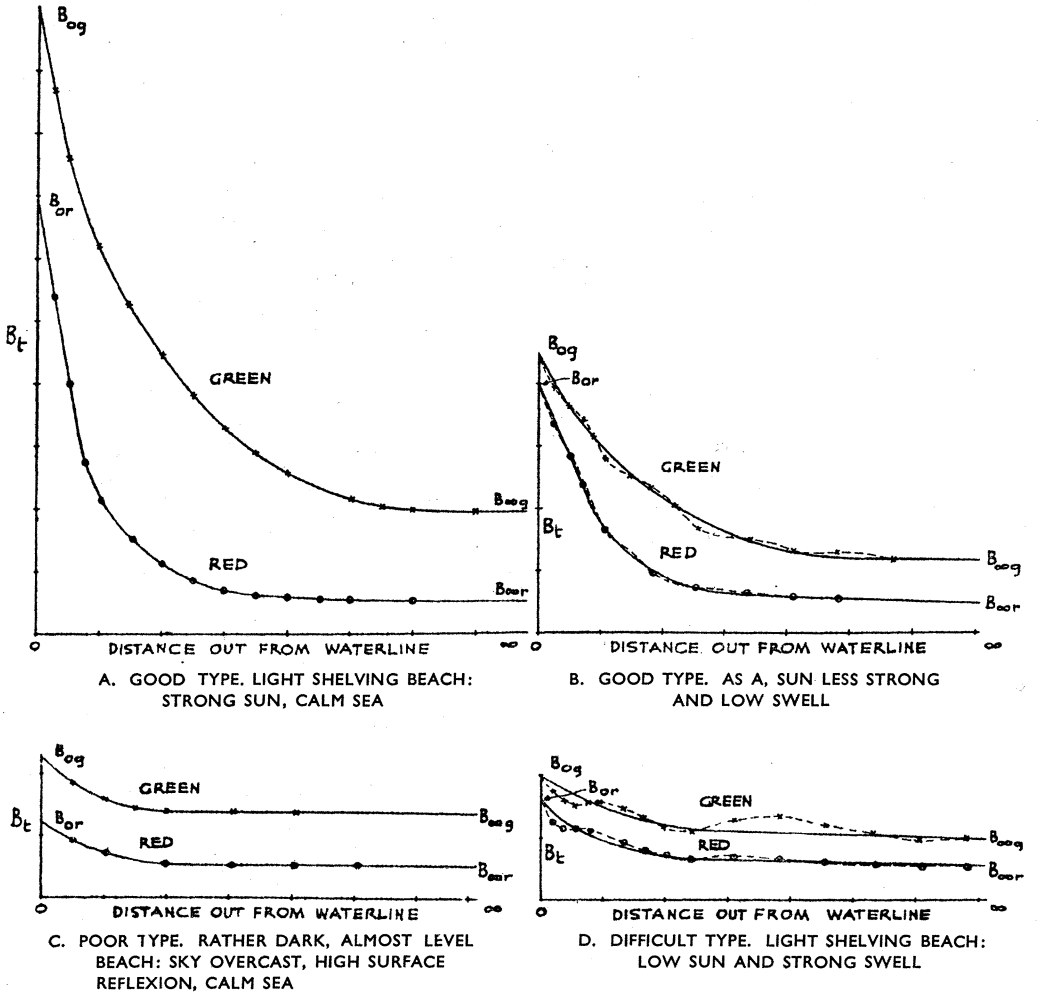

FIGURE 3. Various types of brightness profiles. All diagrams are on the same scale.

relative brightness B_t is exactly half-way between the numerical values of B_0 and B_∞. Then, from equation (3),

$$\log_{10}\frac{B_0-B_\infty}{B_t-B_\infty} = 2(\alpha+\beta)\,t_b = \log_{10} 2{\cdot}0,$$

whence

$$t_b = \frac{0{\cdot}1505}{(\alpha+\beta)}. \qquad (8)$$

This simple relation indicates how the shape of a profile will vary with the extinction coefficient. In conjunction with figure 2, it can be used to estimate the relative shapes of the two profiles which should be obtained with any two selected filters.

(*b*) *Sensitivity.* It can be shown from equation (3) that the sensitivity of the depth determination from a brightness profile is proportional to the value of $(B_0-B_\infty)/B_\infty$. A profile on which B_∞ is high relative to B_0—due to reflexion from atmospheric haze, or from the

water surface, or from particles within the water—will therefore give less accurate depths on analysis than a profile having a relatively low value of B_∞.

(*c*) *Change in reflectivity of the sea-bed.* A sudden change in reflectivity of the sea-bed will produce a discontinuity in the profile. A gradual change will alter the rate of curvature of the profile, and will appear on the calculator as a change in the extinction coefficient or in the beach profile. Generally, changes in sea-bed reflectivity are immediately obvious on

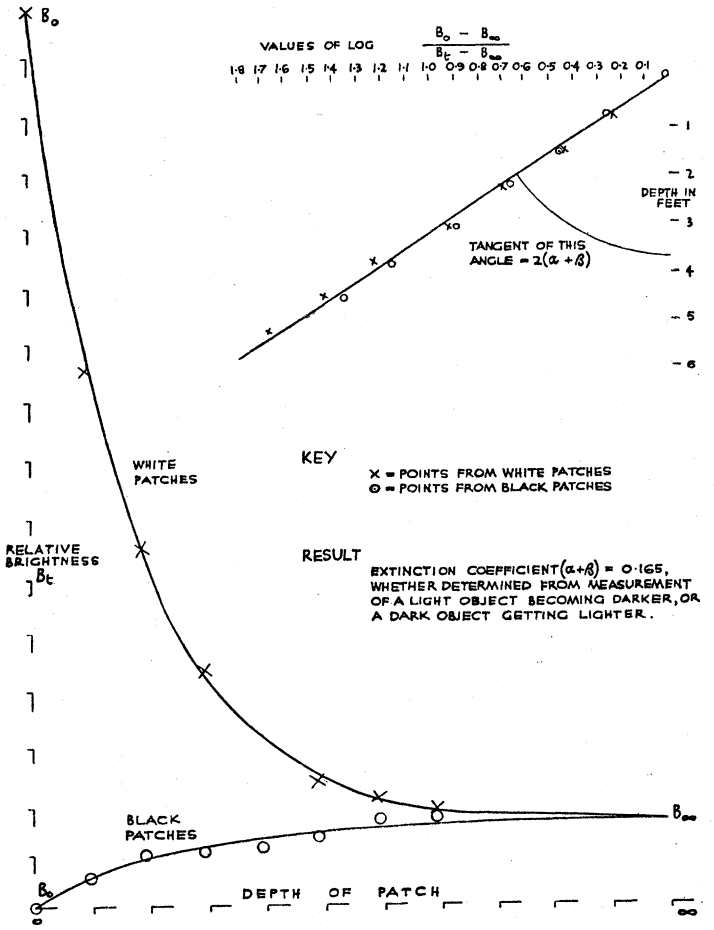

FIGURE 4. Brightness profiles over white and black surfaces.

examining a negative taken through a green filter. If the sea-bed is not of uniform material, it will be necessary to break the profile into short sections of approximately uniform reflectivity, and to analyse each section separately on the calculator.

(*d*) *Waves or swell.* Waves or swell affect the brightness profile in two ways: they increase or decrease the length of the column of water through which the light is passing, and so decrease or increase the values of B_t; they also alter the surface reflexion to an extent depending on the angle of the water surface, the sun altitude and the amount of cloud in the sky, and thus change the value of B_∞ applicable to the point B_t. The relative extent of these two effects has not been determined, but examples of a decaying sinusoidal wave motion superimposed on the brightness profile are common (figure 3).

Wave or swell effects may be distinguished from changes in the gradient or reflectivity of the sea-bed by comparing brightness profiles constructed from overlapping photographs. If the disturbance is found to be moving relative to the horizontal scale of the profile, it may

be ascribed to wave motion. Its amplitude will depend on the depth and extinction coefficient of the water and will therefore vary with the filter used.

Provided the wave motion shown on the profile is of small amplitude, it can be removed by drawing a mean curve through the points concerned. This smoothing process may be carried out more accurately on a log brightness profile, constructing the normal linear brightness profile from the smooth curve obtained; this has the advantage that errors which may have been made when measuring the density of the negatives will be of constant dimensions on the log brightness profile, whereas they vary with the numerical value of B_t on the normal profile.

(*e*) *Comparative values of* B_0. The two values of B_0, whether measured or obtained by extrapolation of the profile, will not necessarily be equal, but if the photography is good (part II), they will not be widely different. Absolute brightness values cannot be determined because the intensity of the incident light and the reflectivity of the sea-bed and of the water surface are unknown; if the beach is coloured, its hue and saturation will also affect the values of B_0, although from equation (1) it will be appreciated that B_0 is not the relative brightness of the beach above the waterline.

(*f*) *Comparative values of* B_∞. If the two values of B_0 are approximately equal, the profile with the higher scattering coefficient will generally have the higher B_∞. A decrease in the extinction coefficient as the water becomes deeper will be indicated by failure of this profile to reach a steady B_∞ value.

(*g*) *Configuration of the sea-bed.* Elevations or depressions in the sea-bed will be reproduced on both profiles and must not be mistaken for wave motion. They may prevent extrapolation of the profile to obtain B_∞, which must then be calculated from figure 1. The presence, for instance, of submerged sandbars will complicate the profile and make necessary an analysis by sections (plates 5–6).

(*h*) *Dark beaches.* It has been assumed in the foregoing that the beach material was sufficiently reflective for the term $\left(R-\frac{cV}{2(\alpha+\beta)}\right)$ in equation (1) to be positive, so that B_t decreased as the depth of the water increased. It will be apparent, however, that if $R=\frac{cV}{2(\alpha+\beta)}$, the brightness of the sea-bed will not change with depth. If R is numerically less than $\frac{cV}{2(\alpha+\beta)}$, B_t will increase with depth due to scattering by particles suspended in the column of water above the sea-bed.

Submerged rocks may in fact appear lighter in tone on vertical air photographs as their depth increases. The brightness profiles shown in figure 4 demonstrate the same effect; they were constructed from a photograph of black and white objects submerged at known depths in a water tank, and it will be noted that both profiles have the same B_∞ value and both give the same extinction coefficient for the water.

Brightness profiles of dark surfaces have a relatively low $(B_0-B_\infty)/B_\infty$ ratio and a relatively low sensitivity to changes in depth. The use of a blue filter when taking the photographs would, from the curves of figure 2, be expected to increase this sensitivity by increasing the scattering recorded within the column of water above the dark surface. The results obtained in this way with a blue filter are described in part III.

The choice of filters and film

It will be apparent from figure 2 that coastal sea water will normally be most transparent to light of wave-length about 4500–5800 A, and therefore a green filter should be used for photography of the sea-bed. In considering the choice between a blue or a red filter for use in the second camera, a blue filter has serious disadvantages: the light it transmits may be scattered selectively by atmospheric haze, is generally not strongly reflected by sandy beaches, and is transmitted too freely by sea-water for the purpose of this work. A photograph of the sea-bed taken with a blue filter lacks contrast, and the brightness profile has a low $(B_0-B_\infty)/B_\infty$ ratio. A red filter is therefore preferred, and the film used must therefore be panchromatic.

From the many commercially available filters which transmit in the required spectral regions, the two selected after considerable experiment were Wratten 56 (green) and Wratten 27 (red); for photography of dark beaches, a blue filter, Wratten 47*a*, was also used. These filters have high and nearly equal transmissions relative to Kodak aero panchromatic film, the transmission ending fairly sharply with the minimum obtainable overlap. The filters are rated stable to light.

Table 3 summarizes their transmission characteristics, determined by spectro-photometric measurement on the samples used in the Cornwall trials. The data on the relative spectral sensitivity of Kodak aero panchromatic film to mean noon sunlight was provided by Kodak Ltd. of Harrow. The product of the filter transmission and the film sensitivity for each 100 A unit interval is also indicated on figure 2. Integration of the latter over the limits of transmission of the filters can be used as a measure of the photographic exposure equivalent of each filter-film combination. The results of these integrations are given at the foot of table 3, for comparison with a similar integration for the minus blue (Ilford 110—R.A.F.

TABLE 3. TRANSMISSION OF FILTERS RELATIVE TO PANCHROMATIC FILM

	transmission of filters (Z_λ)				relative sensitivity of Kodak aero Super XX film to mean noon sunlight (Y_λ)	products ($Z_\lambda Y_\lambda$)				haze correction factor (K'_λ)
wave-length (A)	Wratten 27 (red)	Wratten 56 (green)	Wratten 47*a* (blue)	Ilford 110 (minus blue)		Wratten 27 (red)	Wratten 56 (green)	Wratten 47*a* (blue)	Ilford 110 (minus blue)	
4000	—	—	0·0300	—	1·905	—	—	0·0572	—	0·851
4200	—	—	0·2525	—	2·089	—	—	0·5275	—	0·861
4400	—	—	0·3900	—	2·138	—	—	0·8338	—	0·870
4600	—	0·0000	0·2880	—	1·754	—	0·0000	0·5052	—	0·878
4800	—	0·1350	0·1600	—	1·096	—	0·1480	0·1754	—	0·885
5000	—	0·5900	0·0400	0·001	0·7586	—	0·4476	0·0303	0·0008	0·891
5200	—	0·7600	—	0·50	0·7244	—	0·5505	—	0·3706	0·897
5400	—	0·7350	—	0·87	0·7112	—	0·5227	—	0·6188	0·902
5600	—	0·5900	—	0·89	0·6761	—	0·3989	—	0·6017	0·907
5800	0·0450	0·3850	—	0·89	0·6457	0·0291	0·2486	—	0·5747	0·912
6000	0·5625	0·1850	—	0·89	0·6730	0·3786	0·1245	—	0·5976	0·916
6200	0·8060	0·0975	—	0·89	0·7656	0·6171	0·0747	—	0·6814	0·920
6400	0·8525	0·0100	—	0·89	0·8710	0·7425	0·0087	—	0·7752	0·923
6600	0·8725	0·0050	—	0·89	0·5433	0·4740	0·0027	—	0·4835	0·927
6800	0·8725	0·1375	—	0·89	0·0000	0·0000	0·0000	—	0·0000	0·930
					integrals	0·4548	0·5050	0·4233	0·9481	
					ratio of integrals	1·00	1·11	0·93	2·09	

Type IV) filter commonly employed in air photography. It will be seen that the use of these colour filters only doubles the exposure normally required, and no serious demand is therefore made on the camera or aircraft.

The effect of haze and atmospheric scattering

It has already been shown that the effect of haze on the brightness profile is to reduce the sensitivity of the depth determination, and for this reason it is clear that air photographs for use in this work should be taken when haze is at a minimum, and from as low an altitude as possible. In the general case, however, some selective scattering by the atmosphere will be unavoidable, and it is necessary to determine how this will affect the filter-film combinations described in table 3.

Data on the vertical transmission of the atmosphere at various wave-lengths is scarce (Middleton 1941). There is evidence (Duclaux 1931; Johnson, Meyer, Hopkins & Monk 1939; King 1913) that a 5000 ft. column of dry dust-free air at N.T.P. may reduce the intensity of incident light to about 93·7 % at 4000 A and to about 98·8 % at 6000 A. In the lower atmosphere, however, dust, water in the form of droplets, salt particles from the sea, and minute living organisms will increase this attenuation, and it has been found that there is an increase in the selectivity of atmospheric scattering as the visual range through the atmosphere increases (Middleton 1941).

It is clear that some correction must be made to the filter-film transmission data of table 3 to compensate for the selective attenuation superimposed by the column of air between the camera and the sea surface; it is equally clear that no one correction can precisely compensate for the variety of atmospheric conditions which may be encountered. As an approximation, however, it will be assumed that the column of air between the aircraft and the sea surface reduces the intensity of light of wave-length 5300 A to 90 % in one passage, and that the reduction in intensity at other wave-lengths can be calculated by assuming that the scattering coefficient in this column varies inversely as the 1·5 power of the wave-length (Middleton 1935). These figures assume that flying heights may vary from 5000 to 20,000 ft., and that hazy conditions will be avoided. It will again be noted that as the mean effective wave-lengths of the red and green filter-film combinations are numerically close, errors in these assumptions will not be serious. The last column of table 3 gives correction factors under these conditions; their differences are seen to be small within the limits of any one combination.

For a precise evaluation of the effect of atmospheric scattering, it would be necessary to control each photograph by including in the field of view a series of contrasting neutral-toned objects; this is not convenient in practice, and it will be shown in part III that the above general corrections for atmospheric scattering enable depths to be determined from the calculator without significant loss of accuracy.

The construction of the calculator

The necessity for some graphical form of calculator has already been discussed. A suitable form of calculator may be constructed as follows.

From the data on figure 2 and in table 3, it is possible to calculate the theoretical pairs of extinction coefficients which should be given by the green and red filter-film combinations

over any depth range in any type of water. If for each type of water the theoretical values of the product $2(\alpha+\beta)\,t$ for one combination are then plotted against those for the other, smooth curves will be obtained which may themselves be graduated in terms of t. In this way a chart may be prepared from which the depth and water type may be read if a pair of $2(\alpha+\beta)\,t$ values are known. The latter are, of course, easily determinable from a pair of brightness profiles by the use of equations (3), (4) or (6). The first step in the construction of the calculator is therefore the determination, from figure 2 and table 3, of a sufficient number of theoretical pairs of extinction coefficients for the chosen green and red filter-film combinations.

If equation (1) is written for any one wave-length λ and integrated over the spectrum for the chosen filter-film combination, it is clear that

$$B_t-B_\infty=\frac{J}{\mu^2}K''K'''I_0\int_{\lambda_2}^{\lambda_1}Z_\lambda Y_\lambda(K_\lambda)^2\left(R_\lambda-\frac{V_\lambda c}{2(\alpha+\beta)_\lambda}\right)10^{-2(\alpha+\beta)_\lambda t}\,d\lambda,$$

where Z_λ is the transmission of the filter, Y_λ is the relative sensitivity of the film, K'_λ is the haze correction factor, values for which are given in table 3. Hence

$$\frac{B_0-B_\infty}{B_t-B_\infty}=\frac{\int_{\lambda_2}^{\lambda_1}Z_\lambda Y_\lambda(K'_\lambda)^2\left(R_\lambda-\frac{V_\lambda c}{2(\alpha+\beta)_\lambda}\right)d\lambda}{\int_{\lambda_2}^{\lambda_1}Z_\lambda Y_\lambda(K'_\lambda)^2\left(R_\lambda-\frac{V_\lambda c}{2(\alpha+\beta)_\lambda}\right)10^{-2(\alpha+\beta)_\lambda t}\,d\lambda}=10^{-2(\alpha+\beta)t}$$

from equation (3), where $(\alpha+\beta)$ denotes the mean extinction coefficient given by the particular filter-film combination for a depth t of water whose extinction coefficient at any wave-length is $(\alpha+\beta)_\lambda$.

It is reasonable to assume that the backward scatter V_λ due to an elementary layer is proportional to β_λ. If the scattering particles are similar to those on the sea-bed, V_λ will also be proportional to R_λ. Therefore

$$\left(R_\lambda-\frac{V_\lambda c}{2(\alpha+\beta)_\lambda}\right)=R_\lambda\left(1-\frac{K\beta_\lambda c}{2(\alpha+\beta)_\lambda}\right),$$

where K is some unknown constant.

If absorption by the water were negligible, i.e. $\alpha\simeq 0$, and each successive thin layer acted as a partial diffusing screen with the same reflectivity as the sea-bed, then the reflected brightness would be constant at all depths. This would indicate that

$$\frac{Kc}{2}=1\quad\text{or}\quad K=\frac{2}{c}.$$

If the particles behave as diffuse reflecting spheres whose diameters are large compared with λ, it can be shown that the layers of particles will not behave in the same way as the sea-bed, but will reflect only one-quarter of the light, i.e. $K=1/2c$. On this assumption

$$\left(R_\lambda-\frac{V_\lambda c}{2(\alpha+\beta)_\lambda}\right)=R_\lambda\left(1-\frac{\beta_\lambda}{4(\alpha+\beta)_\lambda}\right).$$

R_λ will normally be constant over the wave-lengths considered and will disappear on integration.

It has been found that the ratio of the two integrals is very insensitive to this factor, so that a more precise determination of its size is unwarranted. Finally, therefore,

$$(\alpha+\beta) = \frac{1}{2t}\log_{10}\left[\frac{\int_{\lambda_2}^{\lambda_1} Z_\lambda Y_\lambda (K'_\lambda)^2 \left(1-\frac{\beta_\lambda}{4(\alpha+\beta)_\lambda}\right) d\lambda}{\int_{\lambda_2}^{\lambda_1} Z_\lambda Y_\lambda (K'_\lambda)^2 \left(1-\frac{\beta_\lambda}{4(\alpha+\beta)_\lambda}\right) 10^{-2(\alpha+\beta)_\lambda t}\, d\lambda}\right]. \qquad (9)$$

Because the terms Z_λ, Y_λ and $(\alpha+\beta)_\lambda$ are not mathematical functions, this integral must be evaluated graphically or by Simpson's rule; using the latter method over 100 A intervals of wave-length, pairs of $(\alpha+\beta)$ values for the selected green- and red-film combinations of table 3 have been calculated over arbitrary depth ranges for a number of the water types given in figure 2; the results are summarized in table 4. As a check, one set of the integrations was repeated using the term $\left[1-\frac{\beta_\lambda}{2(\alpha+\beta)_\lambda}\right]$ in place of the term $\left[1-\frac{\beta_\lambda}{4(\alpha+\beta)_\lambda}\right]$ in equation (9); the results are given in the final columns of table 4, and it will be seen that the effect on the original pairs of $(\alpha+\beta)$ values is in fact negligible.

TABLE 4. THEORETICAL PAIRS OF EXTINCTION COEFFICIENTS FOR THE SELECTED GREEN AND RED FILTER-FILM COMBINATIONS

These $(\alpha+\beta)$ values are based on common logarithms and ft.$^{-1}$. To base them on Naperian logarithms and m.$^{-1}$, divide by the factor 0·132. The water types denoted by the letters *a* to *f* are shown in figure 2. The green and red filter-film combinations are denoted by the letters G and R respectively.

water type ...	*a*		*b*		*c*		*d*		*e*		*f*		*d* checked	
filter-film ...	G	R	G	R	G	R	G	R	G	R	G	R	G	R
depth range (ft.)														
0– 1	0·0058	0·0384	—	—	—	—	0·0475	0·0735	—	—	0·1762	0·1814	—	—
0– 2	0·0057	0·0382	0·0157	0·0463	0·0231	0·0529	0·0473	0·0734	0·0809	0·1019	0·1739	0·1813	0·0478	0·0735
0– 5	0·0055	0·0378	0·0153	0·0459	0·0228	0·0522	0·0471	0·0730	0·0806	0·1015	0·1726	0·1809	0·0474	0·0732
0–10	0·0050	0·0370	0·0152	0·0452	0·0223	0·0517	0·0466	0·0728	0·0802	0·1012	0·1730	0·1812	0·0469	0·0727
0–16	0·0046	0·0359	0·0144	0·0442	0·0218	0·0506	0·0464	0·0719	0·0799	0·1010	0·1721	0·1808	0·0466	0·0719
0–25	0·0041	0·0342	0·0139	0·0426	0·0215	0·0492	0·0459	0·0705	0·0799	0·1008	—	—	0·0459	0·0706
0–50	0·0034	0·0286	0·0132	0·0375	0·0211	0·0443	—	—	—	—	—	—	—	—

It will be seen from table 4 that both the selected filter-film combinations will record a reduction in the extinction coefficient of optically homogeneous water as the depth increases. This effect, due to selective attenuation by the water, is common to all recording systems which do not use monochromatic light. It will also be seen that no single mean effective wave-length can be allotted to a filter-film combination; it is necessary first to specify the water type and depth range and then to determine from figure 2 the monochromatic wave-length which would have given the extinction coefficient listed for these conditions in table 4. As a rough guide, however, the mean effective wave-length of the green combination may be taken as about 5600 A, and of the red about 6300 A. From the relation

$$\log\frac{B_0-B_\infty}{B_t-B_\infty} = 2(\alpha+\beta)\,t$$

(equation (3)) it is clear that if from table 4 the products $2(\alpha+\beta)\,t$ for the green filter are plotted against the corresponding products for the red, a chart will be obtained from which values of t can be read if values of $\log\frac{B_0-B_\infty}{B_t-B_\infty}$ have been calculated from the brightness

profile. The chart is shown in figure 5, with lines of equal depth drawn through the water-type curves *a* to *f*. The chart may also be used for the calculation of depths below *t* from the equation $\log \frac{B_{t_1}-B_\infty}{B_{t_2}-B_\infty} = 2(\alpha+\beta)\,(t_2-t_1)$ without appreciable loss of accuracy, and this will generally be necessary because of the difficulty of extrapolating the brightness profiles to obtain values of B_0.

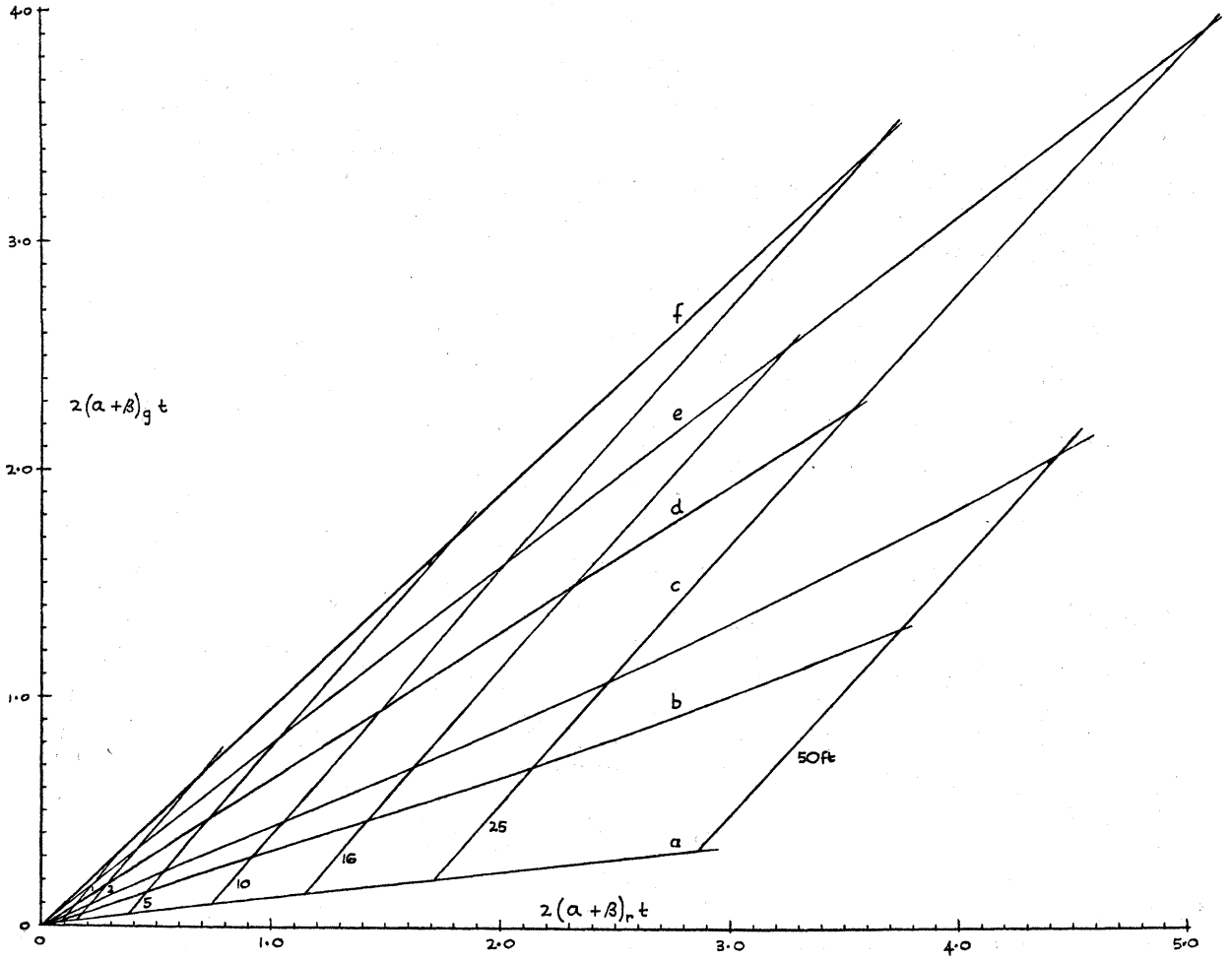

FIGURE 5. Basic data for the calculator.
Water-type curves lettered *a* to *f* (see figure 2). Curves of equal depth are marked in feet.

This chart is not, however, convenient to use for routine work, because it is necessary to calculate for it values of the function $\log \frac{B_0-B_\infty}{B_t-B_\infty}$ or $\log \frac{B_{t_1}-B_\infty}{B_{t_2}-B_\infty}$ from the brightness profiles. By modifying the scales of the chart, and adding geometrical fans to correct for the arbitrary scales of the brightness profiles, it is possible to obtain a more convenient calculator for the determination of depths from a pair of brightness profiles by purely graphical means. In addition to speeding up the interpretation of photographs, this graphical method of analysing the profiles also gives an immediate indication of any changes which may have occurred in the extinction coefficient of the water or in the reflectivity of the sea-bed as the distance from the shore increases.

The finished calculator is shown as figure 17 (facing p. 186), and is reproduced diagrammatically as figure 6. It consists of three parts, which have been superimposed to economize in space:

(*a*) A set of curves of equal depth intersecting curves which represent the selected water types *a–f*; both sets radiate from the bottom left-hand corner of the chart. A smaller set of curves for use in deeper water is placed centrally below them.

(*b*) A geometrical fan *ABC* providing the green ordinates for the above curves; this fan includes a right-angled isosceles triangle *ABD* containing a set of guide lines parallel to the side *BD*. The green brightness profile may be adjusted over this fan so that its brightness

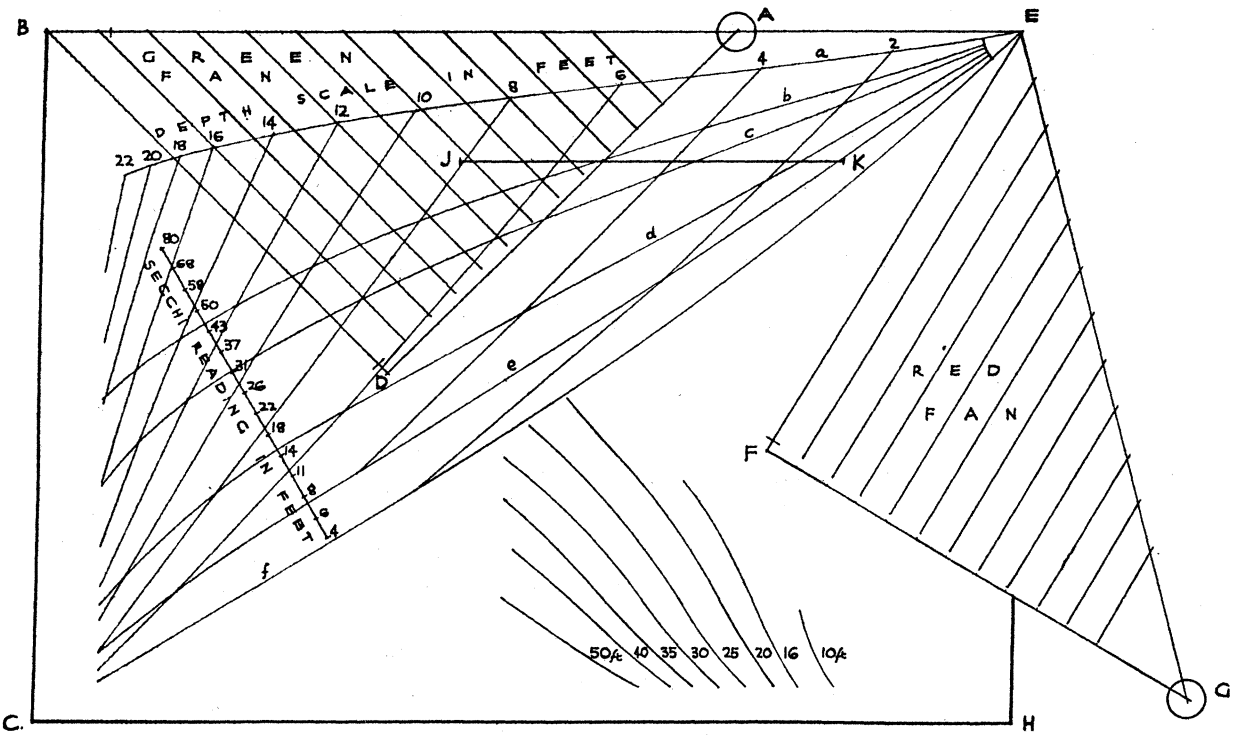

FIGURE 6. Diagram of calculator.

scale is parallel to these guide lines, with B_0 (or B_{l_1}) lying along *AB*, and B_∞ along *AD*. The ordinates for the calculator curves are then given by the intercepts on *BC* of lines drawn from *A* through the desired readings on the brightness scale of the green profile.

(*c*) A second fan *BEG* providing the red abscissae for the depth and water-type curves; this fan is similar in construction to the fan *ABC*. The red brightness profile may be adjusted over it so that the brightness scale of the profile is parallel to *EF*, with B_0 (or B_{l_1}) lying along *EG* and B_∞ along *FG*. The abscissae for the calculator curves are then given by the intercepts on *BE* of lines drawn from *G* through the desired readings on the brightness scale of the red profile.

It is an advantage if the calculator is printed on heavy white paper and in contrasting colours—the two fans green and red, the depth and water-type lines black and blue, the set of deeper water curves purple. Plotting should be carried out on a piece of transparent centimetre-millimetre graph paper pinned over the calculator with its graduations parallel to the frame *BEHC*. By the procedure described above, any point at a given horizontal

distance from the waterline on the green and red brightness profiles will be represented on the calculator by an intercept from A on the scale BC, and by an intercept from G on the scale BE. Perpendiculars from these intercepts will meet at a point within the system of depth lines, from which the required depth may be obtained by interpolation. When the limit of sensitivity of the red brightness profile has been reached, greater depths must be estimated by erecting perpendiculars from the intercepts on BC and from the point of intersection of the appropriate water-type line on JK. These perpendiculars will then meet at a point within the system of deeper water lines. If the water is not homogeneous, the position of the intercept on JK must be estimated from the position of the water-type line at the greatest depth given by the red brightness profile. An example of the use of this calculator is given in part III.

The calculator shown in figure 17 may be constructed from the data on figure 5 by the following procedure. On the assumption that brightness profiles would normally be plotted on centimetre-millimetre graph paper, and the brightness scale could always be so chosen that the vertical distance on the profile between B_0 (or B_{t_1}) and B_∞ need not exceed 20 cm., the fan perpendiculars BD and EF are drawn exactly 20 cm. in length. To off-set to some extent the convergence of the B_t values as the limit B_∞ is approached, the line BD is inclined at an angle of 45° to the calculator ordinate and the line EF at 60° to the calculator abscissae. The overall dimensions and the scale of the calculator are therefore determined. Within this framework the depth and water-type curves are plotted as follows:

The value of $\log_{10}\left(\frac{B_0-B_\infty}{B_t-B_\infty}\right)_g$ and of $\log_{10}\left(\frac{B_0-B_\infty}{B_t-B_\infty}\right)_r$ for any point of known depth t can be read from figure 5, and so the values of $\left(\frac{B_0-B_\infty}{B_t-B_\infty}\right)_g$ and $\left(\frac{B_0-B_\infty}{B_t-B_\infty}\right)_r$ for that depth and particular water type are known. If the line BD on the calculator $= (B_0-B_\infty)_g$ and the line $EF = (B_0-B_\infty)_r$, the positions of B_{tg} and B_{tr} on BD and EF, and hence on BC and EB, can be plotted. The point of intersection of perpendiculars from the latter determines the position of the known value of t on the calculator. In this way all the data on figure 5 can be transferred to the calculator and the smooth curves representing the depths and water types can be drawn. Intermediate depth lines may then be added by graphical interpolation, and the set of deeper water depth lines can be plotted for any arbitrarily chosen position of the line JK.

In practice, however, it was found more convenient to construct a conversion curve showing the relation between arbitrary values of $2(\alpha+\beta)t$ for each filter and the co-ordinates of B_t on arbitrary scales along BC or EB; using this conversion curve, the principal points from figure 5 may be plotted directly on to the calculator.

Atkins has suggested that there is an approximate relationship between the Secchi disk reading of sea water and its extinction coefficient. Expressed in the units used in this paper, this relation becomes

$$\text{Secchi reading (in ft.)} = \frac{0{\cdot}74}{(\alpha+\beta)}. \qquad (10)$$

Assuming that the extinction coefficient concerned is that for green light ($\lambda = 5300$ A), a scale of Secchi disk readings can be placed across the water-type lines on the calculator, since the extinction coefficient for $\lambda = 5300$ A is known from figure 2 for each water type.

It is, of course, appreciated that such a scale is far from exact, but it will be shown later that its use enables a useful estimate to be made of water clarity, in terms of Secchi disk readings, from air photographs.

Notes on the calculator

The graphical procedure for determining depths and Secchi disk readings from a pair of brightness profiles by means of the calculator will be apparent from the preceding section. The plotted points should lie on a smooth curve intersecting the Secchi disk scale.

If errors have been made in selecting values of B_0 (or B_{t_1}) and B_∞, or if the extinction coefficient of the water changes appreciably with depth, the smooth curve may cross one or more of the water-type curves. In this case, a shorter section of the two brightness profiles should be analysed and the best curve should be drawn through the plotted points. A corrected set of depths may be obtained from the intersections of this curve with the perpendiculars from the red fan over the very shallow ranges, and with the perpendiculars from the green fan over the slightly deeper ranges. Depths exceeding the range of the red brightness profile can be estimated from the points of intersection of the water-type curve with the line JK, as before.

The limit to which measurements can be made depends on the clarity of the water. Broadly speaking the value read off the Secchi scale indicates the maximum depth to which reliable measurements can be made over a light-coloured beach, but in practice these depths will not be obtained unless the meteorological and sea conditions are very carefully chosen.

The particular calculator represented in figure 17 can only be used with the selected filter-film combinations. The results obtained with this calculator during the Cornwall trials are recorded in part III. They are believed to justify the theoretical assumptions which it has been necessary to make in the foregoing discussion. In particular, the effects of second- and high-order scattering must be insignificant over the shallow depth ranges concerned.

PART II

The procedure for taking suitable photographs and for making the necessary measurements

The procedure developed for the determination of brightness profiles, and for obtaining an independent check of the depths and extinction coefficients calculated from them will now be considered under the following headings:

(1) Flying technique and the selection of suitable meteorological conditions.

(2) Photographic technique, including sensitometric control and the calibration of the cameras.

(3) Planning a photographic sortie.

(4) Methods of interpreting the photographs.

(5) Methods used for checking depths and extinction coefficients.

Flying technique

Task. The task of the air crew may be summarized as follows:

(*a*) To produce good-quality vertical photographs showing a small amount of beach above water, at a scale between 1/7000 and 1/10,000, the photographs being as free as possible from

tilt, cloud shadows, and reflexion from the water surface; to operate the cameras mechanically and at sufficiently short time intervals that any point will appear on at least three consecutive exposures: if a focal plane shutter is used, the camera should be so orientated that the shutter slot is approximately parallel to the desired profile.

(*b*) To record on each photographic run the time, course, flying height, number and time interval between exposures, frequency of cloud and cloud shadows, the amount of haze, the state of the sea surface, and the colour of the sea and of the beach.

It is unquestionable that the air crew need training and special briefing for this task, but experience has shown that a crew with a small amount of specialist training finds no difficulty in obtaining satisfactory photographs if the briefing is adequate and the meteorological forecasts are good.

Equipment. Any aircraft may be used which can be fitted with at least two vertical air cameras, and can carry a crew of not less than two. Range and endurance permitting, it is an advantage if the photographs are taken from relatively slow-flying aircraft, thereby permitting longer exposures and greater manœuvrability over indented coastlines.

For research purposes where no great coverage was required, a twin-engined Oxford aircraft carrying four vertical R.A.F. F.24 cameras of 8 in. focal length was used at a flying height of 5000 ft.; two of the cameras were carried within the fuselage, and two in the bomb bay. These cameras produce photographs measuring 5×5 in., each covering an area a thousand yards square at a scale of 1/7500.

Where greater range or coverage was necessary, a Mosquito aircraft carrying two vertical R.A.F. F.52 cameras of 20 in. focal length was used at a flying height of 12,000 ft.; this negative measures $8\frac{1}{2} \times 7$ in., and covers an area of about 1700×1400 yd. at a scale of 1/7200. A third vertical camera was loaded with infra-red film.

Increase in the above coverage could probably be obtained by using two pairs of split-mounted cameras, but no trials with these cameras have been carried out.

The smaller F.24 cameras carry 125 or 250 exposure magazines, and the F.52 cameras 500 exposure magazines. It may be possible to change magazines while in the air, so that the number of photographs obtainable in one sortie will be limited rather by the number of hours of suitable flying time than by the capacity of the magazines.

Meteorological and sea conditions. Experience showed that certain well-defined meteorological and sea conditions were essential. After preliminary briefing therefore, the air crew waited for a completely favourable meteorological report before making a sortie. This was not found to be a disadvantage, as so much material was produced from a single sortie under good conditions that frequent sorties were unnecessary.

(*a*) *Sun altitude, cloud and haze.* The sky should either be free from cloud, or fully covered by high cloud. Assuming the use of a lens which does not accept light outside a cone of 48°, the sun should be between 30° and 50° above the horizon, but under very calm conditions the latter limits may be extended to 55°. With a low sun, illumination of the sea-bed is reduced (Poole & Atkins 1926; Powell & Clarke 1936; Sverdrup *et al.* 1942), whereas sun altitudes above about 50° were found to produce specular reflexion from small waves. This was of course more marked with wide-angle lenses; the F.24 8 in. lens has an acceptance angle of 48° compared with the 20 in. F.52 of 31°. A simple calculation shows that with the former lens and a sun altitude of 55°, specular reflexion will be recorded at the corner of the

negative if the inclination of the wave surface from the horizontal exceeds 5°, assuming no tilt on the aircraft. If it is necessary to take photographs under conditions likely to produce reflexion, the time of day should be chosen so that reflexion occurs on the opposite side of the photograph to the beach; that is, a beach facing east should be photographed in the morning rather than in the afternoon. Reflexion from one side of the photograph matters little in the case of beaches facing north or south.

Specular reflexion of the sun from waves does not, of course, occur when the sky is fully overcast, although the total diffuse reflexion from the sea surface may be increased (Atkins & Poole 1933). Broken clouds cast shadows which, if they fall on the target area, will introduce random errors in the brightness profiles. It is possible to obtain satisfactory photographs when there is broken cloud in the sky, but greater skill and patience are required of the pilot.

Haze should be at a minimum. It has been shown statistically that the visual range is greater in the afternoon than in the morning (Middleton 1941); afternoon sorties may therefore produce better photographs, but this is by no means a general rule.

(*b*) *Wind.* Apart from navigational difficulties a wind invariably reduces the value of the photograph by:

(i) Increasing the amplitude of waves on the sea surface and so distorting the brightness profile.

(ii) Stirring up particles from the sea-bed.

(iii) Causing local variations in the reflectivity of the sea surface (Atkins & Poole 1933; Poole & Atkins 1926), particularly if the beach is partly sheltered inshore, or is of configuration favourable to the production of surf.

Without exception, the best photographs for interpretation were taken on days of low or no wind at the sea surface, although useful results have on occasion been obtained from photographs taken with a 10–15 m.p.h. wind blowing off the land. Photographs should not, however, be taken immediately after a storm, even if the wind has dropped.

(*c*) *Tide.* It has been found that there is generally less local pollution in coastal water on an incoming tide; immediately after high tide pollution from harbours and beaches may be very marked.

It is easier to determine the waterline on a beach when the tide is coming in than when it is going out; this is important for fixing the absolute depth scales of a brightness profile. If a choice is possible, therefore, it is preferable for the photographs to be taken on an incoming tide.

Photographic technique

Cameras. Standard type R.A.F. cameras, models F.24 and F.52, were used for these trials. The lenses selected varied in focal length from 8 to 36 in., and each pair of cameras chosen for photography with red and green filters was matched as closely as possible for focal length. The maximum aperture varied from $f4$ to $f6{\cdot}3$. Both models have focal plane shutters and were fitted with the sensitometers described below.

The cameras were mounted in the aircraft with their optical axes parallel and the alinement checked by comparing the field covered by each camera on the resulting photographs. To ensure simultaneous photography the cameras were coupled to a single R.A.F. type 35 automatic control.

THE CALCULATOR

FOR USE ONLY WI
WRATTEN 27 (RED),
Bog

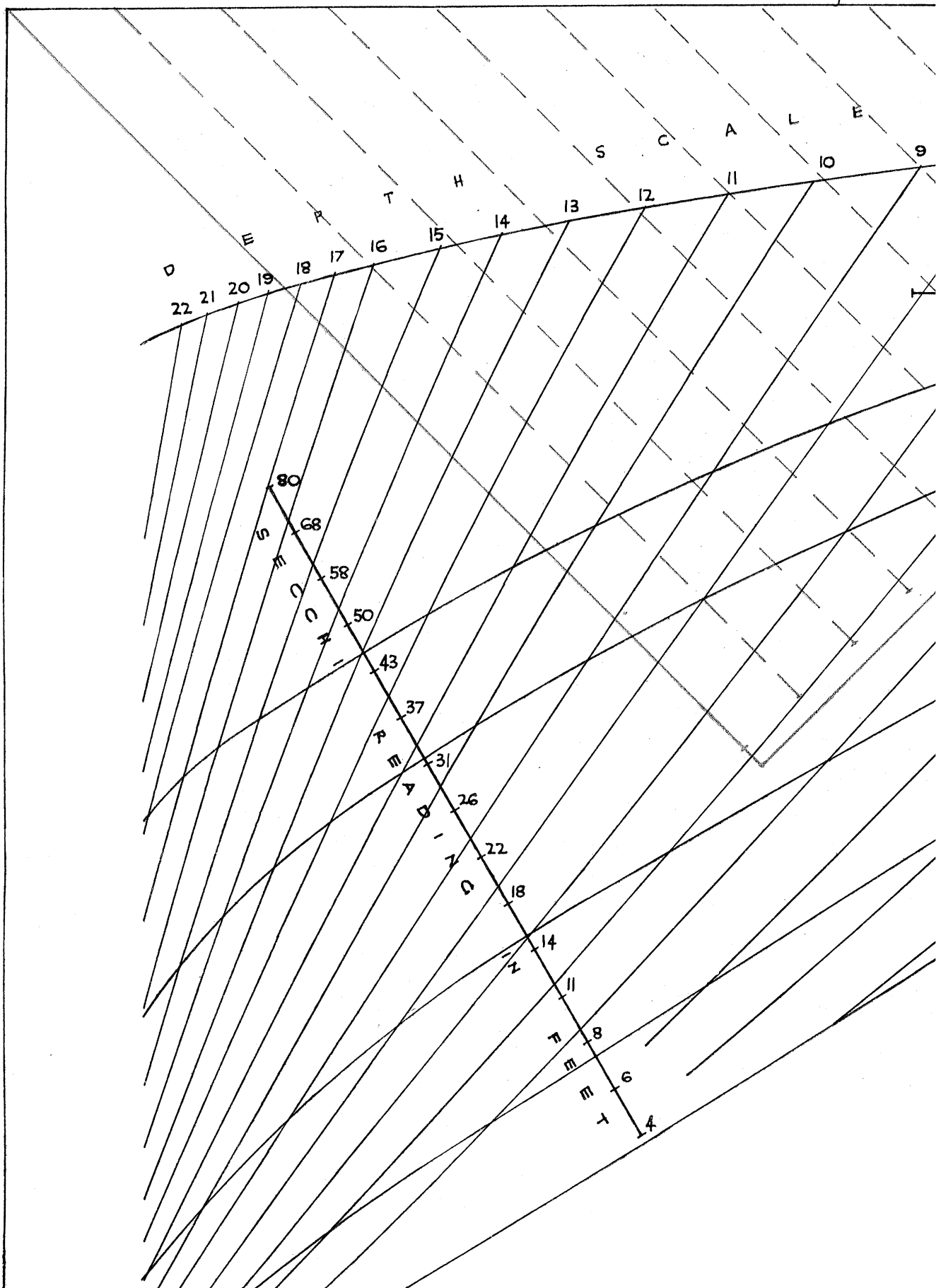

LY WITH BRIGHTNESS PROFILES OBTAINED WITH WRATTEN 56 (GREEN) FIL
RED), AND KODAK AERO SUPER XX PANCHROMATIC FILM.

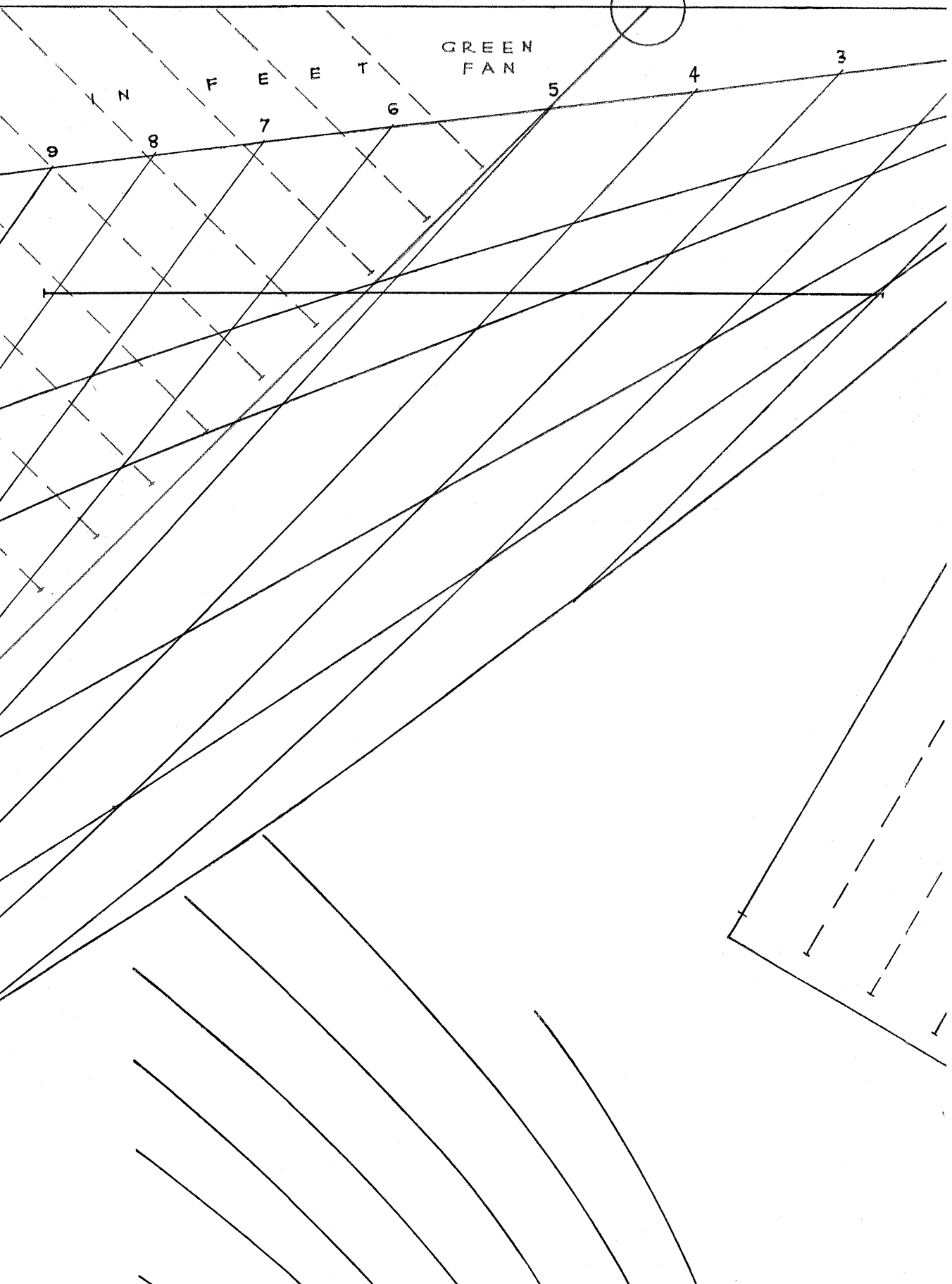

EN) FILTER,

FIGURE 17

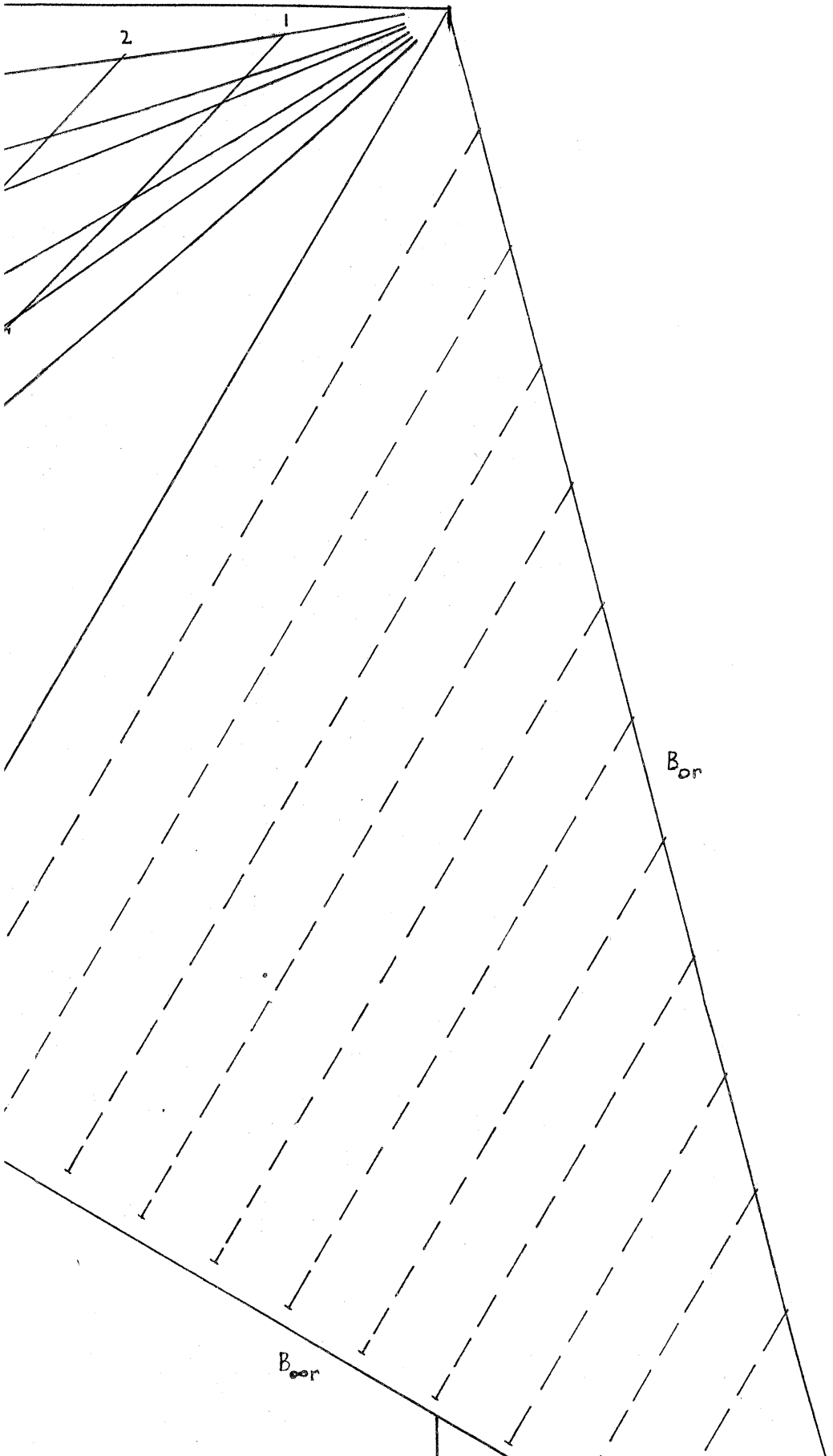

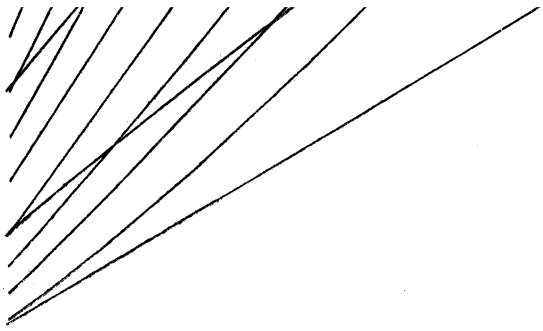

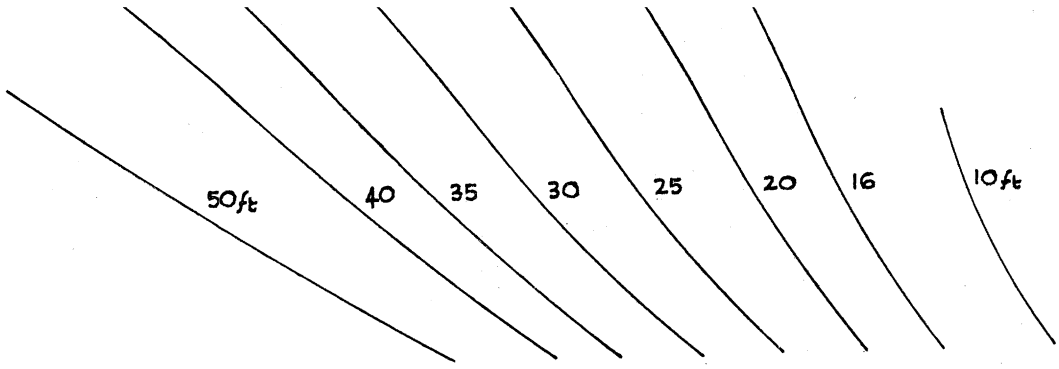
50ft
40
35
30
25
20
16
10ft

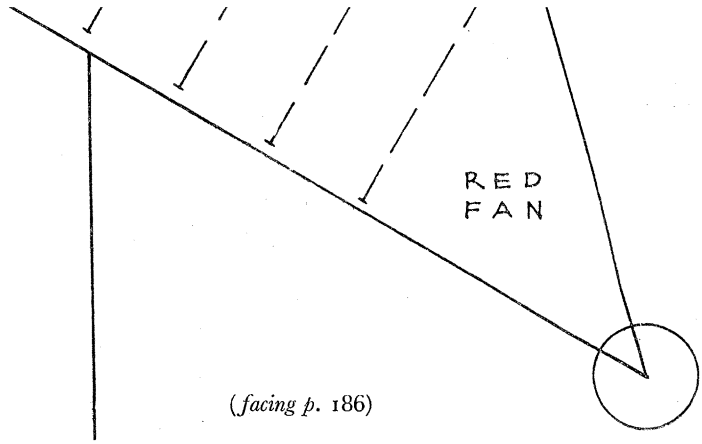

(*facing p.* 186)

This equipment was satisfactory except for the erratic behaviour of the focal plane shutters. The trials showed that for this work the following improvements in camera design were, however, desirable:

(*a*) A lens-shutter system with shutter speeds down to 1/100 sec., giving even illumination over the whole field, or at least uniformity of performance.

(*b*) A lens of the largest possible aperture (f6·3 is too small), whose focal length exceeds 8 in. and whose acceptance angle is under 48°.

Mounting the filters. For the present work the gelatine filters were placed between the lens components by unscrewing the rear element of the lens, and the cameras refocused on an optical bench; packing rings (shims) were used to rack out the lens of the infra-red camera until sharp definition was obtained on photographs.

For routine work the gelatine filters should be cemented between optical flats and mounted with suitable adaptors in front of the lens; this is essential in the tropics where fungus grows rapidly on an unmounted filter (Campbell 1944). Very high quality optical flats are required if good definition is to be maintained.

Chance's glass filters, suitably mounted for air cameras, were not available for this work; for tropical conditions they would be preferable to gelatine filters, but any variation in their spectral transmission characteristics from those of Wratten 27 and 56 would require to be taken into account and the calculator (figure 17) adjusted accordingly.

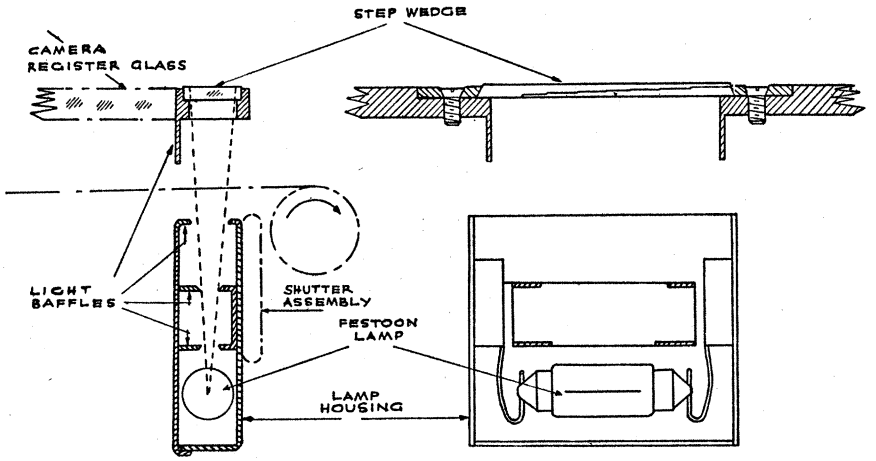

FIGURE 7. Diagram of sensitometer.

Sensitometric control on the cameras. A knowledge of absolute brightnesses is not required for this work, but an accurate measurement of relative brightnesses is essential. Since the relationship between the exposure given to a negative and the density produced after development is not linear, some form of sensitometric control is necessary.

A small sensitometer, consisting of a calibrated step wedge which was evenly illuminated along its length by an electric lamp on each operation of the shutter, was therefore fitted to each camera. The design, construction and calibration of these sensitometers was carried out by the Research Department of Kodak Ltd., Harrow, and excellent control was obtained by their use.

The principle of the design can be appreciated from figure 7, which shows the housing of the 'festoon' lamp and light baffles in position on the underside of the focal plane shutter, and the optical wedge mounted half-way along an inner side of the register glass of the camera

and thus in contact with the film. The lamp is energized from the shutter solenoid and illuminates the wedge through the slot in the shutter blind each time the camera is operated.

In the present design the optical wedge covers the density range 0–3·5 in eleven steps, the density interval between adjacent steps being rather greater at each end of the range than in the centre. The dimensions of the wedge were approximately 55×11 mm., this being the maximum length which could be evenly illuminated by the longitudinal filament of the standard festoon lamp. The individual steps were not reduced in size because of the danger of diffusion during the developing process. If more time had been available a continuous wedge with a scale might have been designed.

The wedge was calibrated photographically using a tungsten source corrected to daylight with a Davis and Gibson filter; it was found that, with a Wratten 15 (minus blue) filter placed over the wedge, the differences between the shapes of the characteristic curves obtained on Kodak Super XX aero film with Wratten 56 (green) and Wratten 27 (red) filters were negligible.

Each wedge was marked with a serial number in such a way that the number was reproduced photographically on the negative. Evenness of illumination was checked by density measurements on a piece of film exposed in the camera with no step wedge in position; if the lamp filament sagged, the illumination became uneven and the lamp had to be renewed. Examples of characteristic curves (Mees 1940) obtained with these sensitometers will be found in figure 10.

For certain of the earlier trials these sensitometers were not available, and some control was exercised by exposing the beginning and end of each roll of film to a gelatine step wedge mounted either on the camera register glass or on the pressure glass of a contact printer. This method was not satisfactory because significant development variations occurred along the length of the film. Although this fault may be overcome by modern Canadian Continuous Processing machines, it will still be desirable to have the wedge recorded on each individual print to enable the print tones to be interpreted.

Calibration of the lens and shutter. The necessity for calibrating each lens and shutter for evenness of illumination will be apparent from the templates in figure 8; the method used to prepare these templates is outlined below.

Calibration negatives were obtained by taking photographs when flying in dense cumulus cloud. Provided the clouds were sufficiently dense, very even illumination was ensured; other methods, such as ground photography of a white screen or air photography of deep sea through a diffusing filter, were less satisfactory, and required a special sortie.

After standard development the calibration negatives were measured on the densitometer at 1 in. intervals over their entire surface. The recorded densities were converted to log brightness values using the characteristic curves obtained from the sensitometer wedges on each negative. A correction template was then prepared on a piece of clear film to the exact size and scale of the negative frame, by drawing contour lines through points of equal log brightness. The contour of greatest log brightness was marked zero correction, the remaining contours being given a correction value numerically equal to the difference between their log brightness value and the log brightness value of the line marked zero.

In use the template is placed over the negative on a light table, and the correction to be added to the log brightness value of any point is read to 0·01 unit from the nearest contour,

or by interpolation between two contours. It will be noted that a boundary line has been drawn on the template at a distance of half an inch from the edges of the negative frame, to indicate that corrections close to the edge of the negative may be unreliable.

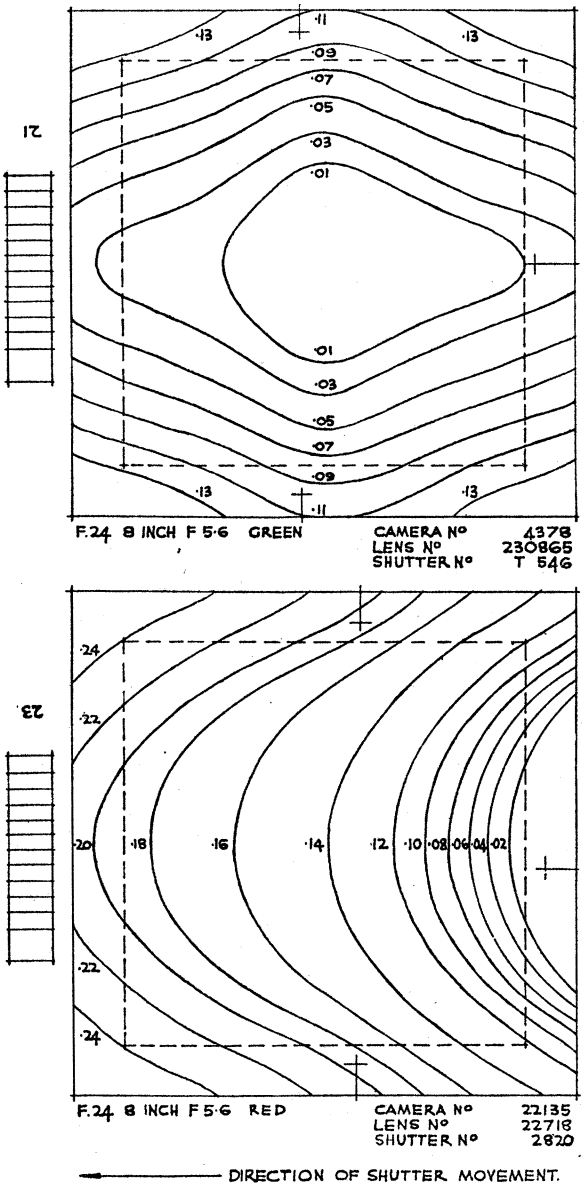

FIGURE 8. Lens shutter calibration templates.

Add these corrections to the log brightness values. Scale: 1 cm. = 0·5 in.

The contours of the template may vary widely in number, shape and spacing. If the shutter slot moved at an exactly uniform speed across the negative frame when the camera operated, the contours would represent only the lens performance and would be more or less concentric. With a well-maintained shutter, reliable measurements may be made along lines not parallel to the shutter slot, but the closer these lines are to the centre of the negative, the less will be the danger of errors due to variations in the shutter performance.

Processing. The cameras were loaded with fresh Kodak aero panchromatic film of the same batch number; after exposure, processing was carried out under standard R.A.F. conditions

using a continuous processing machine known to give nearly constant development along the full length of the film. Short lengths of 5 × 5 in. film were, however, processed in a small spiral unit designed to develop each portion of the negative simultaneously. The conditions of development were chosen to produce, as far as possible, even development to maximum contrast (Mees 1940).

Fixing and washing require to be very thorough to reduce the likelihood of the negatives changing during storage. The use of an alcohol bath to facilitate drying may produce 'bloom' on the negative if the initial bath is too strong; 'bloom' may be removed by re-washing, but the contrast of the negatives may thereby be reduced.

Planning a photographic sortie

Before the sortie a number of lines on which depths or beach gradients are required should be chosen and marked on the pilot's map. If normal air photographs are available, these should also be marked as it is easier to make final course corrections from marked prints than from a map. The chosen lines should, as far as possible, pass over homogeneous material; a projection of the line across the dry beach should intersect some easily recognizable feature. The ideal negative should consist of approximately one-quarter of dry land and three-quarters of water. This balance is impossible to maintain when flying along a sharply indented coastline; it is therefore advisable to fly from the sea into the beach at certain important points and to fly along the length of the beach to get economical coverage. With a focal plane shutter, the camera must be reorientated for each type of sortie, so that the shutter slot is approximately parallel to the required profile.

The time of day at which the photographs are to be taken will be decided after consideration of the light, wind and tide effects discussed previously.

Flying height is determined by the focal length of the cameras used, since the limits of scale for the photographs are 1/7000–1/10,000. A scale of 1/8000 is probably ideal, since a larger scale, apart from giving insufficient cover, may show too much wave detail, and a smaller scale causes errors due to less accurate location of points whose densities are being compared on the red and green negatives. The accuracy obtainable at 1/8000 may be double that which is possible at 1/10,000.

The maximum depth likely to be obtained in any area is indicated by the white Secchi disk reading of the water; if the area is accessible Secchi disk readings should therefore be taken (part III) to ensure that the results will be of value. The Hydrographic Section of the Admiralty Oceanographic Department can also provide charts showing Secchi readings, but the areas covered in detail by these charts are at present limited.

Methods of interpretation of the photographs

Three methods of interpretation were studied:

(*a*) Visual examination of prints without measurements.

(*b*) Construction of brightness profiles from density measurements on the original negatives.

(*c*) Construction of brightness profiles from comparative tone measurements on specially prepared prints.

Visual examination of prints. The prints may be made by contact printing on to a normal grade of printing paper; the printing exposure should be so adjusted that neutral coloured objects above the waterline are slightly under-exposed and of approximately equal tone on the 'green' and 'red' prints.

Two prints should be prepared from each infra-red negative:

(*a*) One normal print recording the maximum detail on the land; on this print the water will be completely black and the exact waterline will be sharply silhouetted against the beach.

(*b*) One very under-exposed print, showing almost no land detail but the maximum detail under the water.

Examples of such prints are shown in this paper, but allowance must be made for unavoidable loss of contrast in the reproduction. These prints have been annotated with depths (in ft.) determined by ground survey.

The following general points will be noted:

(*a*) The 'green' prints show underwater detail to the greatest depth; under favourable conditions detail might be visible at 50 ft. or more.

(*b*) The 'red' prints emphasize the configuration of the shallow areas (plates 7–8) and enable estimates of relative depths to be made in shallow water. Detail is never likely to be visible below 20 ft.

(*c*) The change in tone and in sharpness of outline of the rocks as the water becomes deeper gives an indication of the clarity of the water.

(*d*) Infra-red prints can be used to show either the exact position of the waterline (plate 9) or to assess the depth of very shallow water (plate 10). On these prints seaweed on or just below the surface is very evident because of its high reflectivity for very deep red light (Clarke 1939), causing a contrast against the dark background of the water (plate 13).

It is unfortunate that space does not permit the reproduction of many photographs which have been obtained showing, for instance, submerged pollution in coastal water, seaweed beds in Scotland, the Scilly Isles and the Mediterranean, the effect of headlands on the clarity of coastal water, the underwater configuration of certain Cornish beaches as a result of wave action; nor is it possible to reproduce the many photographs illustrating changes in visibility of the sea-bed under various meteorological and sea conditions. An album of such photographs will be available in the Library of the Royal Society.

Construction of brightness profiles from density measurements on the original negatives. The procedure adopted throughout this work was as follows:

A pair of 'green' and 'red' negatives, free from the defects already discussed, was scaled either by comparison with a reliable map or from focal length and flying height data. The selected profile, parallel if possible to the sensitometer wedge and shutter slot, was then marked on the 'green' negative by a series of needle holes, the interval between holes being least where the density change was most marked.

If the object of the interpretation was to determine beach gradients rather than absolute depths, the horizontal distance of each needle hole from a common point of origin on the line was then measured using a lens and a transparent millimetre scale.

If absolute depths on the photograph were required, it was necessary, in addition, to estimate the position of the waterline, which was defined as the position of the water edge

had the sea surface been dead calm. A needle hole was made at the point of intersection of the waterline and the profile and the horizontal distance of this point from the others recorded. Generally, the waterline will not coincide with the water edge shown on the photograph but will be above or below it according to the wave formation on the beach. The water edge may readily be identified from an infra-red photograph; if the waves are small, the approximate position of the waterline may be taken as midway between the water edge and the line left by the preceding wave on the beach. If the waves are large the waterline and therefore absolute depths will not be determinable, and all depths will therefore have to be recorded as absolute depths below the unknown depth of a chosen point on the profile.

From the above data and the known scale of the photographs the horizontal axis of the brightness profile can be constructed, based either on the distance of each point from the waterline, or from the chosen point of unknown depth, or from a selected point of origin above high-water mark. The last is convenient if it is desired to compare brightness profiles taken at various stages of the tide. It is not necessary for exactly corresponding points to be selected on the red and green negative, but the positions of the waterline or other point of origin must be identical. The precise orientation of the profile on each negative is also important, as the direction of slope of the beach may not be parallel to the profile.

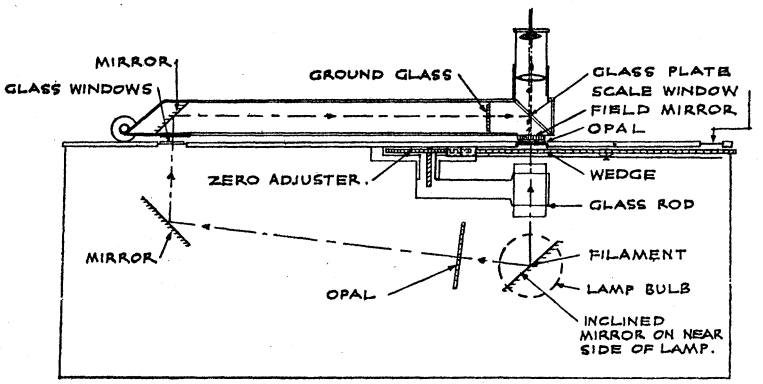

FIGURE 9. Diagram of densitometer.

The relative photographic density of each selected point, and of each step on the sensitometer wedge, was then determined in a darkened room on a modified Capstaff Purdy* density comparator (Kodak, Ltd. 1937; Mees 1940). This instrument (figure 9) was mounted so that density measurements could be made rapidly at any point over the surface of a continuous roll of several hundred 9×9 in. negatives; readings could be estimated to 0·01 over the density range 0·0–3·0.

To make a reading, the needle holes were first located in the eyepiece and then moved until just outside the field of view. This movement corresponded to a lateral shift along the

* There is no doubt that a suitable recording photoelectric densitometer would be preferable both by eliminating the personal factor and by making possible continuous measurements along the whole of the selected line. But for service use the Capstaff Purdy comparator was adopted because of its robust construction and easy maintenance in the field. It will be shown in part III, however, that a considerable increase in accuracy is warranted when determining the rate of curvature of the brightness profile, but because of the limitations imposed by unavoidable variations in the emulsion coating of the negative it is unlikely that density differences of less than 0·005 have any real significance.

beach of 3 ft. on photographs of scale 1/7500. The density of each point was recorded as the mean of two readings.

The same observer then read the relative density of each step on the sensitometer wedge at the side of the negative; these readings were made on three lines parallel to the length of the wedge. The characteristic curve was then constructed by plotting the step density readings against the log exposure values known for each step from the sensitometer calibration data. The speed of the film, the working range of densities employed, and the completion of development, were then checked from the shape and position of the characteristic curve, γ values (slopes of the characteristic curves) of about 1·6 being normal for this type of Kodak film. As the exposure normally used was 1/250 sec. at $f4$, or 1/210 at $f5{\cdot}6$, the values of $\log B_0$ and $\log B_\infty$ lay on the 'straight' portion of the characteristic curve where contrast is at a maximum.

From the characteristic curve, the densities of the points on the selected line were converted to log exposure (or log relative brightness) values and were then adjusted for variations in performance of the lens and shutter using the appropriate lens-shutter-aperture template. From these corrected log brightness values, relative brightness values were calculated and plotted on the vertical scale of the brightness profile.

After constructing the brightness profiles in this way, it was frequently necessary to measure additional points on the selected line in order to define more clearly the rate of curvature of a certain portion of a profile or to assist in the removal from the profile of the effects of waves and swell. Depths and extinction coefficients were then determined from the pair of green and red profiles using the calculator (figure 17).

This method of interpretation is more accurate than interpretation using prints, but a whole day is required by one worker to analyse a pair of red and green negatives. Results can be obtained more rapidly and without sacrifice in accuracy if the work is divided between a team of three, one specializing in the selection, marking and scaling of points, one operating the densitometer, and one plotting the various results and completing the predictions on the calculator; about three pairs of negatives can be interpreted in one day by such a team.

Construction of brightness profiles from comparative tone measurements. The method described below enables measurements to be made from prints without the use of a densitometer. This reduces the time taken in measuring one beach section to about half that required for the analysis from negatives. On the other hand, the accuracy is considerably less; in some cases an accuracy of $\pm 10\,\%$ may be obtainable to a depth of 10–15 ft. No corrections are made either for variations in the performance of the lens and shutter or for slightly uneven illumination of the negative during printing; the application of such corrections would so complicate the procedure that any advantage obtained by using prints rather than negatives would be lost. In what follows, therefore, it will be assumed that the prints are made under optimum conditions, and that the profile lies close to the centre of the photograph and parallel to the shutter slot.

Each print will have at one side a reproduction of the sensitometer step wedge, the relative brightness relationships of which are known from the sensitometer calibration data. The relative brightness of any point on the profile whose tone exactly matches the tone of a wedge step is therefore known, and so a brightness profile may be constructed provided a sufficient number of wedge steps have tones lying within the tone range of the profile. The

wedge can simply be cut off the print and adjusted over the line of points until the required matches are obtained.

Unfortunately, however, this procedure does not give a sufficient number of readings to permit the construction of a brightness profile. The reason for this is that the range of densities which can be reproduced on the print is small compared with the density range of the negative, and therefore only about four of the steps of the wedge are reproduced, even when a soft grade of printing paper is used. Some means of interpolating between the tones of each step on the print is therefore required.

For this purpose, paper comparators were made, consisting of strips printed photographically in steps with smaller tone differences. Each strip covered the reflexion density range 0·0–1·7 in twenty-four steps, the dimensions of each step being about 15 × 15 mm.; the strips were prepared to this specification by the Kodak Research Laboratory. A small round hole of 2 mm. diameter was stamped in the centre of each step and the appropriate reflexion density was written against it. A comparison curve was then constructed for each print, by plotting the known relative brightness value of a given sensitometer step against its reflexion density as determined with the paper comparator. Comparison curves for a number of prints were plotted on one graph so that their forms could be compared and any unlikely points remeasured.

The procedure for determining the tone of points on the profile was then as follows: the line was accurately marked on the print with a very fine hard pencil, and the intersection of the waterline recorded by a needle prick. The interpreter sat with his back to the light, facing a dark corner of the room, so that practically no light was transmitted through the print; holding the print vertically in his left hand, he moved the comparator strip up and down the line until an exact match was obtained through the centre of the hole on a given step. The centre of the hole was marked with a needle prick.

The procedure was then repeated using other holes on the comparator strip until matches had been obtained at a sufficient number of points for a brightness profile to be constructed. The relative brightness of each point was determined from the appropriate comparison curve and plotted against the horizontal distance from the waterline. It was found that tone measurements for the upper half of the brightness profile could best be made from a print on which the reflexion density at the water edge was about 0·2, the lower half being completed from a second print of the same negative on which the reflexion density of the deep sea did not exceed 1·2. Small pieces of exposed printing paper of these reflexion densities were used as controls when preparing the two prints. With practice, the two halves of the brightness profile could be made to overlap quite accurately, and by subsequent use of the calculator (figure 17), depths down to 10 or 15 ft. could be determined and the clarity of the water estimated.

Methods used for checking depths and extinction coefficients

Three types of measurement were made on the ground as a check on the depths and extinction coefficients calculated from the photographs:

(*a*) Ground survey.

(*b*) Secchi disk readings.

(*c*) Measurements with a Pulfrich photometer.

(*a*) *Surveying beach gradients.* The selected line was marked on the beach with banderoles and flags, and had its point of origin at some object which could be clearly defined in three dimensions. The beach gradients from this point of origin to the low-water line were determined at 20 ft. horizontal intervals with a surveyor's level. At half-tide, soundings were made from a small boat over a portion of the same line, thus securing overlapping readings, and on a continuation of this line seawards to depths up to 70 ft. The sounding line was calibrated when wet, and precautions were taken to minimize errors due to drift both of the boat and of the sounding line.

The direction of the boat at each sounding was observed from the shore by two artillery directors on a wide base, and its position obtained by intersection to an accuracy of ± 5 ft. Three or four complete series of soundings were made on each line. Corrections for rise or fall of the tide during any one run of soundings were made by recording the horizontal position of the water edge at frequent intervals and determining the corresponding changes in mean water-level from the accurate beach gradients which had already been obtained above low-water mark. This method of applying corrections was found to give more reproducible results than could be obtained by use of standard tide tables. No attempt was made to take soundings unless the sea was very calm. Since these conditions were also most favourable for photography, no difficulty was experienced in synchronizing the two, and thus errors due to changes in the beach profile caused by storms are believed to have been avoided. A variety of beach gradients was encountered; the most difficult beaches proved to be those in which the direction of slope was at a considerable angle to the survey line.

(*b*) *Secchi disk readings.* Secchi disk readings were taken from the sounding boat at every opportunity, as little extra labour was involved and it was considered that interesting results might be obtained. Following conventional practice, the disks were about 25 cm. in diameter and were lowered on the shady side of the boat, the mean of the depths at which they just disappeared and reappeared being recorded. Readings were taken using white, blue, green, red and black disks of known spectral reflectivity, the disks being painted and measured for this purpose by the Paint Research Station, Teddington. The disks were also observed through various filters. The results are of undoubted interest but their interpretation is difficult. The following general conclusions were, however, drawn; the experimental results are recorded in part III:

(i) The Secchi disk readings were sufficiently reproducible to give a good guide to the clarity of the water provided the water was fairly clear. Any empirical relation between Secchi reading and extinction coefficient which may hold in clearer water was liable to break down in turbid water (Secchi reading less than about 10 ft.). The same Secchi reading (6 ft.) was obtained, for instance, in waters which in the Pulfrich photometer gave widely differing extinction coefficients.

(ii) The Secchi reading with a white disk has no meaning if the disk is close to the bottom; a simple relation, however, exists between the readings obtained with a white and a black disk, in any type of water, the former being approximately twice the latter. In rather shallow water therefore the Secchi reading which would have been obtained with a white disk could be estimated from the reading actually obtained with a black disk, provided that the black disk itself was not too close to the bottom.

(iii) A similar linear relation was found to apply over a wide range between the readings taken with a blue and the readings taken with a red disk (part III). As this relation is not of the form of the probable relationship between the two extinction coefficients, it would appear that the extinction coefficient for a given 'colour' cannot empirically be deduced from the standard Secchi readings given by a disk of that colour. Observations of disks through red and green filters gave similar results (figure 16).

(iv) Atkins suggested privately to the author that the Secchi disks normally used are too small, having regard to Helmholtz's values for the variation of the discrimination coefficient of the eye as the angular dimension of an object changes; this, coupled with the fact that the discrimination factor may vary with both intensity and with wave-length, makes it very difficult to interpret Secchi readings taken with coloured disks, although the readings were extremely consistent amongst themselves. It is unfortunate that a full study of these matters does not exist, as the Secchi reading, despite its difficulty of interpretation (Le Grand 1939), has the great advantage of simplicity and reproducibility.

When the experimental work to be described in part III was being planned, it had been hoped that Secchi disk readings would at least serve to emphasize any irregularities in the various water types. The results with coloured disks were inconclusive. The readings with white or black disks were probably reliable indications of water clarity provided the disk was sufficiently large, the water deep, and the reading not less than about 10 ft. for the white disk or 5 ft. for the black.

(*c*) *Measurement of extinction coefficients in the Pulfrich photometer.* These determinations were made in 1 m. blackened tubes on samples taken at various depths on the profile. The operation of the cameras in the aircraft was synchronized with the sampling by wireless. The samples were measured immediately on board the launch, using a range of narrow cut filters and carefully prepared distilled water as control. Two main conclusions were drawn, of special interest in the present work:

(i) Over the wave-length range covered by the selected red and green filters, the extinction coefficients determined in the Pulfrich photometer varied inversely as about the first power of the wave-length. There was no indication, in a total of forty-seven samples from eight different localities, of third or fourth power variations. Minor irregularities were detected and were ascribable to impurities, but their magnitude was too small to affect the above conclusion.

(ii) The absolute values of the extinction coefficients given by the Pulfrich photometer were higher but of the same order as those calculated from simultaneous air photographs. Exact agreement by two entirely different methods was not to be expected, particularly as the former method measures the extinction coefficient of a sample taken from a given point at a given depth, whereas the latter method measures a mean value over a series of vertical columns of water. Further work of this type is, however, desirable (part III).

A comparison of all available results will be found in part III. It is not intended in the present paper to discuss the technique used, as this will be fully described in a forthcoming paper by Dr L. H. N. Cooper of the Marine Biological Station, Plymouth, who carried out the measurements.

PART III

An analysis of the results obtained between September 1944 and October 1945

Experimental results obtained by the analysis of air photographs, selected from some 10,000 negatives, are presented under the following headings:

(*a*) An example of the production and interpretation of a pair of green and red brightness profiles constructed from negatives.

(*b*) Examples of the determination of mean extinction coefficients from brightness profiles.

(*c*) A summary and comparison of observed extinction coefficients.

(*d*) Examples of beach gradients derived from brightness profiles.

(*e*) An interpretation from prints using the paper comparator.

(*f*) Analysis of Secchi disk readings.

The method described in this paper for the determination of the depths and extinction coefficients of shallow water is then compared with existing methods, and its advantages and limitations deduced on the evidence of the above results; some possible scientific and industrial applications are suggested.

An example of the production and interpretation of a pair of green and red brightness profiles constructed from negatives

The object of this example is to illustrate the various stages in the calculation of the depth of water at selected points on a sandy beach. The photographs used are shown on plates 11–12. Table 5 shows a form of record sheet used for this work. It will be noted that all the relevant information from the pilot's log book and the maker's calibration data for the sensitometers have been entered at the top of the form. The infra-red negative was only used for determining the waterline and no measurements were made on it.

The selected green and red negatives were scaled by comparison with an accurate map and checked from flying height and focal length data. A line approximately at right angles to the water edge and running centrally across the green negative, parallel to the longer dimension of the sensitometer (and therefore to the shutter slot), was chosen and a series of fine needle holes was made along its length. Each hole has been given a serial number in column 1 of the table. From the known scale of the negative, the distance in feet of each hole from the waterline was determined and entered in column 2.

The mean of three density determinations on each step of the sensitometer wedge was entered against the appropriate step number in that portion of the table marked 'Green sensitometer'. From these measurements the characteristic curve for the green negative was drawn and is shown in figure 10. The density adjacent to each hole on the line was then measured and recorded in column 3.

These densities were then converted to relative log brightness values using the characteristic curve, and entered in column 4. The appropriate lens shutter calibration template for this camera was placed over the negative, and the corrections to be applied to each point were added to the values in column 4, and the resulting relative log brightness values recorded in column 5. The relative brightness values for each point were determined using four-figure logarithm tables and entered in column 6.

TABLE 5. RECORD SHEET FOR NEGATIVES 975

place	Porthscatho, Cornwall.
height	5000 ft.
light	sun altitude 48°, no cloud, slight haze.
sea	calm, no surf; 87 min. after high water.
beach	yellow sand.

green sensitometer number 21 gamma produced 1·65

step number	1	2	3	4	5	6	7	8	9
log exposure	3·45	3·12	2·83	2·54	2·26	1·97	1·71	1·43	1·13
mean density reading	3+	2·97	2·68	2·35	1·95	1·51	1·03	0·55	0·26

green negative

point number (1)	distance from waterline (ft.) (2)	density (3)	log B_g (4)	log B_g corrected by template (5)	B_g (6)
1	0	—	—	—	—
2	45	1·96	2·25	2·29	195·0
3	101	1·91	2·215	2·245	175·8
4	116	1·87	2·195	2·225	167·9
5	140	1·83	2·17	2·19	154·9
6	166	1·81	2·16	2·18	151·4
7	182	1·80	2·15	2·17	147·9
8	203	1·79	2·145	2·165	146·2
9	223	1·77	2·13	2·15	141·3
10	247	1·73	2·10	2·12	131·8
11	274	1·68	2·07	2·09	123·0
12	321	1·64	2·045	2·065	116·1
13	330	1·63	2·035	2·055	113·5
14	379	1·57	2·00	2·02	104·7
15	409	1·53	1·985	2·005	101·2
16	426	1·52	1·975	1·995	98·9
17	457	1·48	1·95	1·97	93·3
18	489	1·45	1·93	1·95	89·1
19	529	1·41	1·91	1·93	85·1
20	555	1·39	1·90	1·91	81·3
21	589	1·38	1·895	1·905	80·3
22	619	1·37	1·89	1·90	79·4
23	650	1·36	1·885	1·885	76·7
24	678	1·35	1·88	1·88	75·9
25	722	1·34	1·875	1·875	75·0
26	750	1·33	1·87	1·87	74·1
27	795	1·32	1·865	1·865	73·3
28	835	1·30	1·855	1·855	71·6
29	940	1·27	1·84	1·84	69·2

sortie number	28.
date/time	3 August 1945, 1420 G.M.T.
scale	1/7500.
exposure	1/250 sec. f 5·6.
focal length	8 in.

red sensitometer number 23 gamma produced 1·90

step number	1	2	3	4	5	6	7	8	9
log exposure	3·45	3·12	2·83	2·54	2·26	1·97	1·71	1·43	1·13
mean density reading	3+	3+	3+	2·87	2·43	1·97	1·44	0·83	0·38

red negative

point number (7)	distance from waterline (ft.) (8)	density (9)	log B_r (10)	log B_r corrected by template (11)	B_r (12)
1	0	—	—	—	—
2	24	2·17	2·09	2·11	128·8
3	51	2·11	2·055	2·075	118·9
4	67	2·00	1·995	2·015	103·5
5	86	1·86	1·92	1·94	87·1
6	109	1·77	1·88	1·90	79·4
7	127	1·64	1·815	1·825	66·8
8	148	1·59	1·79	1·80	63·1
9	180	1·45	1·72	1·73	53·7
10	191	1·44	1·71	1·72	52·5
11	208	1·34	1·67	1·68	47·9
12	221	1·30	1·65	1·66	45·7
13	234	1·27	1·64	1·65	44·7
14	255	1·17	1·59	1·60	39·8
15	300	1·10	1·565	1·575	37·6
16	322	1·08	1·555	1·565	36·7
17	378	0·95	1·51	1·52	33·1
18	408	0·93	1·48	1·49	30·9
19	428	0·90	1·465	1·475	29·8
20	460	0·86	1·44	1·45	28·2
21	523	0·81	1·415	1·425	26·6
22	575	0·79	1·410	1·420	26·3
23	622	0·77	1·395	1·405	25·4
24	688	0·75	1·39	1·39	24·5
25	758	0·74	1·38	1·38	24·0

The green brightness profile shown in figure 10 was then constructed from the data in columns 2 and 6. A smooth curve was drawn through these points, allowing for the slight wave motion visible in the upper half of the brightness profile.

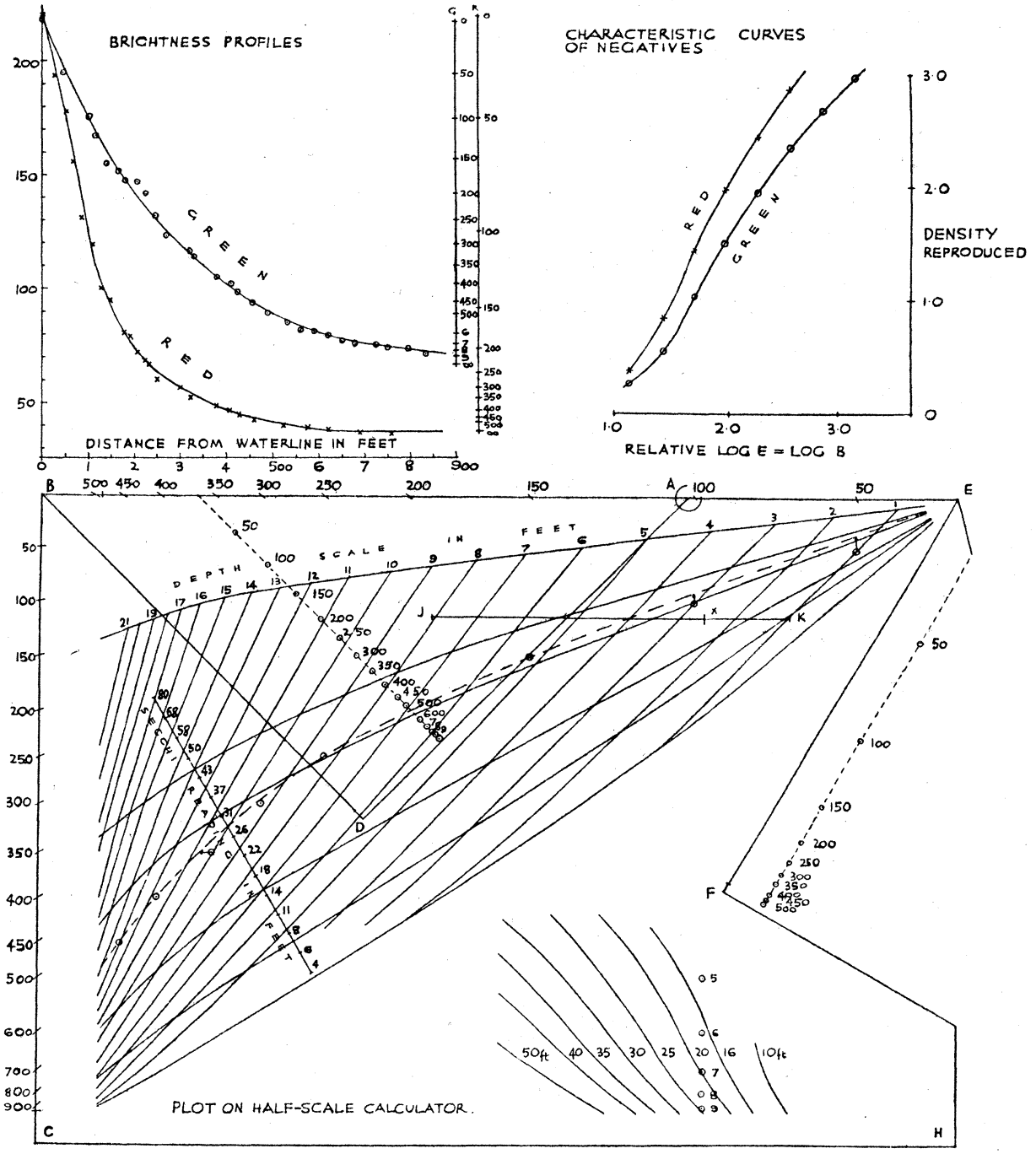

FIGURE 10. Complete analysis of a pair of brightness profiles.

The procedure was then repeated for the red negative; no attempt was made to choose exactly corresponding points, but the orientation of the chosen line and the position of the waterline were of course identical on the two negatives. The measurements on the red negative were entered in columns 7–12, from which the red brightness profile in figure 10

was constructed. (The scales of the two brightness profiles have been adjusted for convenience of reproduction.)

On the vertical scale (figure 10, column *G*) the brightness values were marked from the green profile for all points between B_0 and B_∞ at 50 or 100 ft. intervals from the waterline. This column was placed over the green fan so that it was parallel with the guide lines, and B_0 and B_∞ lay on the sides of the fan.

The position of each point was marked on the green fan, as shown in the half-scale calculator in figure 10. Through these points fine lines were drawn from point *A* on the calculator to give intercepts on the ordinate *BC*.

The procedure was repeated for column *R* on the red fan, giving a set of intercepts on the line *BE*.

Perpendiculars from corresponding intercepts on *BC* and *BE* were then erected, and a smooth curve drawn through their points of intersection. It will be seen that the smooth curve follows one of the water-type lines closely and crosses the Secchi scale at a reading of about 27 ft. At a depth of about 14 ft., however, the curve reaches the limit of the shallow portion of the calculator, because the limiting sensitivity of the red brightness profile has then been reached. To estimate depths greater than this, the set of deeper water curves on the calculator was used as follows:

The position of the smooth curve, at 14 ft., indicates that at still greater depths the water was approaching a type which would have intersected the index line *JK* at about the point marked *X*. A perpendicular from *X* on to the line *CH* was therefore drawn to represent the water type below 14 ft., and the position of the remaining intercepts on *BC* were plotted on it; the depths of these points were then read from the set of deeper water curves on the calculator.

In table 6 the depths obtained in this way are compared with those given by ground survey and soundings; at 24 ft. depth the error does not exceed 1 ft.

TABLE 6. COMPARISON OF RESULTS

distance from waterline (ft.)	depth predicted by calculator (ft.)	depth determined by ground survey (ft.)	error in predicted depths (ft.)
0	—	—	—
50	1·3	1·8	−0·5
100	3·2	3·7	−0·5
150	5·2	5·4	−0·2
200	7·0	7·2	−0·2
250	8·4	8·8	−0·4
300	9·4	9·7	−0·3
350	10·6	10·7	−0·1
400	11·8	12·0	−0·2
450	13·2	13·6	−0·4
500	14·0	14·2	−0·2
600	17·0	17·1	−0·1
700	19·6	19·1	+0·5
800	22·3	21·5	+0·8
900	24·5	23·8	+0·7

In this example the limiting depth of 24 ft. obtainable from the green negative was obviously set by the extinction coefficient of the sea water. A separate analysis of extinction

coefficients by method 2 (described in part I of this paper) gave the following values over the depth range 4–18 ft.:

extinction coefficients	$(\alpha+\beta)$ ft.$^{-1}$ $\log_{10}$	$(\alpha+\beta)_m$ m.$^{-1}$ $\log_e$
green profile	0·0235	0·318
red profile	0·0525	0·71

Examples of the determination of mean extinction coefficients from brightness profiles

Mean extinction coefficients were obtained using method 2 as follows:

Green and red brightness profiles were constructed by plotting observed brightness values against depths determined by survey, and values of the functions $(B_{t_1}-B_{t_2})/(B_{t_1}-B_{t_3})$ were calculated from the smooth curves for selected depths t_1, t_2 and t_3. Corresponding values of $2(\alpha+\beta)\,t$ were read from theoretical sets of curves based on equation (6); the green and red extinction coefficients were then determined from the slopes of the straight lines obtained by plotting these values of $2(\alpha+\beta)\,t$ against known depths. As a check, theoretical brightness profiles based on these calculated extinction coefficients were superimposed on the observed brightness profiles.

The examples in figure 11 show:

(*a*) Observed green and red brightness values plotted against survey depths.

(*b*) Calculated values of $2(\alpha+\beta)\,t$ plotted against survey depths.

(*c*) Theoretical brightness profiles superimposed on the observed brightness values.

It will be seen that the agreement between the observed and theoretical values is excellent despite the presence of some wave motion. Two of the examples include an additional blue brightness profile analysed by the same procedure. The relative effect of haze and scattering on these profiles may be judged by comparing the green and blue values of B_∞, as the brightness scales have been adjusted to make the relative B_0 values approximately equal.

A considerable number of extinction coefficients have been calculated by this procedure; the results are examined below.

A summary and comparison of observed extinction coefficients

Extinction coefficients calculated from brightness profiles have been:

(*a*) Analysed for variation with wave-length.

(*b*) Compared with values obtained on the same water using the Pulfrich photometer.

The extinction coefficients were calculated by method 2, and have been arranged in table 7 in order of decreasing sun altitude. Only a few blue profiles were analysed, since generally the contrast on the blue negatives had been greatly reduced by haze.

The following points may be noted:

(*a*) The accuracy of the determinations is known to depend primarily on the contrast of the negatives and on the absence of wave motion on the brightness profiles. In the last column of table 7 the estimated accuracy of each pair of green and red coefficients has been recorded. The *relative* errors in the green and red coefficients are less than those indicated because faults due to wave motion or incorrect choice of the water line are common to both profiles.

(*b*) The sun altitude, amount of cloud, or the state of the tide may affect the extinction coefficients, but there is no evidence of this in table 7.

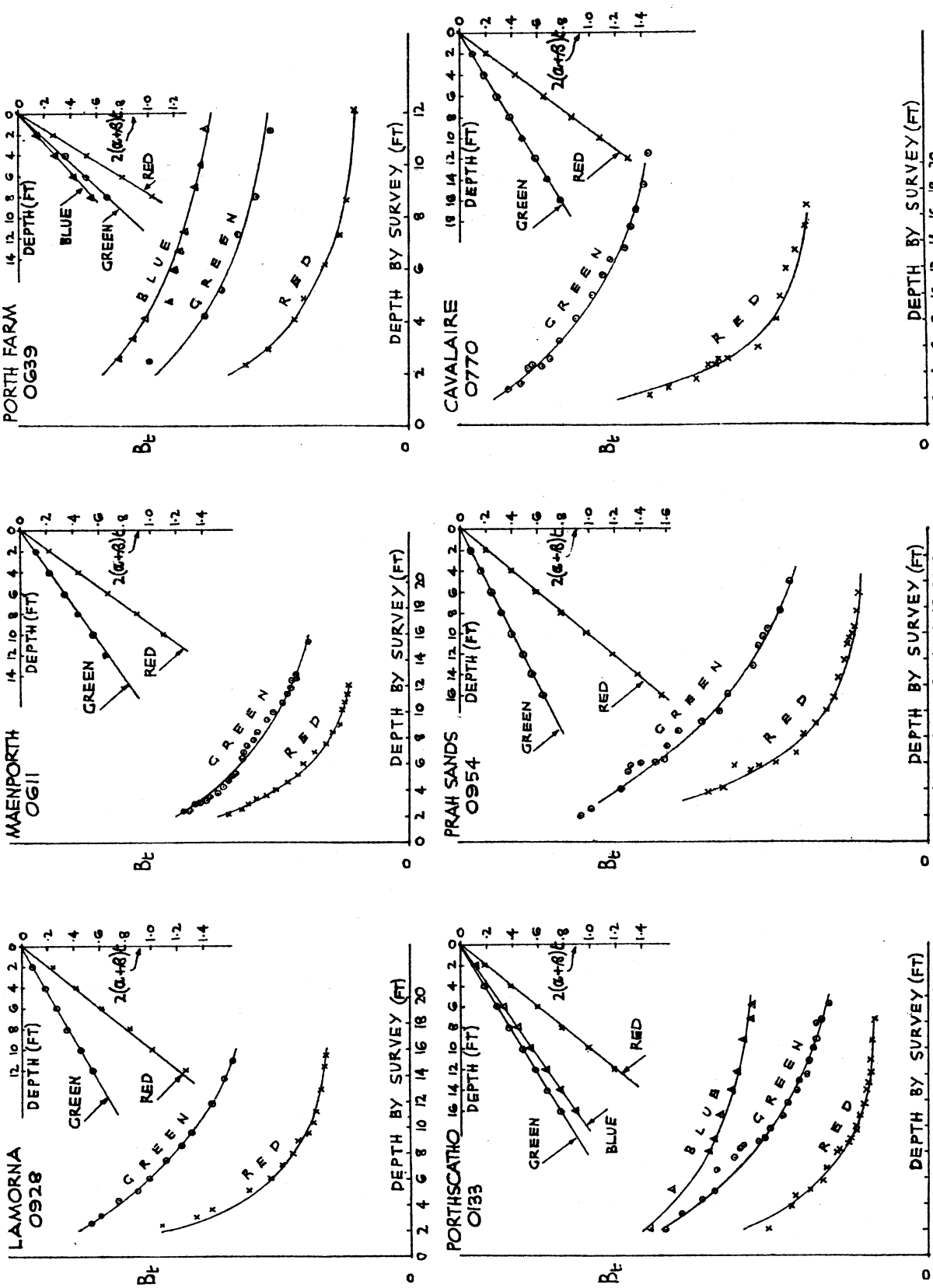

FIGURE 11. Determination of extinction coefficients.

All points on the above graphs were determined from density measurements on negatives. The smooth curves were calculated from extinction coefficients given by the slope of the straight lines shown in the top right-hand corner of each graph.

TABLE 7. SUMMARY OF EXTINCTION COEFFICIENTS

negative number	date and time (G.M.T.)	place: (1) = near Falmouth (2) = near Penzance (3) = south of France (4) = Mull of Kintyre, Scotland	sun altitude degrees above horizon	cloud in tenths	tide, min. before (−) or after (+) high water	depth range (ft.) over which $(\alpha+\beta)$ was calculated	mean extinction coefficients $(\alpha+\beta)$ per ft. blue	green	red	estimated accuracy ±
0639	24 July 1018	Porth Farm (1)	53	7	+350	2–12	0·034	0·042	0·066	0·004
1170	3 Aug. 1107	Porth Farm (1)	53	0	−106	4–22	—	0·024	0·054	0·004
1160	3 Aug. 1021	Maenporth (1)	50	0	−152	4–14	—	0·029	0·059	0·003
1154	3 Aug. 1013	Swanpool East (1)	50	0	−160	3–13	—	0·040	0·068	0·005
1155	3 Aug. 1015	Swanpool West (1)	50	0	−148	10–20	—	0·026	0·057	0·004
1134	3 Aug. 0950	Porth Farm (1)	47	0	−183	7–21	—	0·023	0·052	0·005
1057	4 Aug. 0954	Swanpool East (1)	47	0	−255	3–17	0·045	0·041	0·069	0·003
0900	2 Aug. 1444	Porthscatho (1)	46	1	+194	2–12	—	0·026	0·055	0·003
0975	3 Aug. 1420	Porthscatho (1)	46	0	+ 87	4–24	0·024	0·024	0·053	0·003
0976	3 Aug. 1421	Porthscatho (1)	46	0	+ 90	2–12	—	0·027	0·056	0·003
0979	3 Aug. 1423	Porthscatho (1)	46	0	+ 95	2–16	—	0·021	0·051	0·003
1053	4 Aug. 0847	Porthscatho (1)	46	0	−272	2–12	—	0·025	0·054	0·003
0847	4 Aug. 1443	Swanpool East (1)	45	0	+ 34	3–13	—	0·045	0·070	0·005
0049	17 June 1532	Swanpool West (1)	42	0	+305	2–16	—	0·031	0·059	0·003
0133	18 June 0840	Porthscatho (1)	42	1	−167	4–18	0·028	0·022	0·051	0·004
1033	4 Aug. 0808	Prah Sands (2)	42	0	−274	3–21	—	0·020	0·049	0·003
0928	2 Aug. 1527	Lamorna (2)	41	1	+254	2–16	—	0·023	0·050	0·003
0770	19 July 0820	Cavalaire (3)	40	0	nil	2–16	—	0·024	0·054	0·004
1032	4 Aug. 0902	Lamorna (2)	40	0	−280	2–12	—	0·019	0·048	0·004
0061	17 June 1550	Penzance (2)	39	0	+350	4–14	—	0·019	0·048	0·005
1008	3 Aug. 1535	Porthscatho (1)	38	0	+162	4–18	—	0·033	0·063	0·003
1012	3 Aug. 1537	Porthscatho (1)	38	0	+162	2–16	—	0·027	0·056	0·003
0757	19 July 0806	Beauvallon (3)	37	0	nil	7–17	—	0·036	0·063	0·005
0074	17 June 1557	Lamorna (2)	37	0	+ 35	4–18	—	0·019	0·049	0·003
0075	17 June 1557	Lamorna (2)	37	0	+ 35	4–18	—	0·020	0·050	0·003
0801	2 Aug. 1029	Porthscatho (1)	36	1	+214	10–24	—	0·024	0·053	0·005
0954	2 Aug. 1558	Prah Sands (2)	35	1	+285	3–21	—	0·020	0·050	0·003
0611	24 July 0758	Maenporth (1)	34	1	+195	2–12	—	0·028	0·055	0·004
0093	18 June 0739	Swanpool West (1)	34	1	−225	4–14	0·030	0·038	0·065	0·005
5087	8 Sept. 1100	Gigha (4)	30	3	nil	3–13	—	0·077	0·100	0·010

(*c*) The interdependence of the green and red extinction coefficients is very marked over a wide range. The left-hand portion of figure 12 shows the thirty green extinction coefficients of table 7 plotted against the corresponding red values. The points lie on either side of a line which has been obtained by plotting the green and red extinction coefficients (0–10 ft.) for the theoretical water types *a* to *f* from table 4. The agreement between the theoretical coefficients and those calculated from the most accurate portions of thirty pairs of brightness profiles is considered to justify Le Grand's contention (part I) that a ρ value of about 1 is generally applicable to coastal water, although the green and red filter-film combinations are not particularly sensitive to it. The blue extinction coefficients shown in table 7 are also similar in value to the observed green coefficients, as would be expected for a ρ value of 1 (figure 2). A ρ value of 4, for instance, would require the blue coefficients to be approximately twice the green.

Extinction coefficients determined with the Pulfrich photometer. The procedure used has already been outlined; those portions of the results relevant to this work are summarized below:

(*a*) A direct comparison of extinction coefficients could only be made on nine of the results listed in table 7, as the Pulfrich photometer was not available when the remaining photographs were taken. The extinction coefficients of each of the nine samples were plotted against the estimated mean wave-lengths of the eight 'monochromatic' filters used during the determinations; the extinction coefficients for the wave-lengths 5600 A (green) and 6300 A (red) were then read from the smooth curves. The results are compared in table 8

TABLE 8. COMPARISON OF EXTINCTION COEFFICIENTS

negative number (see table 7)	place	extinction coefficients from brightness profiles: green	red	depth range (ft.)	extinction coefficients from Pulfrich photometer: green	red	depth of sample (ft.)
0801	Porthscatho	0·024	0·053	10–24	0·038	0·076	1
0900	Porthscatho	0·026	0·055	2–12	0·045	0·083	15
0975	Porthscatho	0·024	0·053	4–24	0·037	0·074	1
0976	Porthscatho	0·027	0·056	2–12			
0979	Porthscatho	0·021	0·051	2–16	0·048	0·086	15
1008	Porthscatho	0·033	0·063	4–18	0·040	0·080	1
1012	Porthscatho	0·027	0·056	2–16	0·046	0·080	2·5
1134	Porth Farm	0·023	0·052	7–21	0·040	0·078	4
1170	Porth Farm	0·024	0·054	4–22	0·039	0·077	10

with extinction coefficients calculated from the green and red brightness profiles. The latter are seen to be consistently lower than the extinction coefficients given by the Pulfrich photometer. Both sets of results are reproducible and the variations with wave-length are consistent in both cases with a ρ value of about unity. The discrepancy is real and cannot be due to the following causes:*

(i) The effects of sun altitude or of haze. Theoretical corrections which might be made for sun altitude (part I) would decrease rather than increase the extinction coefficients

* In some of the earlier trials indications of a ρ value of 3 or 4 were recorded; these results could not be repeated, and as they were obtained without adequate sensitometric control and using estimated values of B_∞, they cannot be considered reliable.

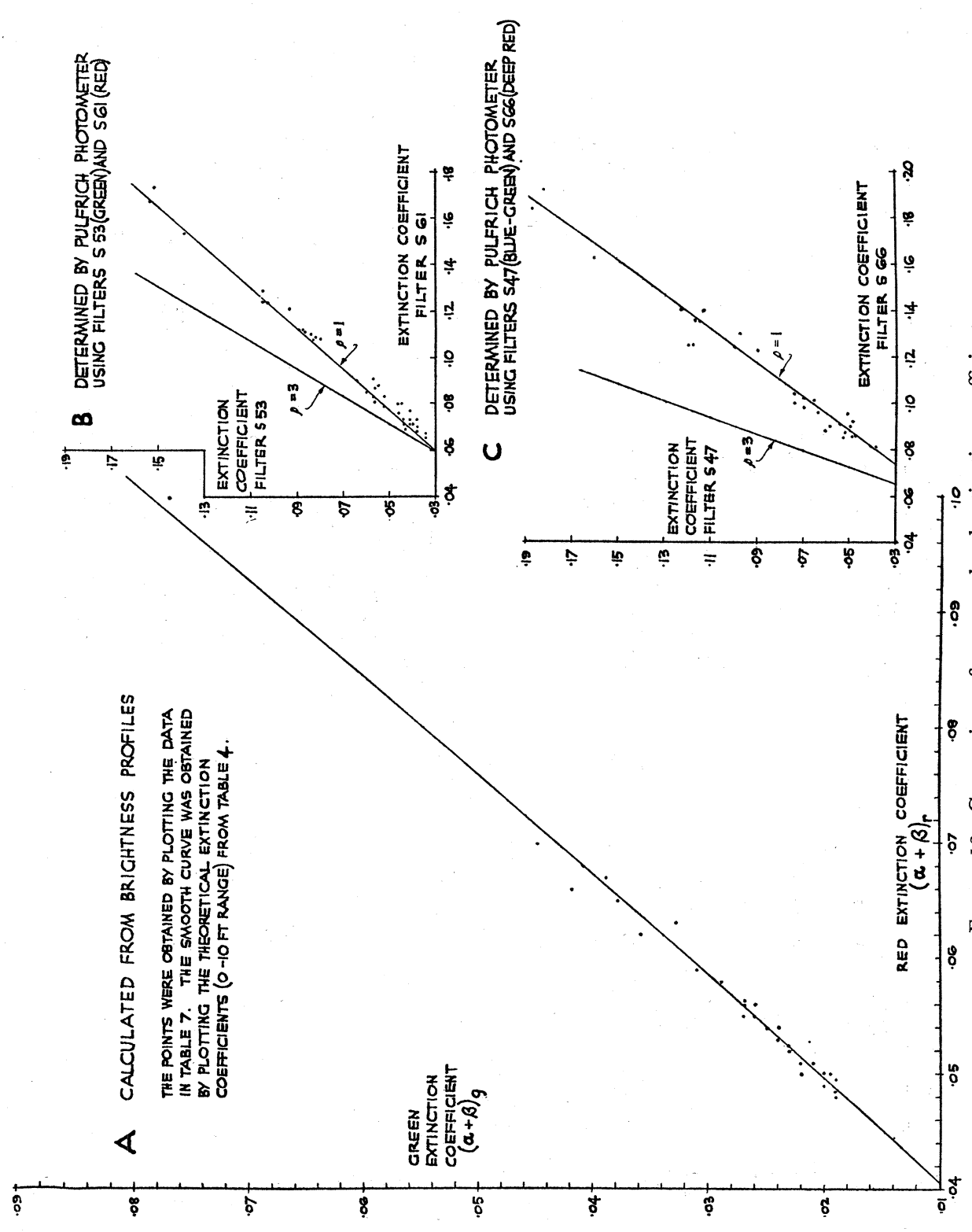

FIGURE 12. Comparison of green and red extinction coefficients.

All extinction coefficients are based on feet and common logarithms.

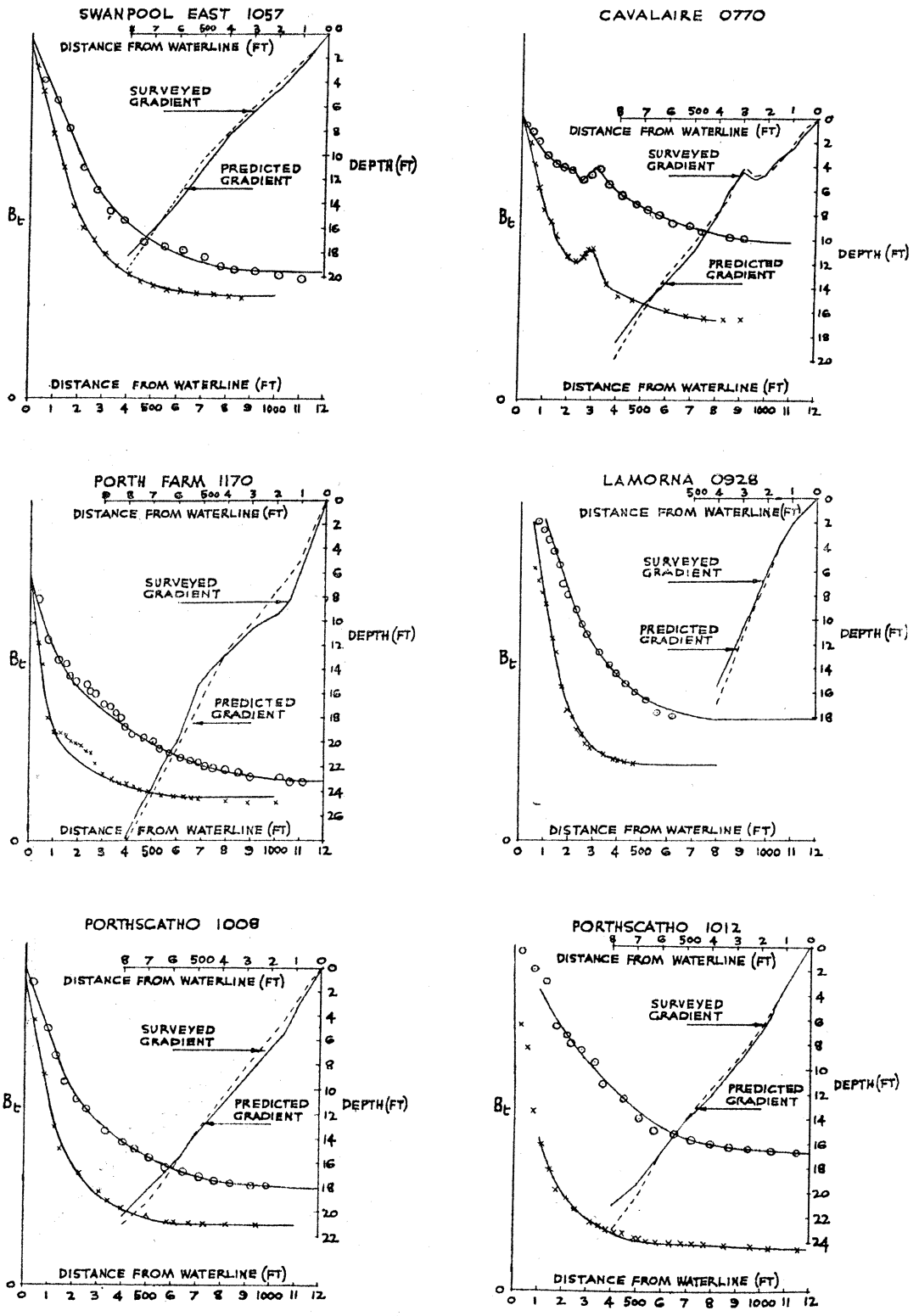

FIGURE 13. A comparison of beach gradients predicted from the calculator and gradients determined by ground survey.

calculated from brightness profiles, nor could any reasonable correction for haze produce a significant increase in the red extinction coefficients.

(ii) Non-homogeneity of the water. Samples taken at greater depths and at greater distances from the shore gave in fact somewhat higher extinction coefficients in the Pulfrich photometer than those recorded in table 8.

(iii) Errors in survey. It would require a 4 ft. error in a 6 ft. sounding to explain the discrepancy.

(iv) Random photographic errors. It is not possible to fit theoretical curves based on the photometer extinction coefficients to the observed brightness profiles (figure 11).

When these trials were planned, both Atkins and Cooper pointed out that the standard Pulfrich photometer was unsuitable for the determination of extinction coefficients in relatively clear water. As it was not possible at the time to use submerged photo-cells, the Pulfrich photometer was modified so that the determinations could be made in tubes 1 m. long. In view of the above discrepancy, it would be interesting to compare extinction coefficients obtained with the modified Pulfrich photometer and those obtained by the submerged photo-cell technique. It is appreciated that the latter is more likely to give results comparable to those obtained from brightness profiles, because in the Pulfrich photometer light once scattered is largely lost by absorption at the tube walls. The comparison, however, would assist materially in assessing the accuracy of extinction coefficients determined from air photographs.

(*b*) As the extinction coefficients given by the modified Pulfrich photometer were, however, consistent amongst themselves, they have been analysed for variation with wavelength. On the right-hand portion of figure 12 extinction coefficients obtained with the following pairs of filters are plotted against each other:

S 66 (deep red) against S 47 (blue-green),
S 61 (red) against S 53 (green).

Curves have been added to show the theoretical relationships which would be expected with these filters for various values of ρ. It will be seen that the observed values in both cases lie on either side of the curve representing a unit ρ value.

Examples of beach gradients derived from brightness profiles

The procedure for calculating beach gradients from density measurements on pairs of green and red negatives was described in part I and illustrated by a worked example at the beginning of part III. Additional examples are shown in figures 13 and 14. The six beach profiles in figure 13 were obtained using the calculator. The agreement between the calculated depths and the depths obtained by survey is satisfactory, but the limiting depths vary from 15 to 30 ft. according to the contrast on the negatives, the homogeneity of the water and the calmness of the sea surface.

The reproducibility of the results is illustrated by the examples in figure 14. These have been taken from eight separate sorties over one beach. The sorties were made at the beginning of these trials and the results were interpreted using equation (7*a*), as the calculator had not at that time been developed. Random errors may therefore be greater than in the examples in figure 13, but the gradients are of interest as they show reproducibility and a good depth range.

An interpretation from prints using the paper comparator

The prints used in this example were made from the pair of negatives (plates 11–12) described in table 5, so that a direct comparison of the results of the two methods of interpretation is possible.

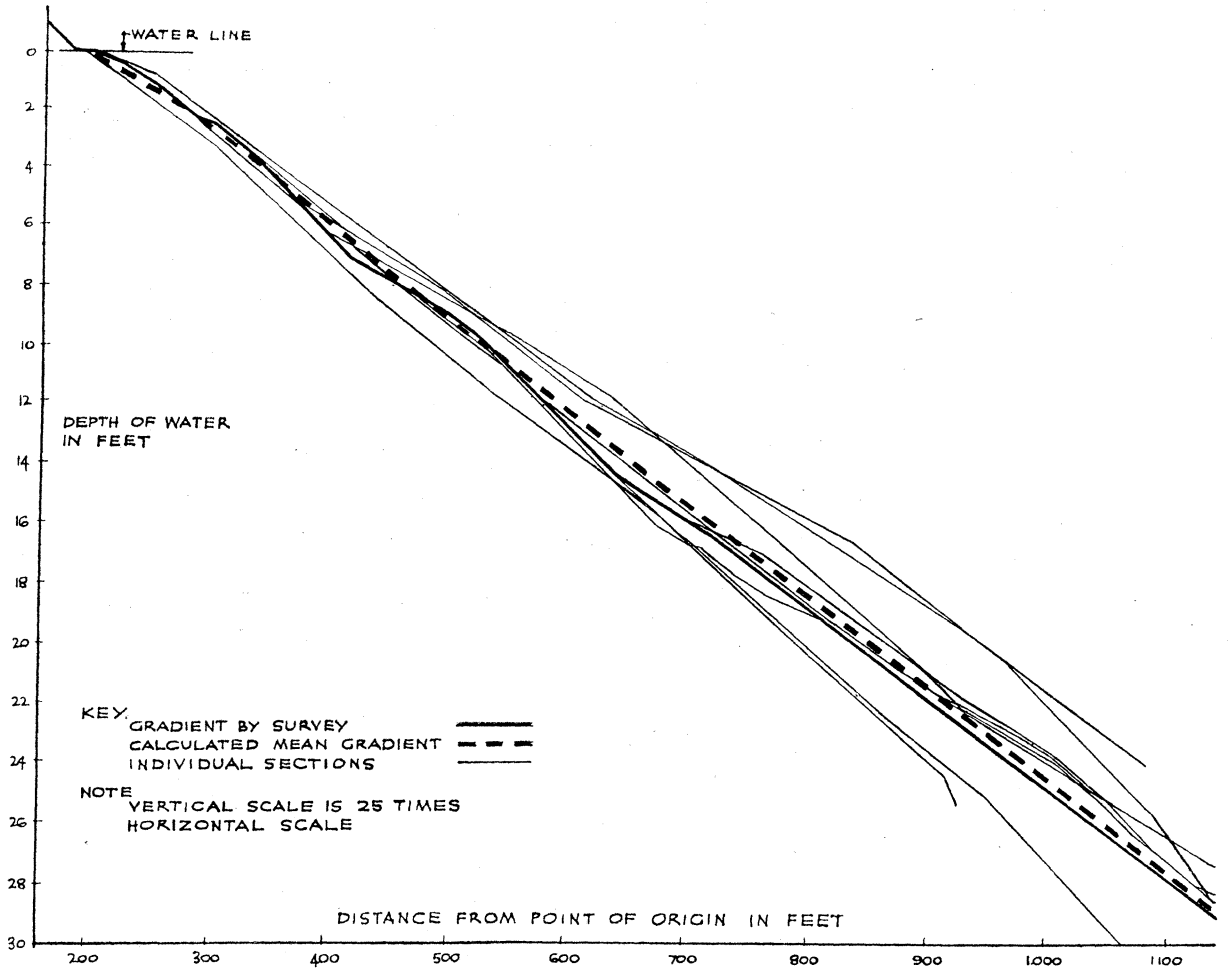

FIGURE 14. Beach gradients determined from eight sorties over Prah Sands, Cornwall. These gradients were obtained without using the calculator, by use of equation (7*a*).

Two prints were prepared from the red negative; the first, referred to by the letters *Ra*, had a reflexion density near the waterline of approximately 0·2; the second, which will be called *Rb*, had a reflexion density in the deep water of 1·4. Only one print was required to cover the contrast range on the green negative; it will be referred to as print *G*.

Comparison curves for these three prints, constructed from the data at the head of table 9, are shown in figure 15. It will be noted that each curve can be drawn with considerable certainty, despite the few points on it, by comparison with the form of the other two.

The points which were pricked on the green print are numbered in column 1 of table 9; the horizontal distance of each from the waterline is shown in column 2. The reflexion density of the matching step on the paper comparator is recorded in column 3, and its corresponding relative brightness as read from the green conversion curve is given in

column 4. Similar data for the two red prints *Ra* and *Rb* are entered in columns 5–8 and 9–12 respectively.

The green brightness profile, constructed from the values in columns 2 and 4, is shown in figure 15. The upper half of the red profile was derived chiefly from the measurements on print *Ra*, and the lower half from print *Rb*; the agreement where the two portions overlap is satisfactory.

TABLE 9. INTERPRETATION FROM PRINTS OF NEGATIVES 975

(For description of negatives see head of table 5.)

data for comparison curves:							
sensitometers 21 and 23: step number		4	5	6	7	8	9
equivalent log exposure		2·54	2·26	1·97	1·71	1·43	1·13
relative brightness value		347	182	93·3	51·3	26·9	13·5
reflexion density of matching step on paper comparator:	print *G*	0·01	0·14	0·75	1·40	—	—
	print *Ra*	—	0·05	0·34	1·18	1·62	—
	print *Rb*	—	—	0·01	0·26	1·12	1·54

	green print *G*			red print *Ra*			
point number (1)	distance from waterline (ft.) (2)	reflexion density (3)	relative brightness (4)	point number (5)	distance from waterline (ft.) (6)	reflexion density (7)	relative brightness (8)
1	0	—	—	1	0	—	—
2	20	0·18	160	2	19	0·18	118
3	112	0·25	137	3	41	0·25	104
4	180	0·38	115	4	60	0·45	87
5	225	0·49	107·5	5	71	0·51	84
6	308	0·65	98·8	6	97	0·65	78
7	382	0·80	90·5	7	116	0·80	72
8	495	0·96	81·0	8	135	0·96	64
9	698	1·10	72·0	9	165	1·24	49
10	—	—	—	10	199	1·39	41

	red print *Rb*		
point number (9)	distance from waterline (ft.) (10)	reflexion density (11)	relative brightness (12)
1	0	—	—
2	100	0·06	78
3	142	0·18	58
4	169	0·32	48
5	202	0·51	42
6	221	0·73	38
7	255	0·88	35
8	319	1·03	30
9	397	1·24	23
10	495	1·31	20

The depths obtained from these profiles by use of the calculator are shown in figure 15 as a profile of the beach on an exaggerated vertical scale. Comparison of the first 10 ft. of this profile with that obtained by survey suggests that the constant error of about 9 in. in the former is probably due to inaccurate selection of the waterline on prints. At depths

below 13 ft. the error increases and at 20 ft. has become serious, no doubt due to the absence of lens-shutter corrections. A comparison of the errors made in the two methods of prediction is given in table 10.

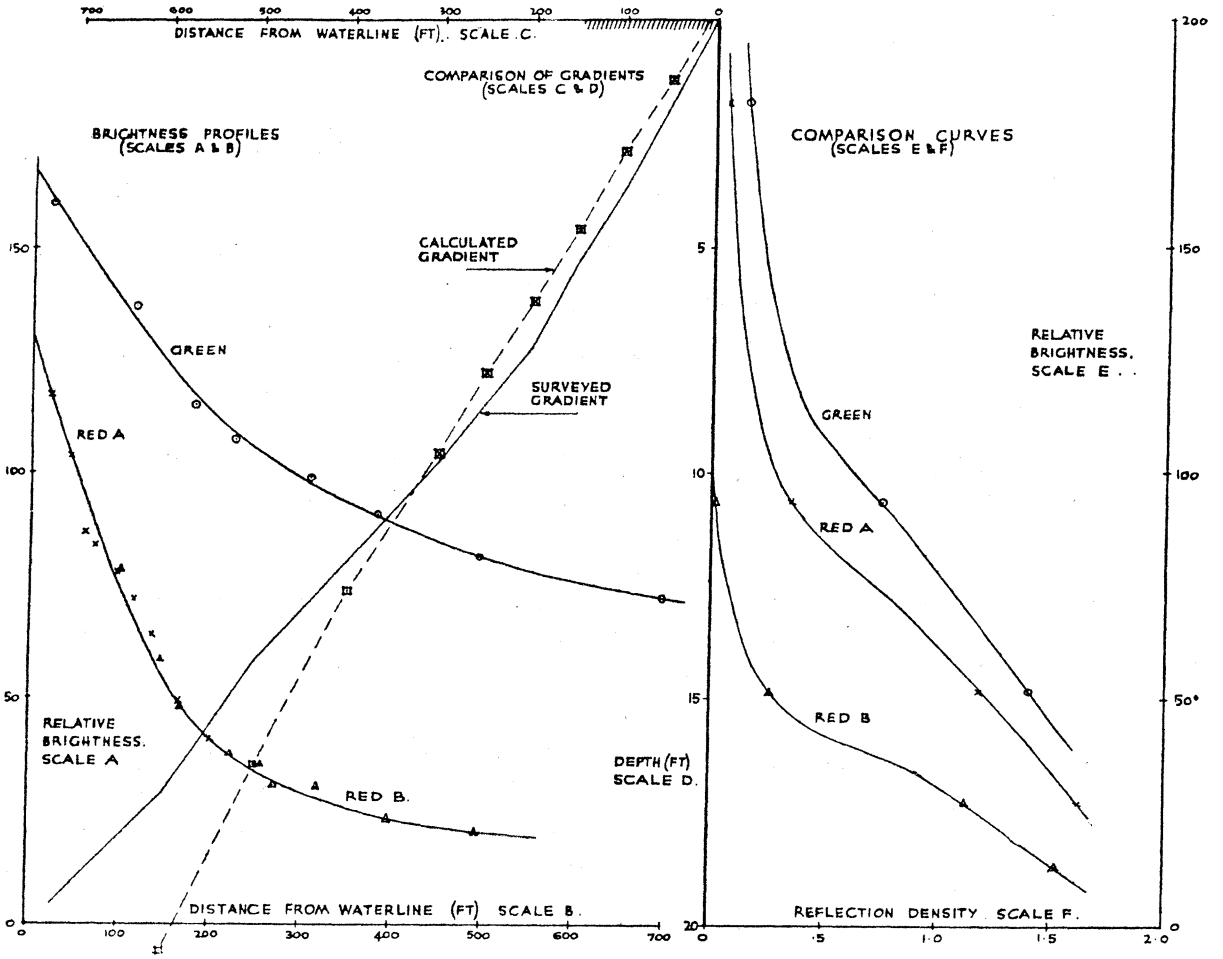

FIGURE 15. Example of interpretation using the paper comparator.

TABLE 10. COMPARISON OF ERRORS

distance from waterline (ft.)	depth by survey (ft.)	error in depth predicted from negatives (table 6)	error in depth predicted from prints
100	3·7	−0·5	−0·8
200	7·2	−0·2	−1·0
300	9·7	−0·3	−0·1
400	12·0	−0·2	+0·6
500	14·2	−0·2	+2·3
600	17·1	−0·1	+3·7
700	19·1	+0·5	+6·0
800	21·5	+0·8	—
900	23·8	+0·7	—

It is interesting to note that the Secchi scale reading obtained from the prints was 26 ft., and that from the negatives 27 ft. The reading recorded in the water at the time of photography was 31·5; this was at a point several hundred feet further along the profile, as the water closer to the shore was too shallow for the white disk to be used.

Analysis of Secchi disk readings

Five interchangeable metal disks were prepared, each of 25 cm. diameter. Four of the disks were finished with a urea-formaldehyde stoving lacquer of refractive index 1·55; the fifth disk was painted a dull matt black.

The spectral reflectivities of the lacquered disks were measured and from the results their effective mean wave-lengths, relative to the human eye, were estimated (table 11).

TABLE 11. PROPERTIES OF THE SECCHI DISKS

disk	approximate spectral limits of reflectivity (A)	estimated effective mean wave-length to human eye (A)	calculated visual lightness under C.I.E. illuminant B %
white	uniform from 4000 to 7000	—	85
blue	<4000–5100	4900	2·7
green	4700–6000	5400	6·1
red	5800–>7000	6120	12·6
black	uniform from 4000 to 7000	—	probably <1

The disks were used in the normal way. No polarizing device was used to remove surface reflexion, but all readings were taken on the shady side of the launch. Numbered tallies were fixed to the calibrated line to minimize errors when recording the depths. Four out of five tested observers were able to obtain consistent readings; the fifth observer was consistent with the coloured disks, but his readings for the black disk were erratic and generally too great; his results were therefore discarded.

All observers noted that the blue, green and red disks appeared to change colour as they were lowered through the water. The blue disk became a deeper blue and then increasingly green; the red disk appeared to be brown; at the limits of visibility the disks appeared greenish grey, tinged slightly with their particular colours. Except for the green disk, the limits of visibility were quite sharp.

Readings were taken in all types of water, some through coloured filters. The filters were prepared by mounting pieces of Wratten 47*a* (blue), 56 (green) and 27 (red) gelatine filters between glass plates.

The principal results, summarized in figure 16, have already been discussed (part II); the linear relationships given by the coloured disks were not expected, and the significance of the slope of the lines is not clear. A continuous series of readings was also made, without filters, along the channel of the Fal river; the series was started in coastal water outside the river (station A) and was continued right up the river to Ruan Creek, about three miles from Truro (station F). The sky was overcast throughout and the water was slightly 'choppy'. The results are summarized in table 12.

It will be seen that the readings are consistent and vary almost linearly with distance downstream. It is considered that the Secchi disk is valuable for obtaining a rapid estimate of water types but it is clear that further research is required before reliable extinction coefficients can be calculated from the readings.

TABLE 12. SECCHI DISK READINGS IN THE FAL RIVER

station	distance downstream from Ruan Creek (yd.)	tide, min. before (−) or after (+) low water	Secchi readings (ft.) white	black	blue	green	red
A	13,400	−144	35	18	29	26	25
B	10,300	− 60	30	15	23	22	21
C	7,400	− 30	22	12	17	15	15
D	4,700	0	16·5	9·5	11·5	9·5	11·5
E	2,000	+ 20	9·5	7·0	9	7	9
F	0	+ 50	4·5	3·3	4	4·3	4·3

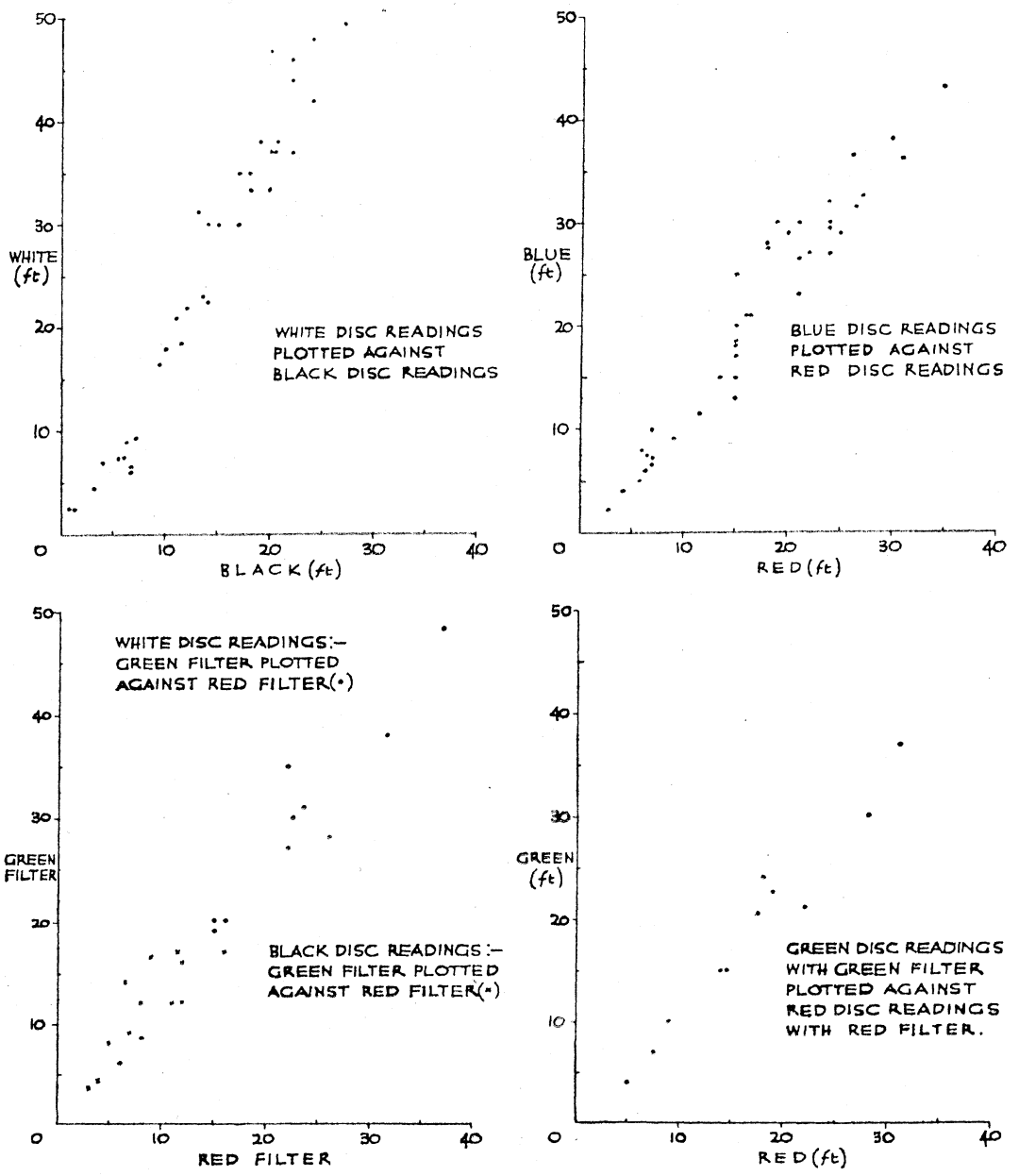

FIGURE 16. Analysis of Secchi disk readings.

Conclusions

Comparison with existing methods

It has been shown that, if the water is calm and fairly clear and the photographic conditions are properly chosen:

(1) The underwater detail can be recorded over large areas of the sea-bed to depths exceeding 30 ft.

(2) Depths can be determined over light-coloured beaches with an accuracy better than 10 % over a depth range exceeding 20 ft. Independent depth information is not required, but, if available, permits the elimination of one camera or can be used as a check on the results obtained with two.

(3) The clarity or state of pollution of the water can be assessed in terms of mean extinction coefficients or predicted Secchi disk readings; these measurements can be made practically simultaneously over large areas of sandy beaches.

Distribution of underwater detail. There is probably no satisfactory alternative method to air photography for recording the detailed distribution of rocks, weeds, sandbars, obstacles, etc., on the sea-bed.

The determination of depths and gradients. The peculiar advantage of the present method for determining depths or beach gradients in shallow water is that a large number of records can be made over a big area within a very short time interval; the records can then be examined at leisure, and the effect of factors such as tides, currents, etc., which vary with time can be compared over the whole area. Alternative methods of recording depths, for instance, by line or echo sounding, will give more accurate results over greater ranges, but the records cannot be obtained over a large area at anything like the speed permitted by air photography, nor are they automatically related to the geological configuration of the sea-bed.

The operational method of depth determination, known as the wave-velocity method, is complementary to the present method, as it can be used when the sea conditions are unsuitable for photography of underwater detail; but it cannot be used when the sea is calm or if the coastline is strongly indented, conditions most suited to the present work.

Depths can, of course, be predicted operationally from normal photographs if accurate tide tables are available and the water edge is photographed at known times at various stages of the tide; the range of depths obtainable is, however, limited to the range of the tides, and this method is therefore useless wherever the tide range is small (e.g. the Mediterranean); where it can be used it may be applied as a check on the shallower depths given by the present method.

Stereoscopic photographs have been used to determine the depths of shallow water; suitable conditions may, however, be difficult to obtain.

The measurement of water clarity. All the existing methods are based on some form of measurement at or below a point on the water surface. They cannot be used to give information over an area, and therefore there is at present little knowledge of the effect of tides, currents, sun altitudes, seasons, etc., on the clarity of coastal water. The direct or indirect dependence of marine life on photo-synthesis is, however, well known, and therefore it is considered that the present method provides a new and important tool for the marine biologist. Whether

or not the extinction coefficients determined from air photographs are capable of exact physical explanation has not been determined, but they appear to be directly related to the clarity of sea water, and are extremely sensitive to the effects of pollution.

Some possible scientific and industrial applications

No practical work on the following possible uses of the method has been attempted, but it is clear that promising results might be obtained either by application of the technique described in this paper, or by some suitable modification of it.

Uses based on photography of underwater detail

Study of the geology and marine biology of the sea-bed (plate 13).

Detection of submerged obstacles to navigation, including reefs, wrecks, etc.

The control of industrial pollution.

Archaeological study of submerged areas (e.g. the Scilly Isles).

Uses based on determination of depths and gradients

The preparation of charts of shallow-water areas.

The control of erosion and deposition on beaches, and in navigable channels and harbours (plates 14–15).

Study of the effects of current and tides on the formation and movement of sandbars, beach gradients, etc.

Research on wave motion and tides in shallow water.

Recording depths of water for engineering purposes. (This may be particularly valuable in relatively inaccessible areas.)

Uses based on the determination of water clarity

Study of the effects on marine life of light of various wave-lengths and intensities.

Control of pollution.

Identifying water types and recording coastal currents.

Planning engineering operations (e.g. diving and salvage) in which submarine visibility is important.

Suggested future research

In addition to an examination of the applications outlined above, further research would be valuable on the following aspects of the technique described in this paper:

(*a*) Improvements in camera and shutter design (see part II).

(*b*) The use of a continuous sensitometric wedge and scale.

(*c*) The use of narrow-band filters and longer exposures.

(*d*) The effect of using split mounted cameras to increase coverage.

(*e*) The use of a continuously recording densitometer.

(*f*) Development of a printer giving even illumination over the whole negative.

(*g*) The effect of coloured material in solution or in suspension in the sea water or on the sea-bed.

(*h*) Application to inland lake waters (this may require the use of a third filter).

(*i*) The identification of sea-bed materials.

(*j*) Alternative corrections for haze, multiple scattering, sun altitude, cloud conditions, etc.

(*k*) Modifications necessary to increase the range of depths obtained.

The assistance given by Professor J. D. Bernal, F.R.S., has already been acknowledged.

It is particularly desired to record the help given throughout this work by Dr W. R. G. Atkins, F.R.S., whose knowledge of oceanographical literature has proved invaluable; and of Professor Yves Le Grand whose comprehensive paper (1939) was used as a basis for the theoretical procedure for calculating extinction coefficients.

Dr L. H. N. Cooper, of the Marine Biological Association Laboratories, Plymouth, carried out the extinction coefficient determinations with the Pulfrich photometer, and in addition gave considerable help during the theoretical discussions on this work; for the facilities provided by the Director of the Marine Biological Association Laboratories, the author wishes to record his thanks.

The modification to the densitometer and the design of the sensitometers were carried our by Mr E. D. Eyles and Mr A. L. Shuffrey of the Kodak Research Laboratories, Harrow, who also rendered invaluable assistance and advice on the properties of films and filters and in the production of the comparator strips. Arrangements for the production and supply of all the photographic equipment were made by Dr D. A. Spencer, Mr B. Sugarman and Mr J. C. Shepherd of R.D.Photos, Ministry of Aircraft Production.

Modifications to camera shutters and the controlled processing of films were carried out by the staff of the Photographic Division, Royal Aircraft Establishment, Farnborough. The coloured Secchi disks were prepared, by permission of Dr L. A. Jordan, by the staff of the Paint Research Station, Teddington.

Flying facilities were provided in particular by the Officers Commanding R.A.F. Stations at Old Sarum and Portreath, and R.N.A. Station, Machrihanish, and the assistance given by the staffs at these stations is very gratefully acknowledged.

All the photographic sorties in the south of France were carried out by 106 Group R.A.F. Benson, and it is desired to thank W/Comdr. G. Buxton for organizing these sorties, and F/O M. D. Mackins, and F/O R. S. Flight, D.F.C., who rapidly became expert in the type of air photography required.

Ground survey and soundings in Cornwall and the Scilly Isles were made from H.M. Launch *Vita* from 644 Water Transport Company, R.A.S.C., Falmouth; this launch frequently had to operate under exacting conditions and the skipper, Mr R. West, and the staff of the 644 Company gave every possible assistance throughout the trials.

Lt.-Col. J. R. Merton, M.B.E., commanding the Army Photographic Research Unit, made the original suggestion that comparative air photographs might be used for determining depths in shallow water; he made many other useful suggestions and criticisms, and provided every possible facility throughout the work. Major P. K. C. Wiggs, R.A., gave invaluable assistance with the theoretical calculations and the trials in Scotland. Captains V. J. Cooper and N. H. Fowler, R.A., were responsible for a large proportion of the computations.

Of the remaining staff of the Army Photographic Research Unit, it is particularly desired to mention the tireless efforts and willing co-operation throughout these trials of Sgt. M. J. E. Fuche, R.A., Cpl. J. Dodd, R.A.F., Cpl. H. Loxton, A.T.S., L/Bdrs. E. Browning and A. Shepherd, and L.A.C. G. Alden, R.A.F. Additional personnel attached from the Survey Wing of the School of Artillery included Sgt. L. F. Collings, R.A., and Bdrs. M. Thurston and R. Riley, who, under Lieut. K. Travis, R.A., gave considerable help in the ground survey.

The Oxford aircraft was piloted throughout the trials by F/Lt. K. Partis, R.C.A.F., and F/Lt. K. Crist, R.N.Z.A.F. The photographs were taken by F/Lt. J. Van Panhuys, Netherlands Air Force, and F/Lt. R. H. Thomson, R.A.A.F.; the latter officer was attached to A.P.R.U. by S/Ldr. N. Everingham, R.A.A.F. H.Q., who showed considerable interest in these trials.

Finally, it is especially desired to thank the War Office (D.Air), Air Ministry (D.D.Photos), and the Ministry of Aircraft Production, for their inexhaustible patience in arranging many facilities at short notice.

References

Atkins, W. R. G. 1932 *J. Cons. int. Explor. Mer.* **7**, no. II, 171–211. B.

Atkins, W. R. G., Clarke, G. L., Pettersson, H., Poole, H. H., Utterback, C. L. & Angström, A. 1938 *J. Cons. int. Explor. Mer.* **13**, 37–57. B.

Atkins, W. R. G. & Poole, H. H. 1933 *Phil. Trans.* B, **222**, 129–164. B.

Atkins, W. R. G. & Poole, H. H. 1936 *Phil. Trans.* A, **235**, 245–272.

Atkins, W. R. G. & Poole, H. H. 1940 *J. Mar. Biol. Ass. U.K.* **24**, 271–281.

Bhagavantam, S. 1942 *Scattering of light and the Raman effect.* New York: Chemical Publishing Co.

Blumer, H. 1926 *Z. Phys.* **39**, 195–214.

Campbell, I. G. 1944 *Development of fungus, fogging and filming in optical instruments under tropical conditions.* London: Director Mech. Engrs, War Office.

Clarke, G. L. 1936 *J. Cons. int. Explor. Mer.* **101**, pt. II. B.

Clarke, G. L. 1938 *Ecology*, **19**.

Clarke, W. 1939 *Photography by infra red.* London: Chapman and Hall, Ltd.

Clarke, G. L. & James, H. R. 1939 *J. Opt. Soc. Amer.* **29**, 43–55.

Cooper, L. H. N. & Milne, A. 1938 *J. Mar. Biol. Ass. U.K.* **22**, 509–528.

Debye, P. 1909 *Ann. Phys., Lpz.*, **30**, 57–136.

Duclaux, J. 1931 *Bull. Obs. Lyon*, **13**, 239–255.

Erikson, N. A. 1933 *J. Opt. Soc. Amer.* **23**, 170.

Hardy, C. A. 1936 *Handbook of colorimetry.* Cambridge, Mass.

Hulbert, E. O. 1932 *J. Opt. Soc. Amer.* **22**, 408–417.

James, H. R. & Birge, E. A. 1938 *Trans. Wis. Acad. Sci. Arts Lett.* **31**, 1–154.

Jenkins, Bowen & Rogers 1941 *Report C4-Sr* 30–024, Univ. of California, Div. NIR. B.

Johnson, N. G. & Liljequist, G. 1938 *Svenska hydrogr.-biol. Komm. Skr.* N.S. Hydrogr. **14**, 1–15.

Johnson, E. A., Meyer, R. C., Hopkins, R. E. & Monk, W. H. 1939 *J. Opt. Soc. Amer.* **29**, 512–517.

Jorgenson, W. & Utterback, C. L. 1939 *J. Mar. Res.* **2**, 30–37.

Kalle, K. 1938 *Ann. Hydrogr. Berl.* **66**, 1–13.

Kimball, H. H. & Hand, I. F. 1930 *Mon. weath. Rev. Wash.* **58**, 280.

King, L. V. 1913 *Phil. Trans.* A, **212**, 375–433.

Kodak, Ltd. 1937 *J. Sci. Instrum.* **14**, no. 1, 30–32.

Krishman, R. S. 1925 *Phil. Mag.* **50**, 697.

Le Grand, Y. 1939 *Ann. Inst. Oceanogr. Monaco*, **19**, 393–436. B.

McDermott, L. H. 1943 *Report RC (G)* **40**, Civil Defence Research Committee, Ministry of Home Security, London.

Mees, C. E. K. 1940 *Theory of the photographic process.* New York: Macmillan and Co. B.

Middleton, W. E. K. 1935 *Beitr. Geophys.* **44**, 358–375.

Middleton, W. E. K. 1941 *Visibility in meteorology.* Univ. Toronto Press. B.

Mie, G. 1908 *Ann. Phys., Lpz.*, **25**, 377–445.

Orr, A. P. 1933 *Scientific Reports*, **2**, no. 3. British Museum of Natural History.

Pettersson, H. 1935 *J. Cons. int. Explor. Mer.* **10**, 48–65.

Poole, H. H. & Atkins, W. R. G. 1926 *J. Mar. Biol. Ass., U.K.*, **14**, no. 1.
Powell, W. M. & Clarke, G. L. 1936 *J. Opt. Soc. Amer.* **26**, 111–120.
Raman, C. V. 1922 *Proc. Roy. Soc.* A, **101**, 64.
Rayleigh, Lord 1910 *Proc. Roy. Soc.* A, **84**, 25–46.
Sawyer, W. R. 1931 *Contr. Canad. Biol. Fish.* **7**, no. 8, 75–89.
Subow, N. M. & Czihirin, N. J. 1940 *Oceanographical tables.* Oceanographical Institute, U.S.S.R. Moscow.
Sverdrup, H. U., Johnson, M. W. & Fleming, R. H. 1942 *The oceans, their physics, chemistry and general biology.* New York: Prentice Hall, Inc.
Utterback, C. L. 1936 *J. Cons. int. Explor. Mer.* **101**, pt. II, no. 4.
Utterback, C. L. & Jorgenson, W. 1936 *J. Opt. Soc. Amer.* **26**, 257–259.
Utterback, C. L. & Williams, E. A. 1935 *J. Opt. Soc. Amer.* **25**.
Whitney, L. V. 1941 *J. Mar. Res.* **4**, 122.
Young, R. T. & Gordon, R. D. 1939 *Bull. Scripps Inst.* **4**, 197–218. Univ. of California.

Note. References followed by the letter B contain bibliographies.

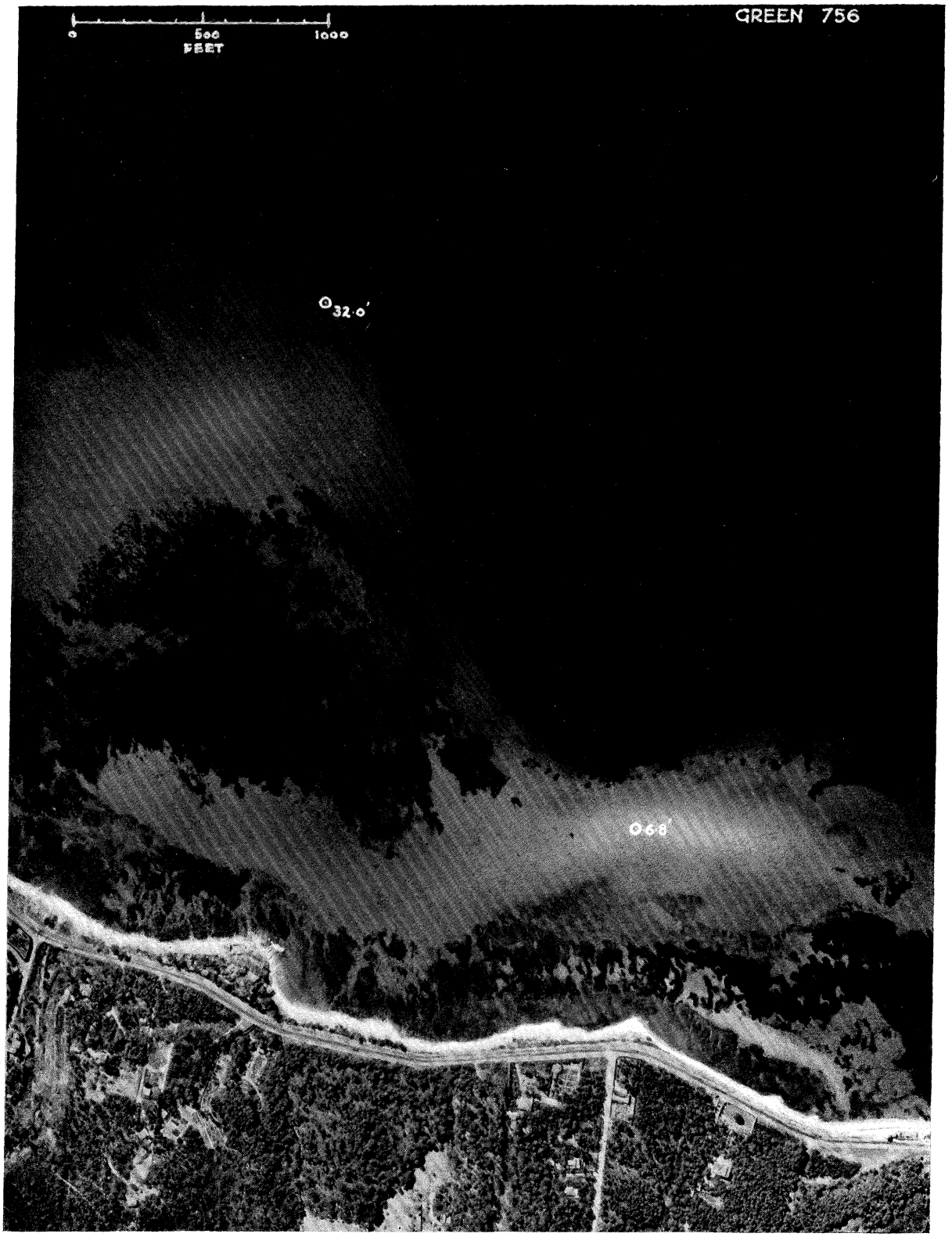

PLATES 1–2. MEDITERRANEAN BEACH TAKEN FROM OPERATIONAL AIRCRAFT (756)

Description. Green and red prints of Beauvallon beach, near St Maxime, France. 19 July 1945. Taken at 12,000 ft. by Mosquito aircraft of 106 Gp R.A.F. Benson, with 20 in. F.52 cameras; 1/120 sec. at *f* 6·3. Contact prints, sensitometer wedges removed in printing; scale 1/7200. Sun altitude 37°, slight haze, cloudless sky; calm sea.

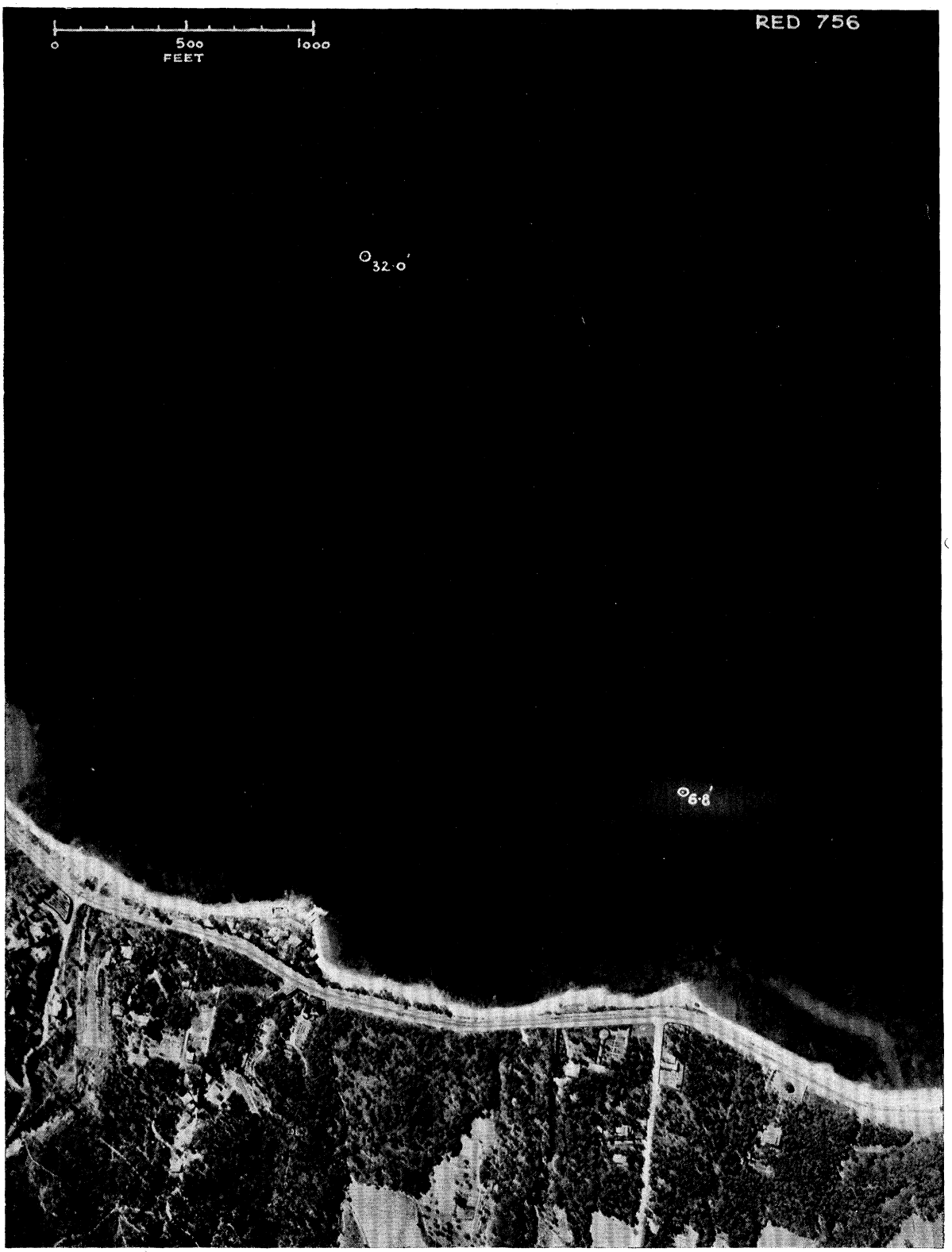

Comment. A rocky beach with patches of sand and a few prominent sandbars. The presence of so much rock made depth prediction difficult, but two satisfactory pairs of profiles were obtained through the sandbar at the spot depth marked 6·8 ft. Detail of the sea-bed at points more than half a mile from the shore is visible on the green print at a depth exceeding 32 ft.

PLATES 3–4. MEDITERRANEAN BEACH TAKEN FROM OPERATIONAL AIRCRAFT (770)

Description. Green and red prints of Cavalaire beach, south of France. 19 July 1945. Conditions as for plates 1–2.

Comment. Undulating sandy beach giving place to continuous rocks at about 24 ft. depth. The undulatory nature of the beach is clearly shown by the tone changes on the red print. A line of submerged military obstacles is visible at point *a* at a depth of about 8 ft. A second line of smaller obstacles can be seen at point *b*. A good prediction of the beach gradient was made along a line through the two spot depths; the results were included in figures 11 and 13.

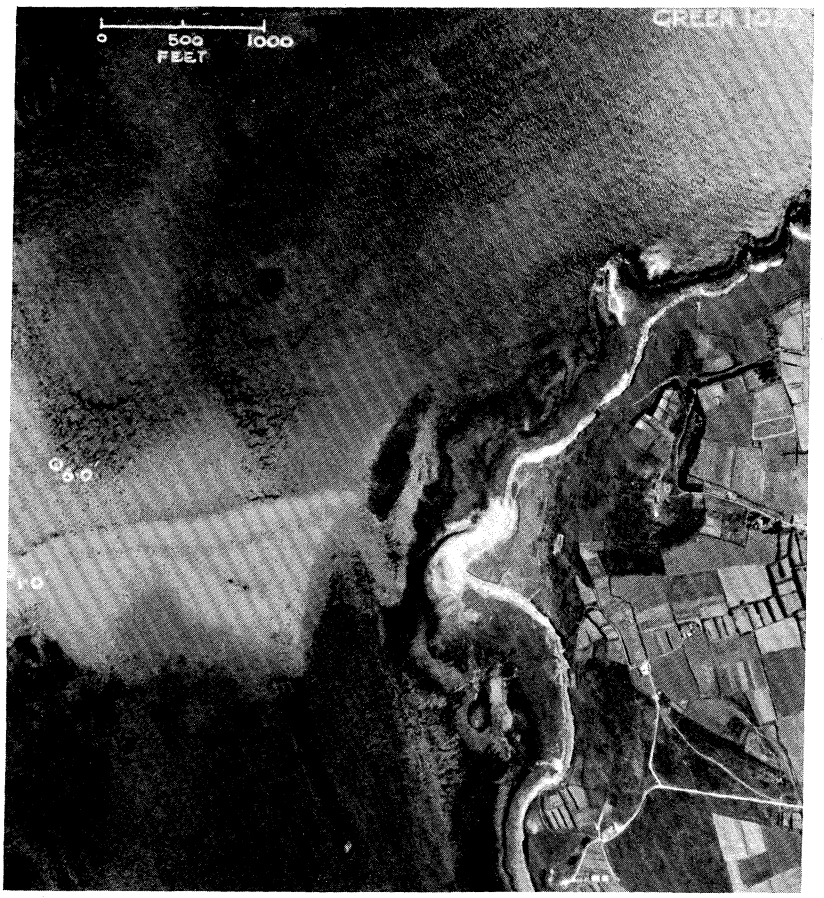
0 500 1000
FEET
6·0'

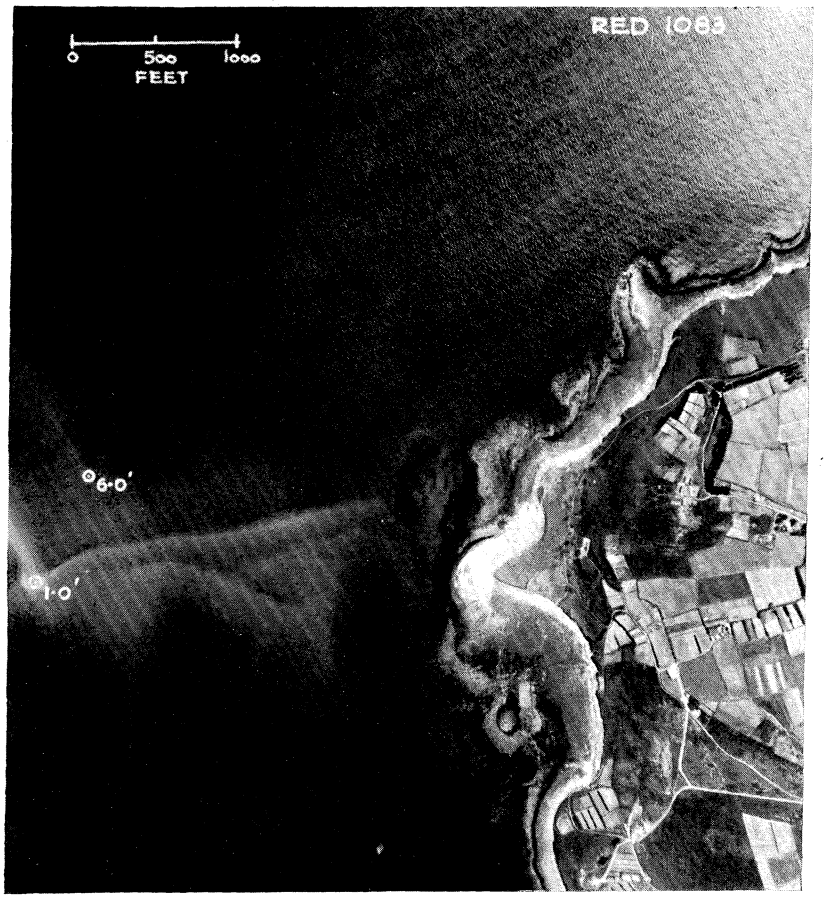
RED 1083
0 500 1000
FEET
6·0'
1·0'

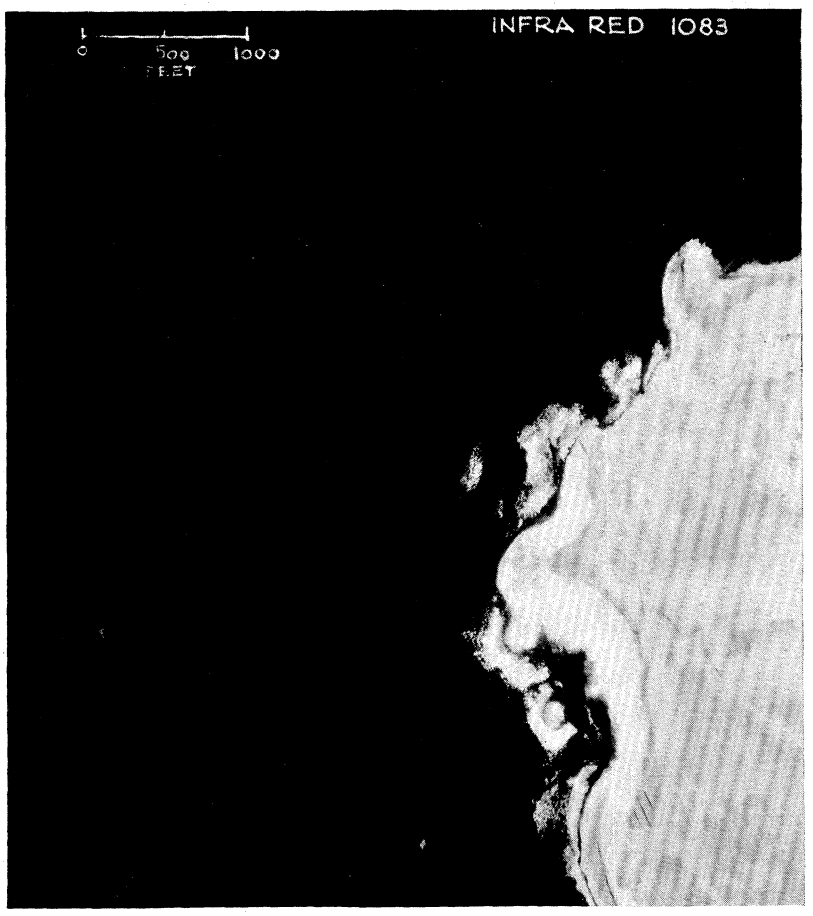

PLATES 5–6. SANDBARS WITH ROCKS AND WEED (1083)

Description. Bar Point, St Mary's, Scilly Isles. 5 August 1945. Taken at 10,000 ft. with 8 in. F.24 cameras; 1/250 sec. at f 5·6. Contact prints; scale 1/15,000. Sun altitude 50°, slight haze; cloudless sky.

Comment. Alinement of the cameras was not perfect and the sun altitude was sufficiently high to cause specular reflexion from waves on one corner of the photograph. The water was shallow and therefore details of the complex system of sandbars are shown most clearly on the red print.

It is clear from the infra-red print that the entire sandbar was submerged; patches of weed are visible on this print in the water close to the shore.


GREEN 1088

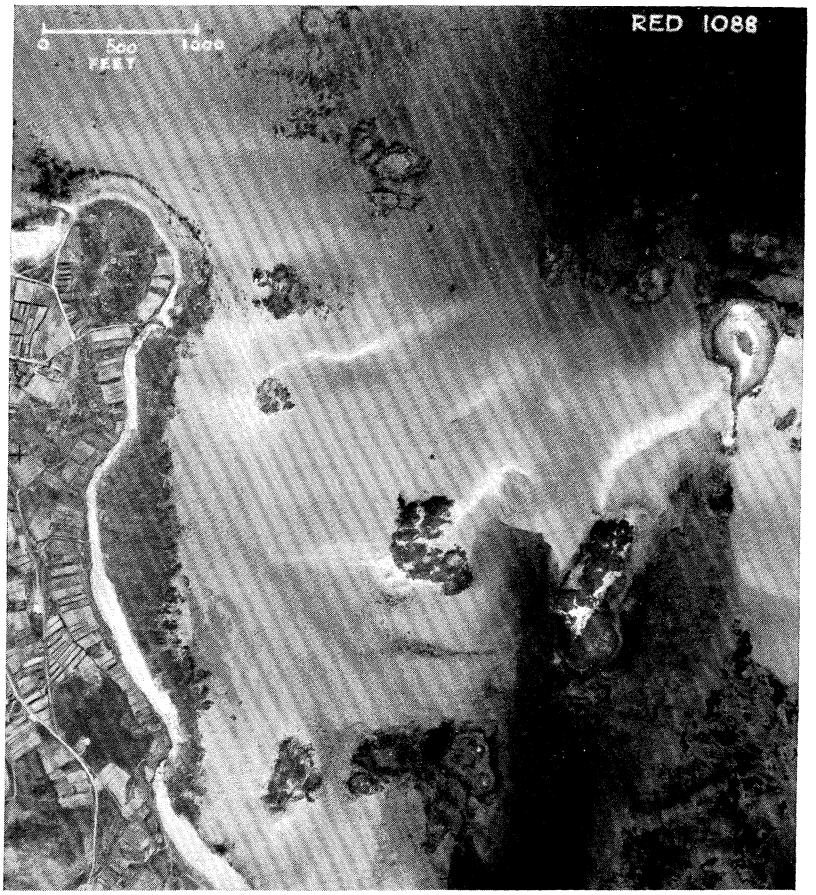
RED 1088
0
500
1000
FEET

PLATES 7–8. SHALLOW UNDERWATER DETAIL (1088)

Description. St Mary's, Scilly Isles. 5 August 1945. Conditions as for plates 5–6.

Comment. The water is shallow, except in the channel on the bottom right-hand quarter of the photograph. The distribution of sand and rock and the effects of water currents are clearly shown. The infra-red photograph indicates which portions of the beach are above the water surface.

EXPOSED SAND BEACH (1025)

Description. Porth Curno, near Land's End. 4 August 1945. Taken at 5000 ft. with the cameras used for plates 5–6. Scale 1/7500. Sun altitude 38°, slight haze, no cloud.

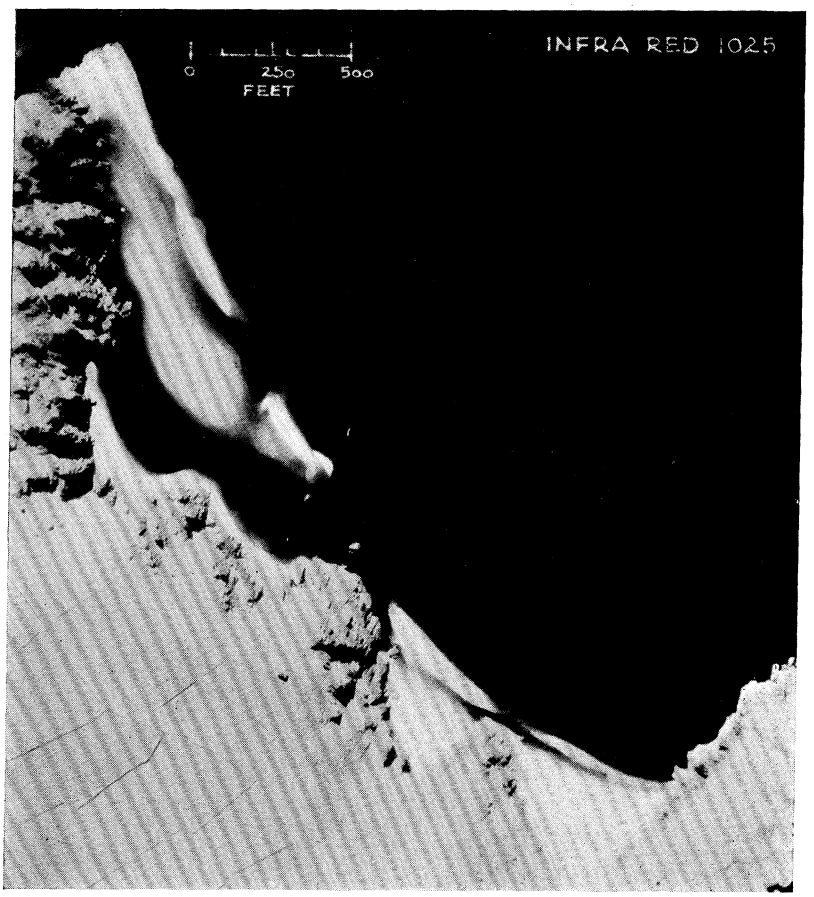

Comment. The green print shows no clearly defined waterline because the sea water is clear and fairly calm, and the surface of the beach has been eroded into a complex shape by storms. The infra-red print demonstrates that there is quite deep water inshore behind the beach. This must not, however, be confused with shadows cast by the cliffs—the limits of the shadows are obvious from the green print.

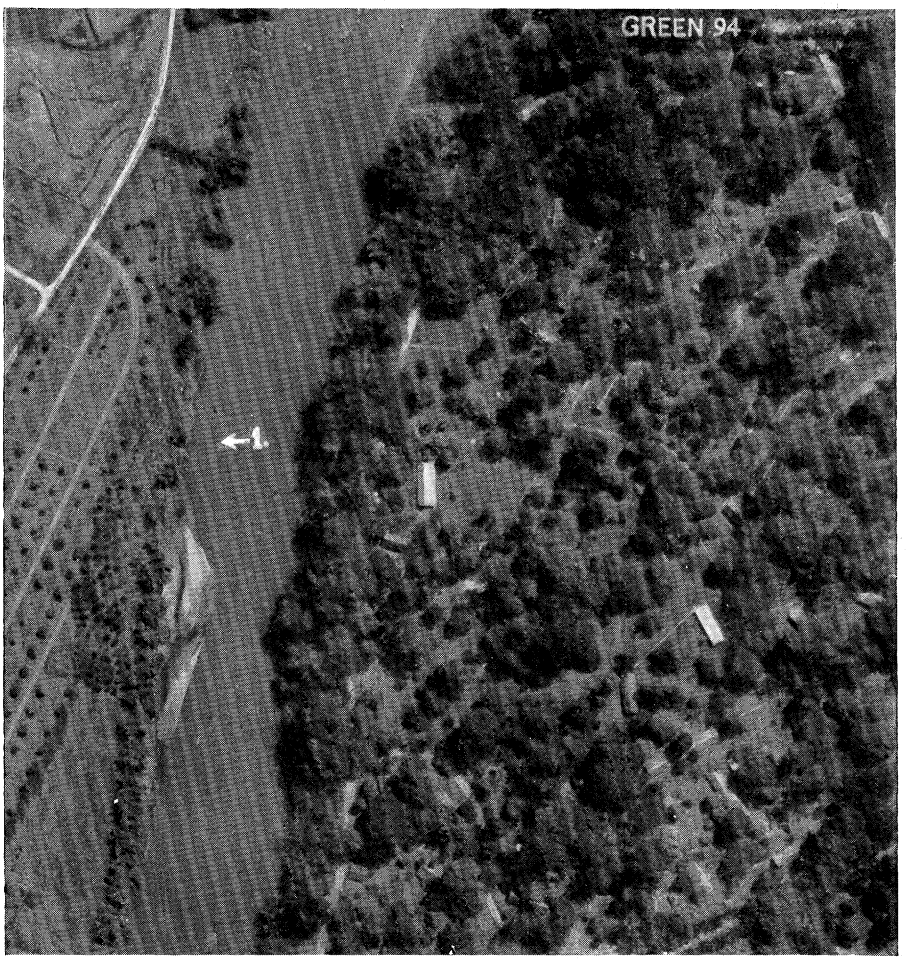

River channels (94)

Description. Mahaweli Ganga, Kandy, Ceylon. 15 January 1945. Taken at 13,000 ft. with 20 in. F.52 cameras; 1/210 sec. at *f* 6·3. Portions of contact prints; sun altitude 49°, nearly cloudless sky.

Comment. The channels are clearly shown on the infra-red photograph which was taken through a Wratten 27 (red) filter, whereas little can be seen on the panchromatic photograph which was taken through a Wratten 56 (green) filter.

Estimates of the depth of the water at various parts of the river can be made by an experienced interpreter; the value of infra-red photography of rivers for finding fording places and channels navigable by small craft will be appreciated.


RED 975
0
FEET
500
8
7
6
5
4
3
2
1
R.A.

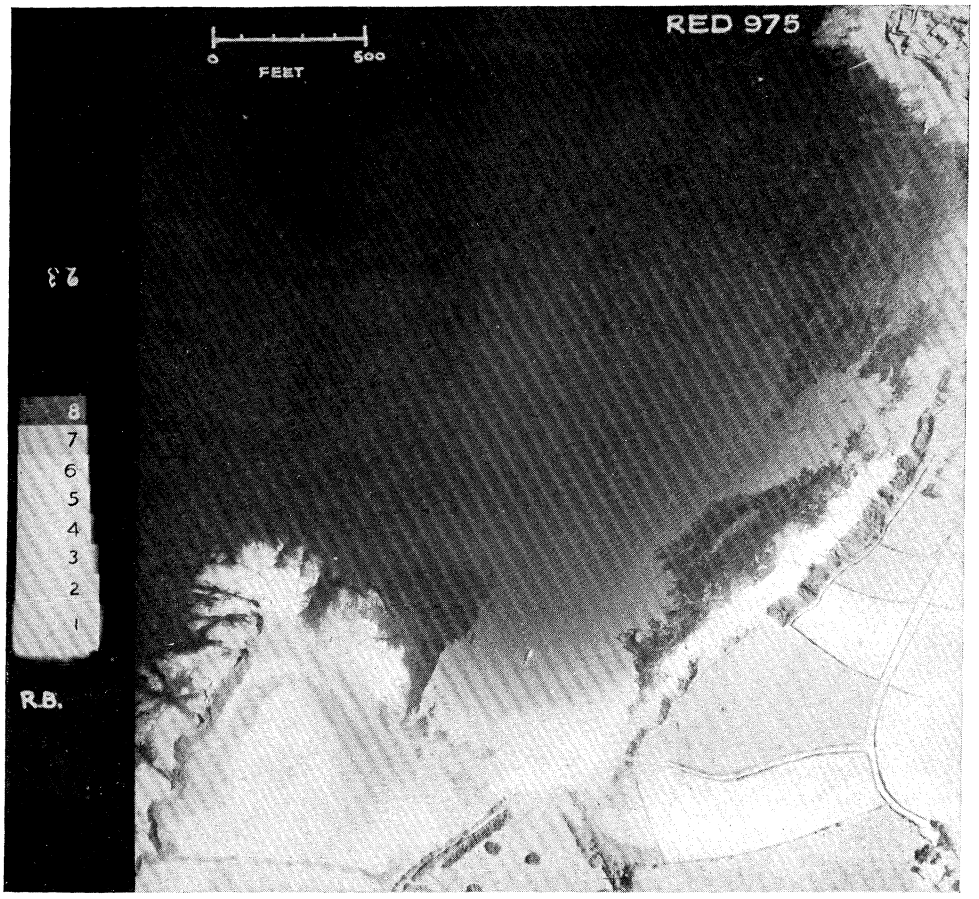
RED 975
0
FEET
500
8
7
6
5
4
3
2
1
R.B.

PLATES 11–12. A SANDY CORNISH BEACH (975)

Description. Porthscatho, near Falmouth. 3 August 1945. Taken at 5000 ft. with 8 in. F.24 cameras; 1/250 sec. at *f* 5·6. Sun altitude 46°, slight haze, cloudless sky, calm sea. Contact prints; scale 1/7500.

Comment. These are the photographs on which measurements were made to illustrate the methods of calculating depths from negatives and from prints. The sensitometer wedges have not been removed from these prints, and their step numbers have been shown (tables 5 and 9).

The position of the selected profile is shown by a series of needle holes; on the photographs it passes across the launch from which the water samples were taken.

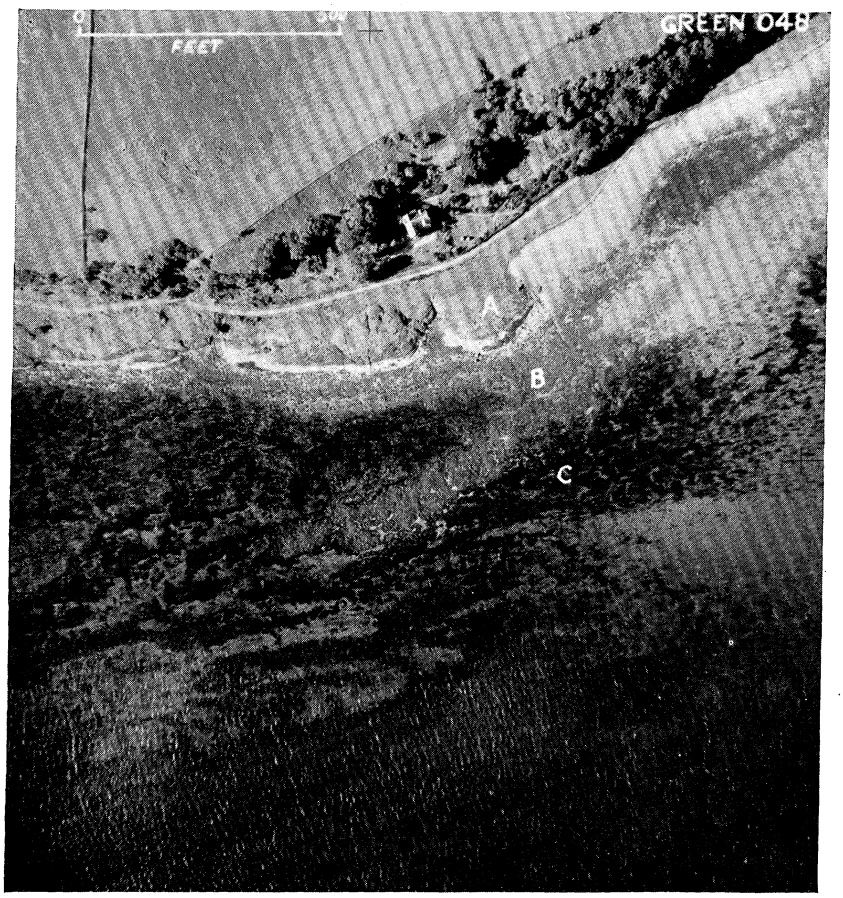

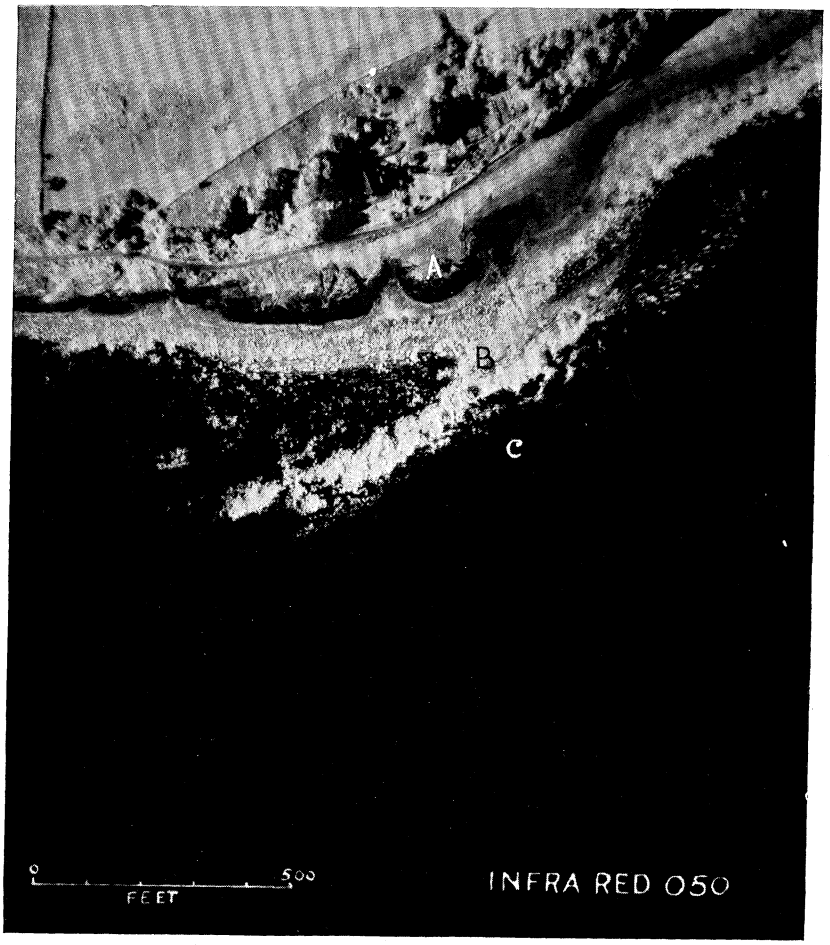

DETECTION OF COMMERCIALLY VALUABLE SEAWEED (048/050)

Description. Lismore Island (west coast of Scotland). 25 September 1945. Taken at 3000 ft. with 8 in. F.24 cameras; 1/250 sec. at f4. Sun altitude 25°, cloudless sky, calm sea. Contact prints, scale 1/7500.

Comment. The green print shows a belt of probable rock weed (*B*) and a belt of bottom weed (*C*). That belt (*B*) is weed and not dark toned or wet bare rock is clear from the infra-red print, on which the weed appears very bright owing to its high reflectivity in deep red light.

Bare rock (*A*) or sand and shingle appear dark on the infra-red print in contrast to the weed. Underwater weed (*C*) is invisible on the infra-red print except for isolated plants covered by a few inches of water; stereoscopic examination of green prints, however, confirms bottom weed at (*C*).

PLATES 14–15. A HARBOUR ENTRANCE (072)

Description. Penzance, Cornwall. 17 June 1945. Conditions as for plate 13. Sun altitude 38°, low tide. Contact prints from enlarged negatives.

Comment. Rock detail on either side of the harbour approaches is clearly visible on the green print; unfortunately, it is not possible to reproduce the full set of overlapping photographs which show the rock detail at greater depths. (*Contd. on plate* 15.)

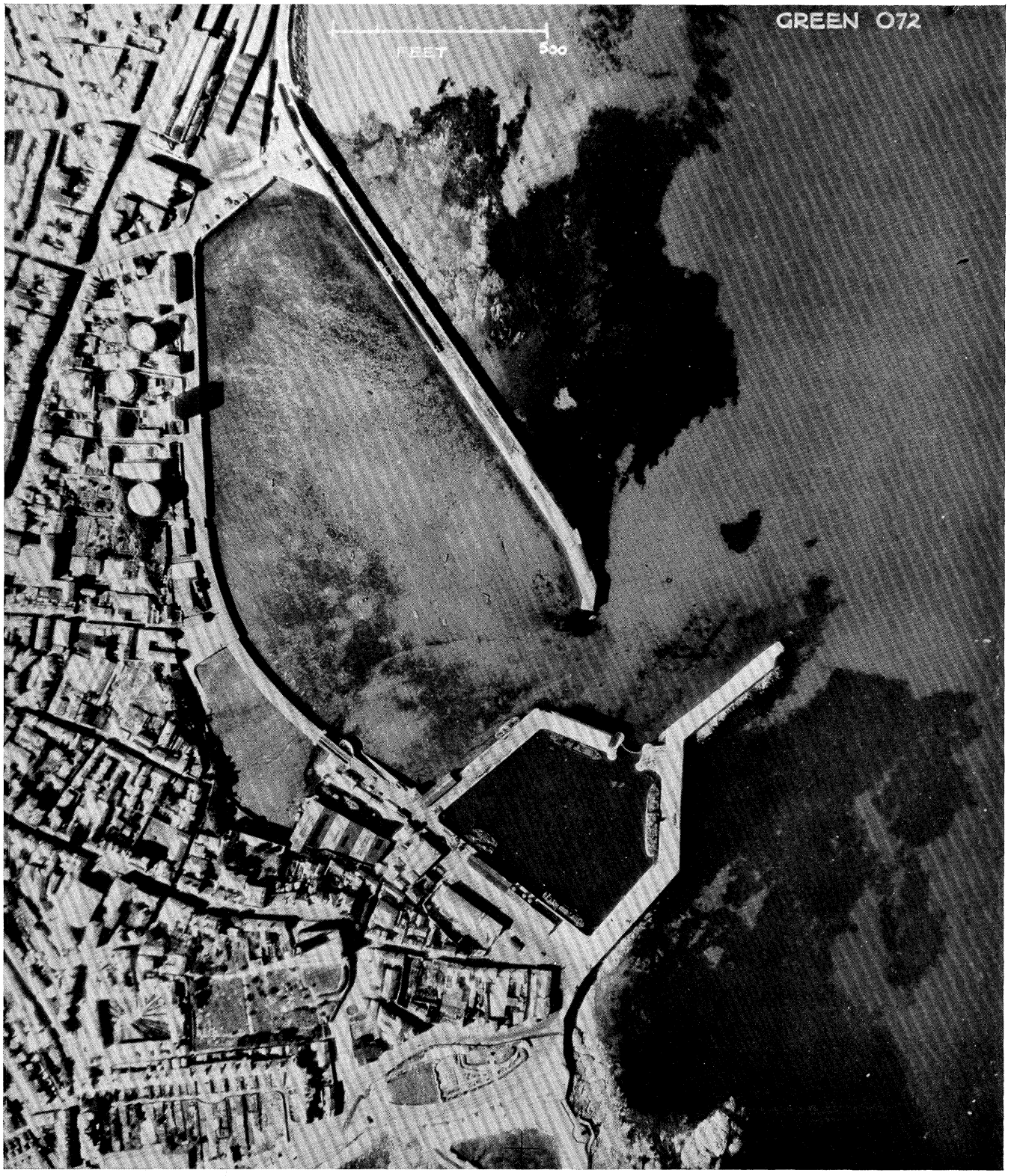

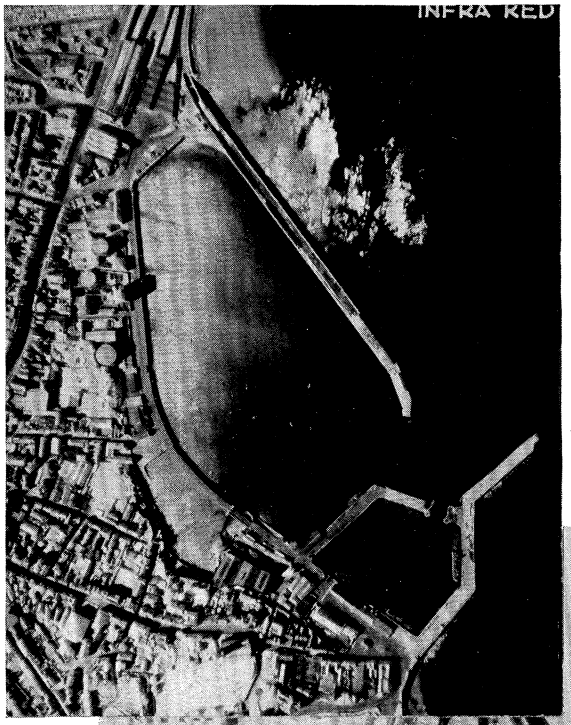

(*Contd. from plate* 14.)

The photographs were taken at low water; the position of the waterline is shown on the smaller scale infra-red print.

A bank of sand is visible at the harbour entrance; from a study of its tone on the red print, the shape of this sand bank appears to have altered since the 1943 Admiralty Chart was issued. The value of this type of photograph for the control of harbour works will be apparent.

THE CALCULATOR

FOR USE ONLY WITH BRIGHTNESS PROFILES OBTAINED WITH WRATTEN 56 (GREEN) FILTER, WRATTEN 27 (RED), AND KODAK AERO SUPER XX PANCHROMATIC FILM.

FIGURE 17

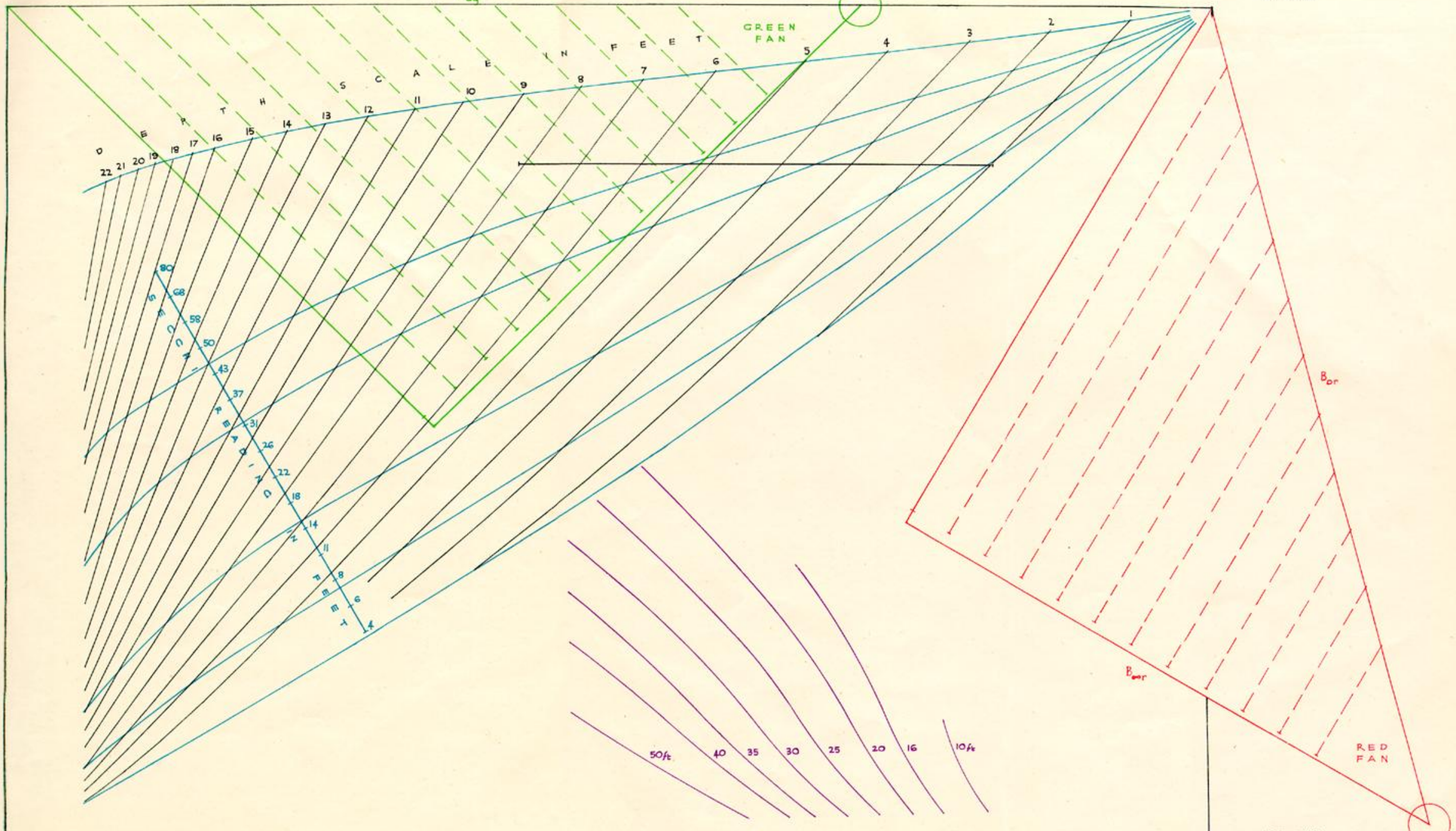

(facing p. 186)

THE CALCULATOR

FOR USE ONLY WI
WRATTEN 27 (RED),
B09

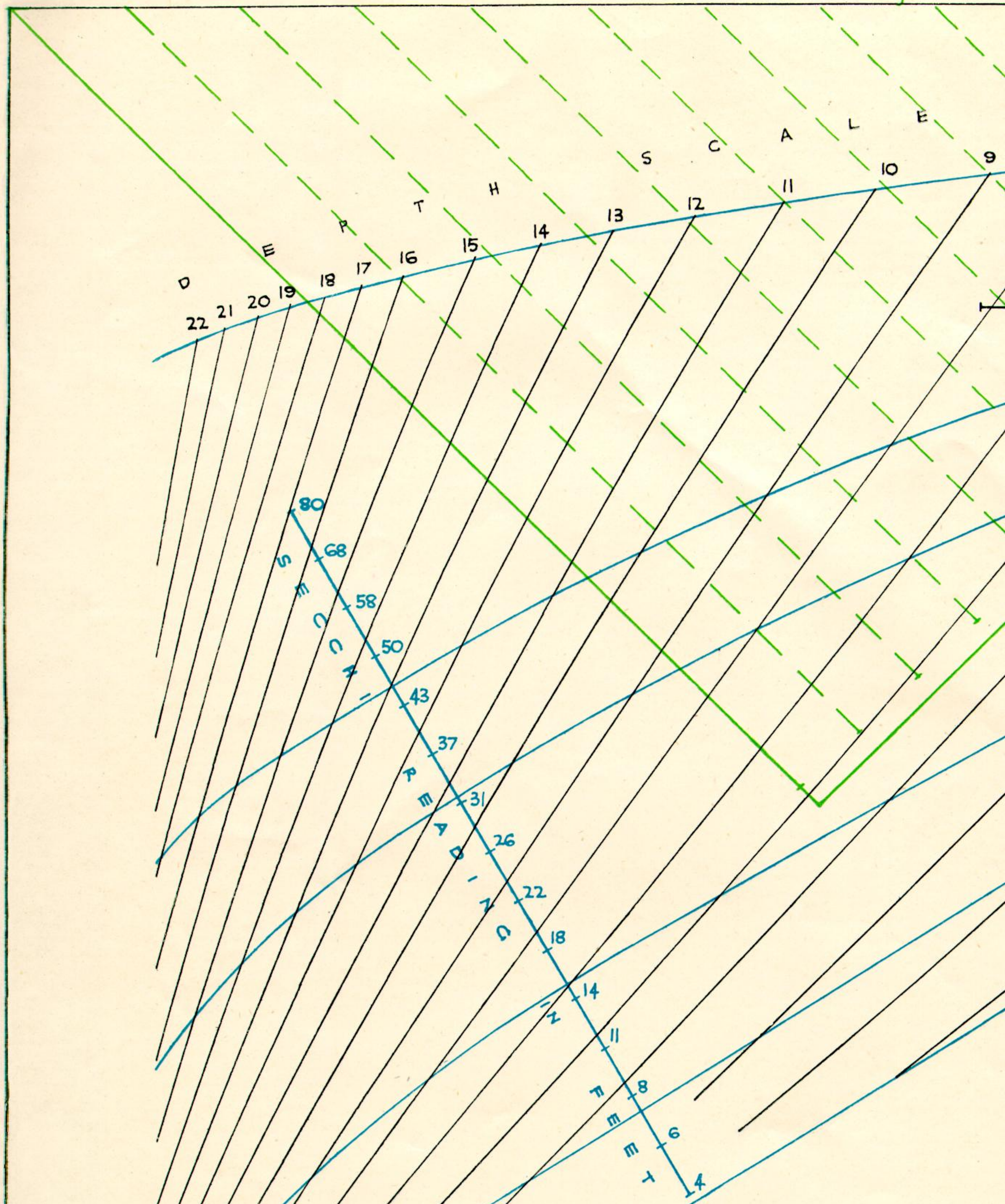

LY WITH BRIGHTNESS PROFILES OBTAINED WITH WRATTEN 56 (GREEN) FIL
RED), AND KODAK AERO SUPER XX PANCHROMATIC FILM.

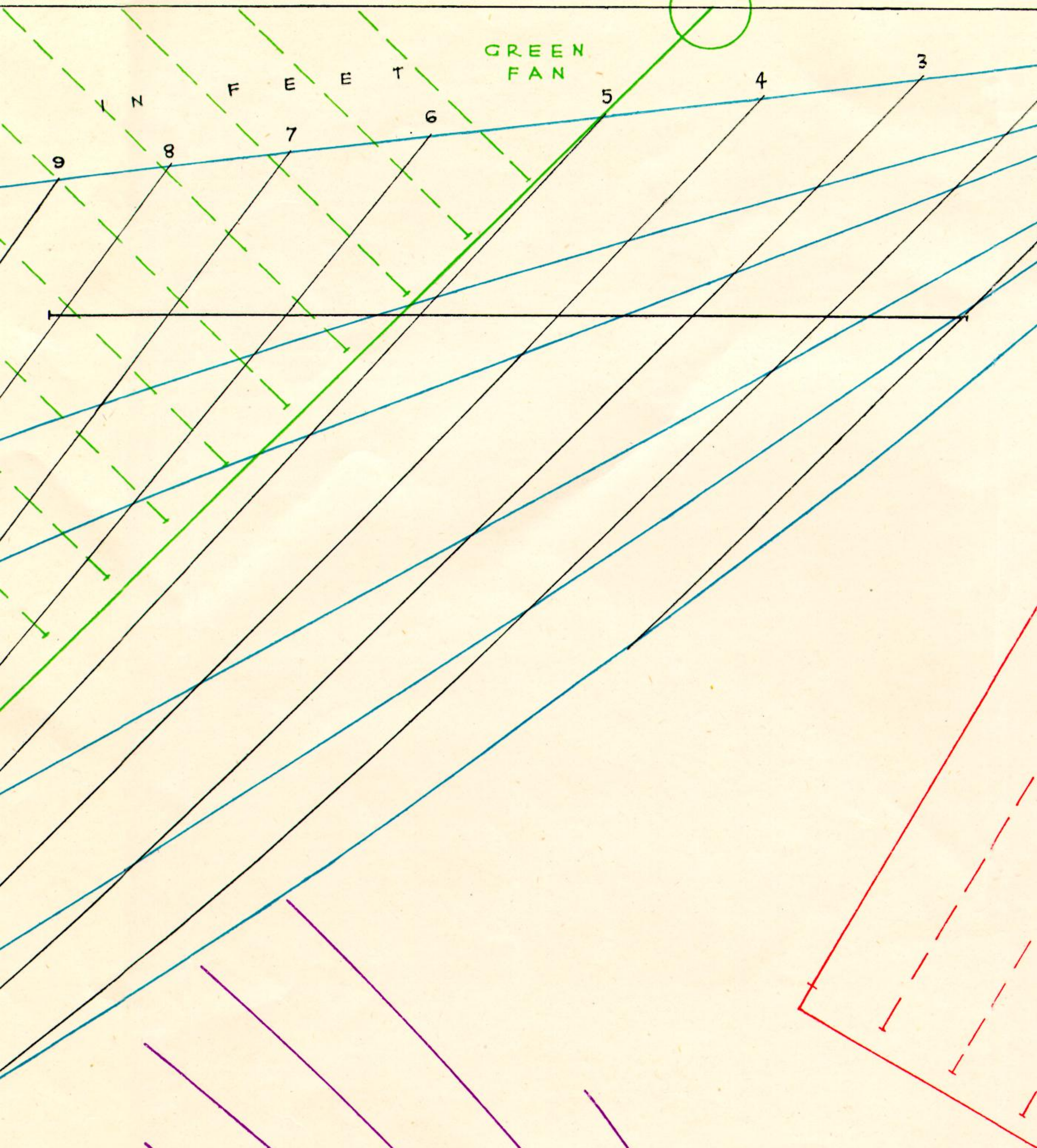

EN) FILTER,

FIGURE 17

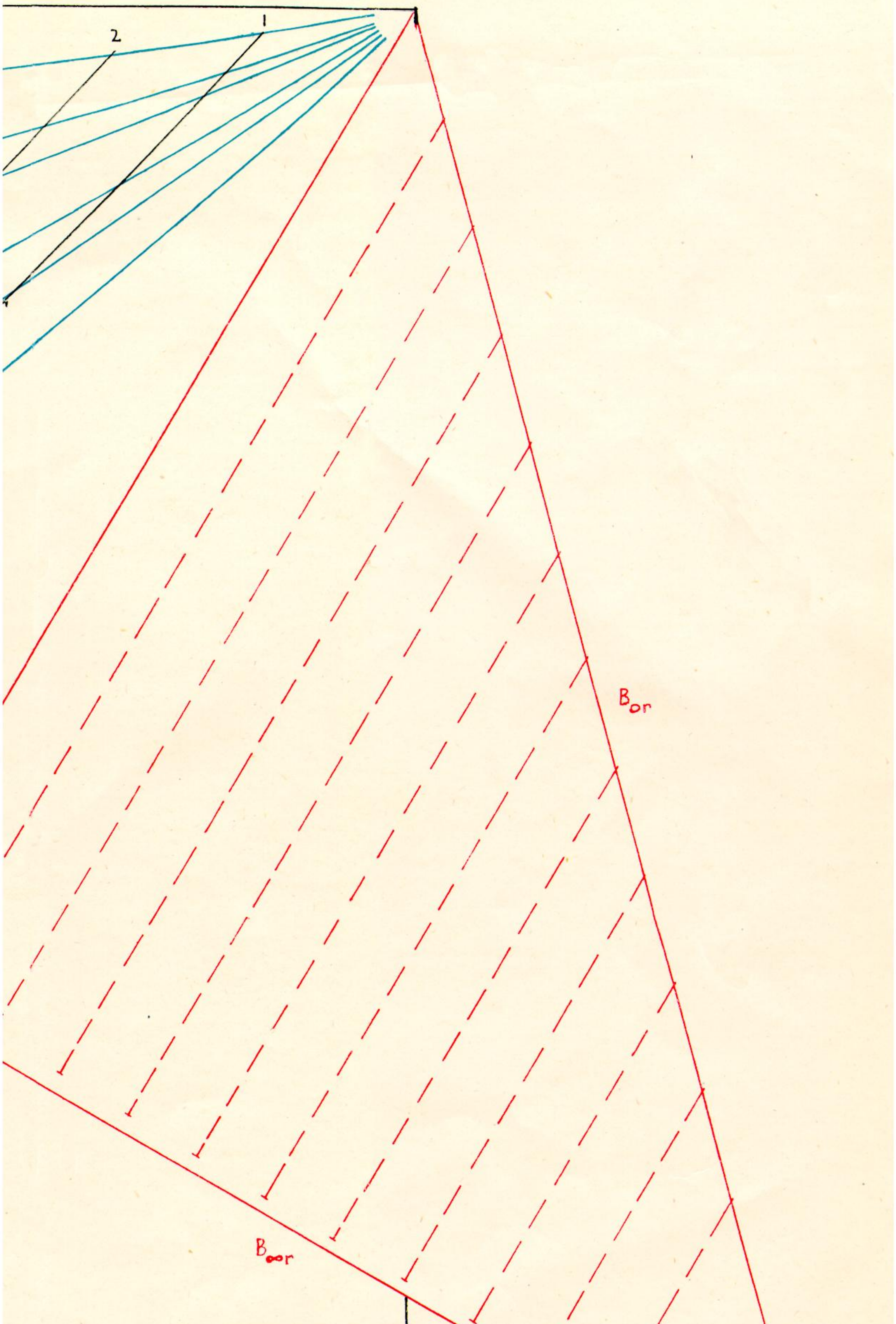

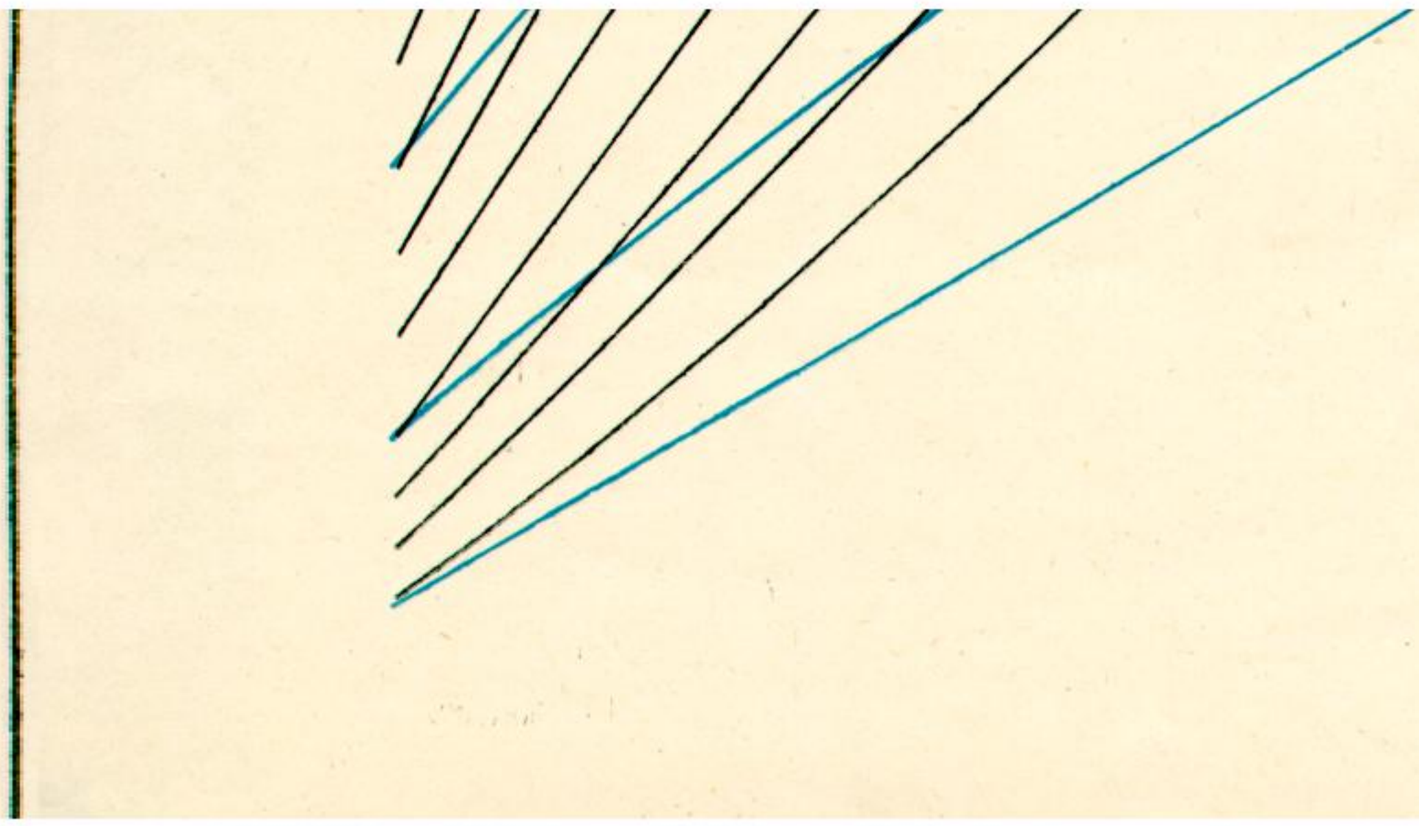

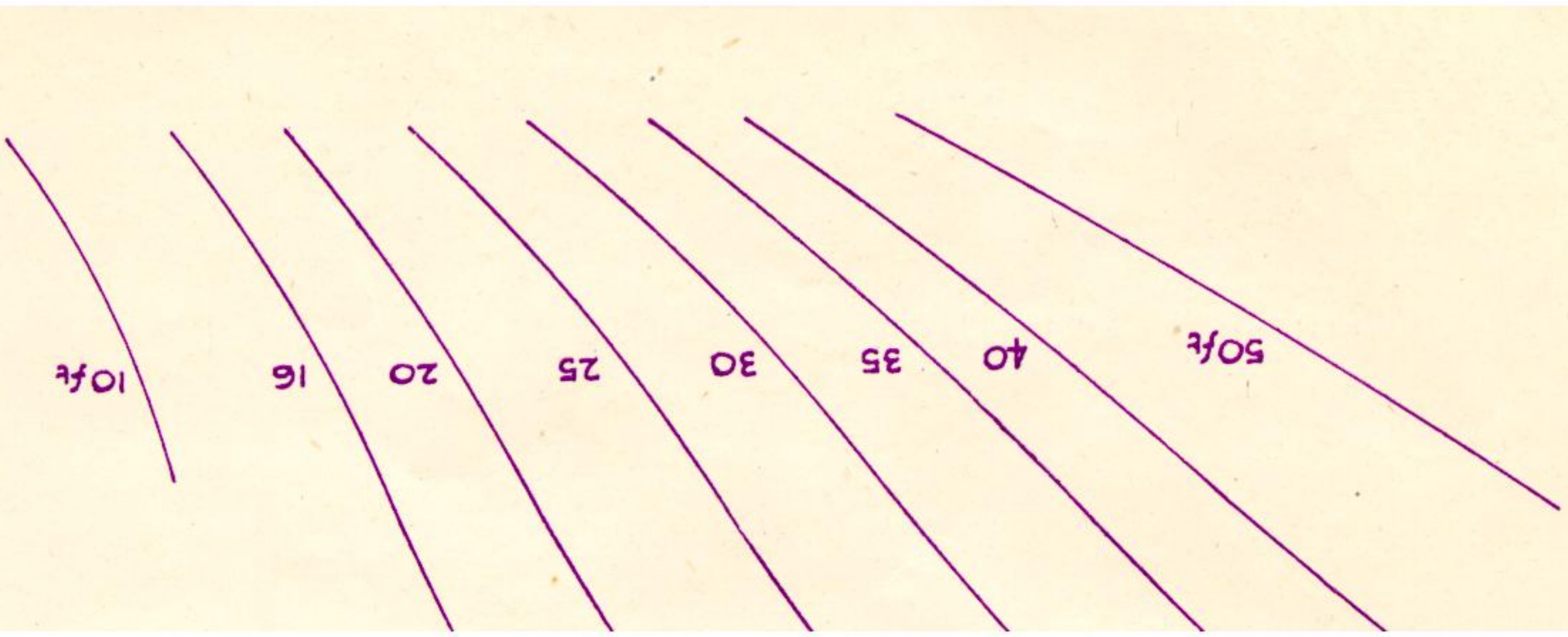
10ft
16
20
25
30
35
40
50ft

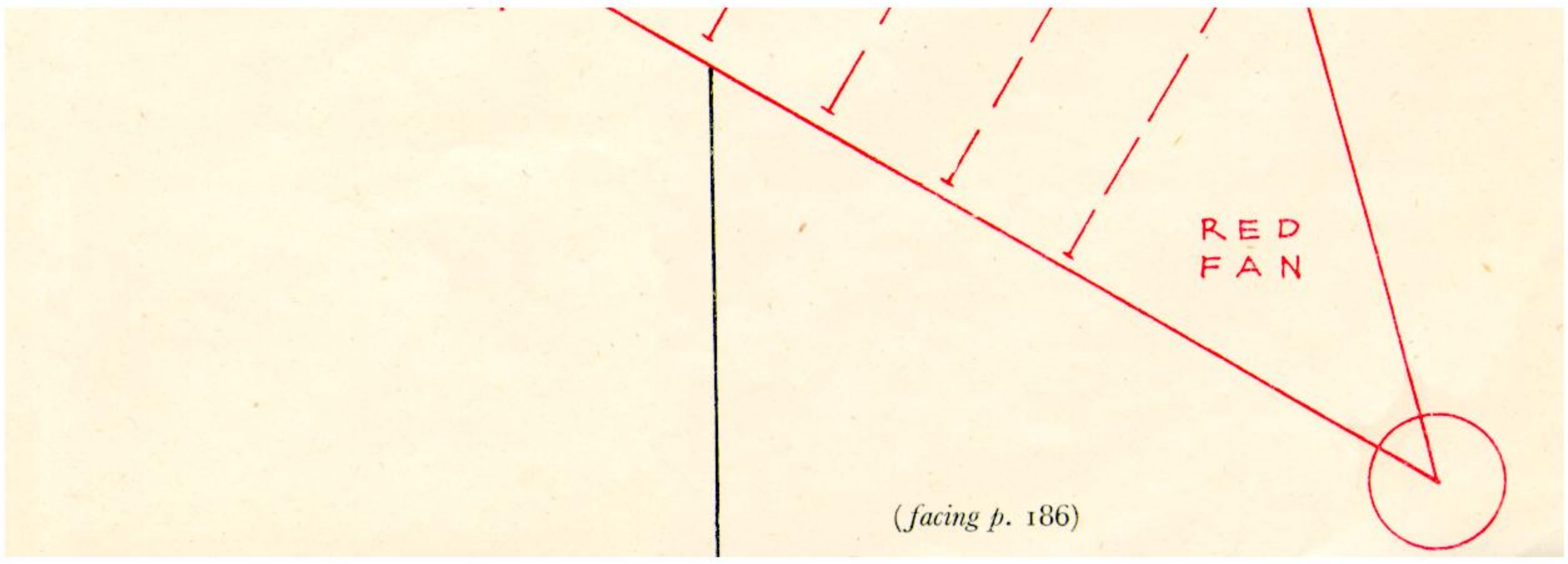

(*facing p.* 186)

PLATES 1–2. MEDITERRANEAN BEACH TAKEN FROM OPERATIONAL AIRCRAFT (756)

Description. Green and red prints of Beauvallon beach, near St Maxime, France. 19 July 1945. Taken at 12,000 ft. by Mosquito aircraft of 106 Gp R.A.F. Benson, with 20 in. F.52 cameras; 1/120 sec. at *f* 6·3. Contact prints, sensitometer wedges removed in printing; scale 1/7200. Sun altitude 37°, slight haze, cloudless sky; calm sea.

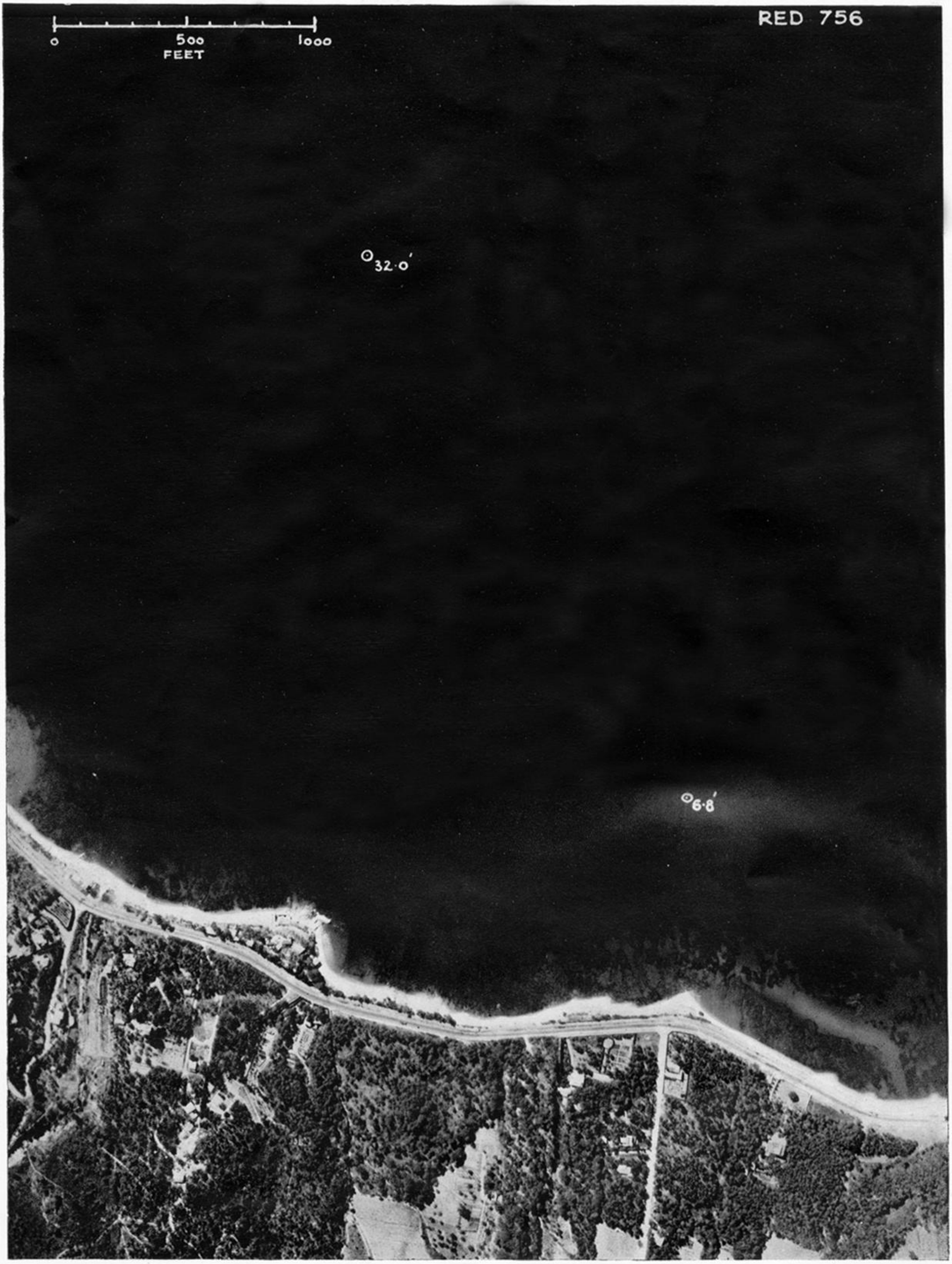

Comment. A rocky beach with patches of sand and a few prominent sandbars. The presence of so much rock made depth prediction difficult, but two satisfactory pairs of profiles were obtained through the sandbar at the spot depth marked 6·8 ft. Detail of the sea-bed at points more than half a mile from the shore is visible on the green print at a depth exceeding 32 ft.

PLATES 3–4. MEDITERRANEAN BEACH TAKEN FROM OPERATIONAL AIRCRAFT (770)

Description. Green and red prints of Cavalaire beach, south of France. 19 July 1945. Conditions as for plates 1–2.

Comment. Undulating sandy beach giving place to continuous rocks at about 24 ft. depth. The undulatory nature of the beach is clearly shown by the tone changes on the red print. A line of submerged military obstacles is visible at point *a* at a depth of about 8 ft. A second line of smaller obstacles can be seen at point *b*. A good prediction of the beach gradient was made along a line through the two spot depths; the results were included in figures 11 and 13.

0
500
1000
FEET
6·0′
1·0′

RED 1083
0
500
1000
FEET
6·0′
1·0′

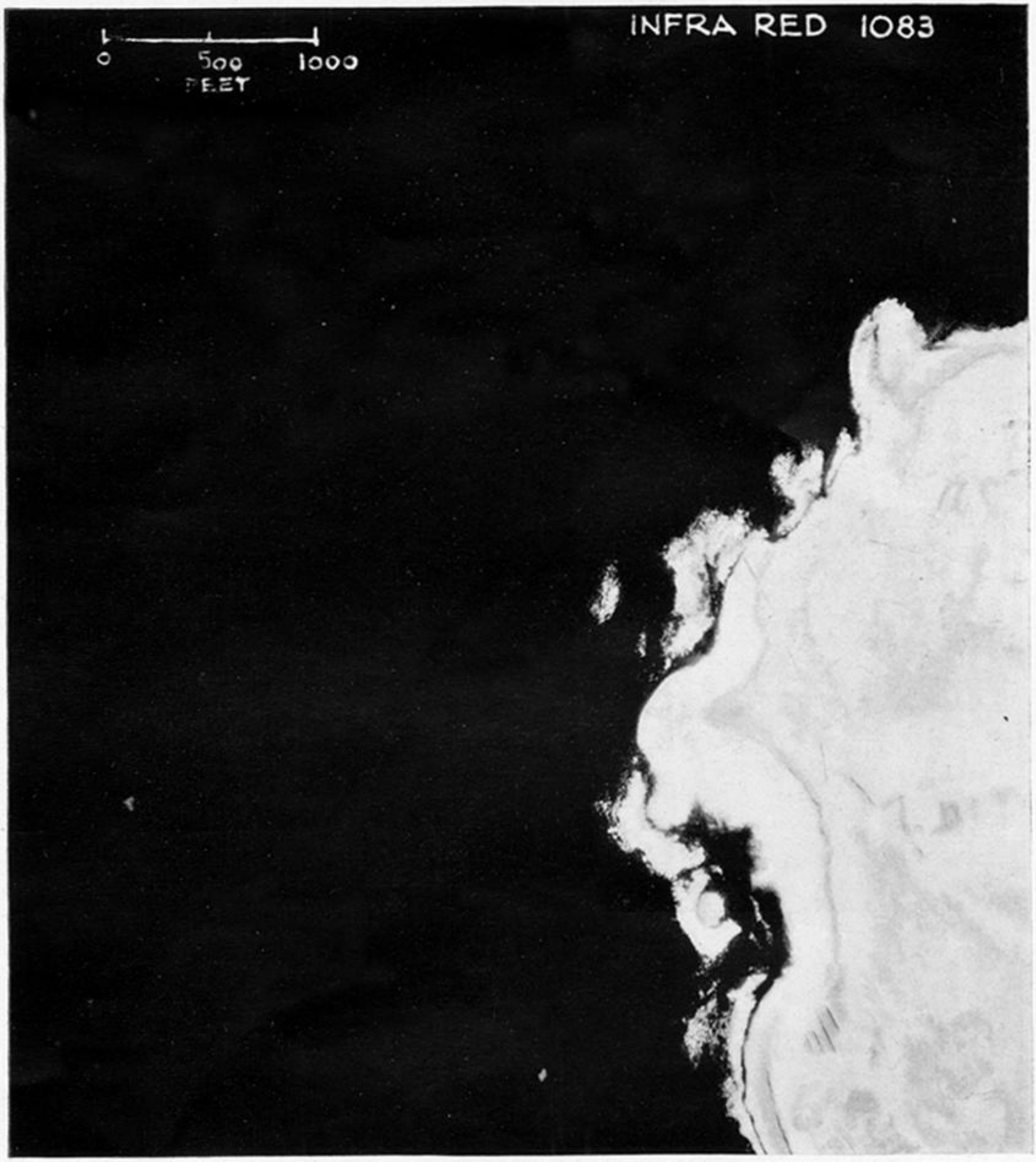

PLATES 5–6. SANDBARS WITH ROCKS AND WEED (1083)

Description. Bar Point, St Mary's, Scilly Isles. 5 August 1945. Taken at 10,000 ft. with 8 in. F.24 cameras; 1/250 sec. at *f* 5·6. Contact prints; scale 1/15,000. Sun altitude 50°, slight haze; cloudless sky.

Comment. Alinement of the cameras was not perfect and the sun altitude was sufficiently high to cause specular reflexion from waves on one corner of the photograph. The water was shallow and therefore details of the complex system of sandbars are shown most clearly on the red print.

It is clear from the infra-red print that the entire sandbar was submerged; patches of weed are visible on this print in the water close to the shore.

GREEN 1088

RED 1088
0
500
1000
FEET

PLATES 7–8. SHALLOW UNDERWATER DETAIL (1088)

Description. St Mary's, Scilly Isles. 5 August 1945. Conditions as for plates 5–6.

Comment. The water is shallow, except in the channel on the bottom right-hand quarter of the photograph. The distribution of sand and rock and the effects of water currents are clearly shown. The infra-red photograph indicates which portions of the beach are above the water surface.

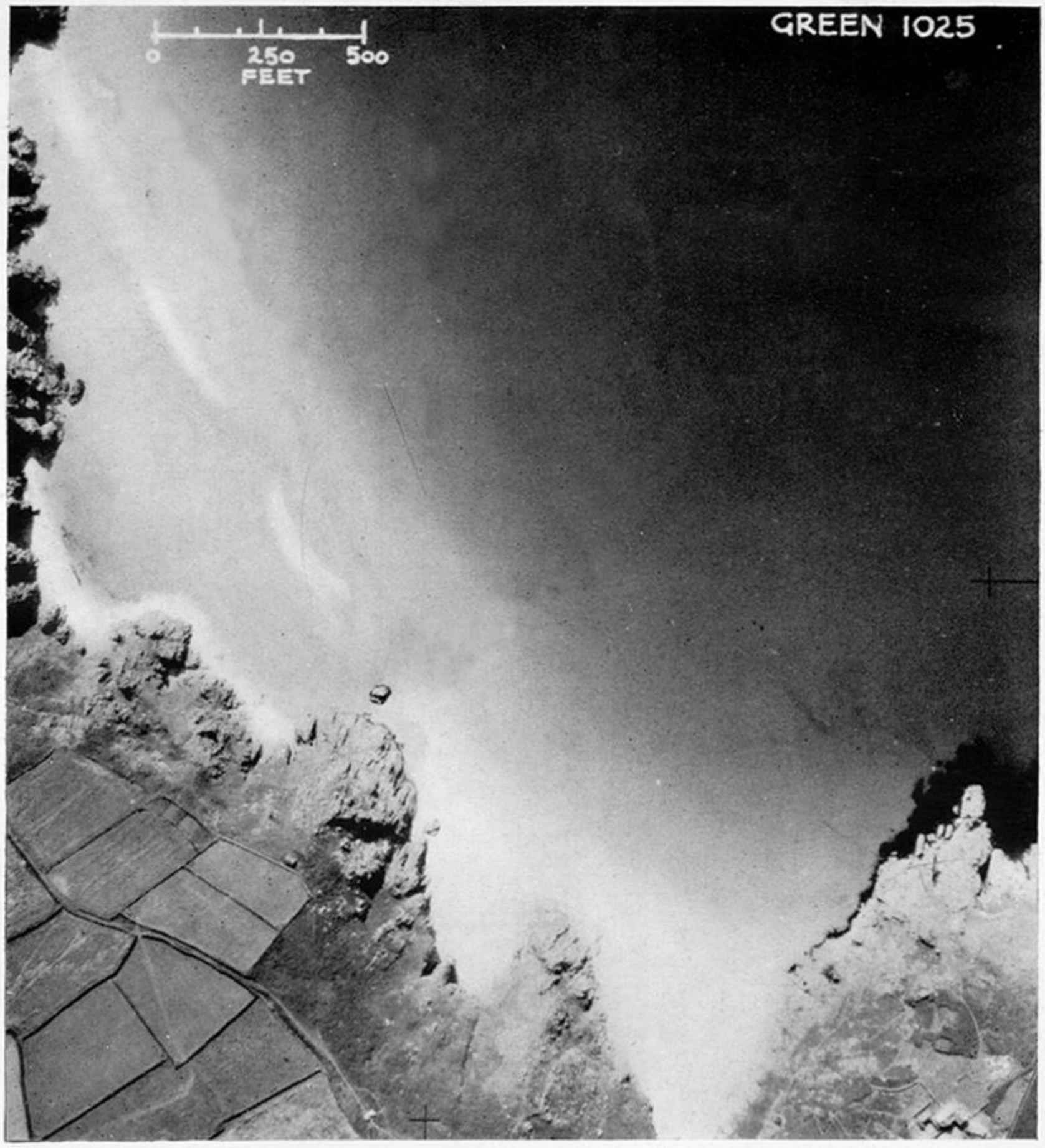

EXPOSED SAND BEACH (1025)

Description. Porth Curno, near Land's End. 4 August 1945. Taken at 5000 ft. with the cameras used for plates 5–6. Scale 1/7500. Sun altitude 38°, slight haze, no cloud.

Comment. The green print shows no clearly defined waterline because the sea water is clear and fairly calm, and the surface of the beach has been eroded into a complex shape by storms. The infra-red print demonstrates that there is quite deep water inshore behind the beach. This must not, however, be confused with shadows cast by the cliffs—the limits of the shadows are obvious from the green print.

River channels (94)

Description. Mahaweli Ganga, Kandy, Ceylon. 15 January 1945. Taken at 13,000 ft. with 20 in. F.52 cameras; 1/210 sec. at *f*6·3. Portions of contact prints; sun altitude 49°, nearly cloudless sky.

Comment. The channels are clearly shown on the infra-red photograph which was taken through a Wratten 27 (red) filter, whereas little can be seen on the panchromatic photograph which was taken through a Wratten 56 (green) filter.

Estimates of the depth of the water at various parts of the river can be made by an experienced interpreter; the value of infra-red photography of rivers for finding fording places and channels navigable by small craft will be appreciated.

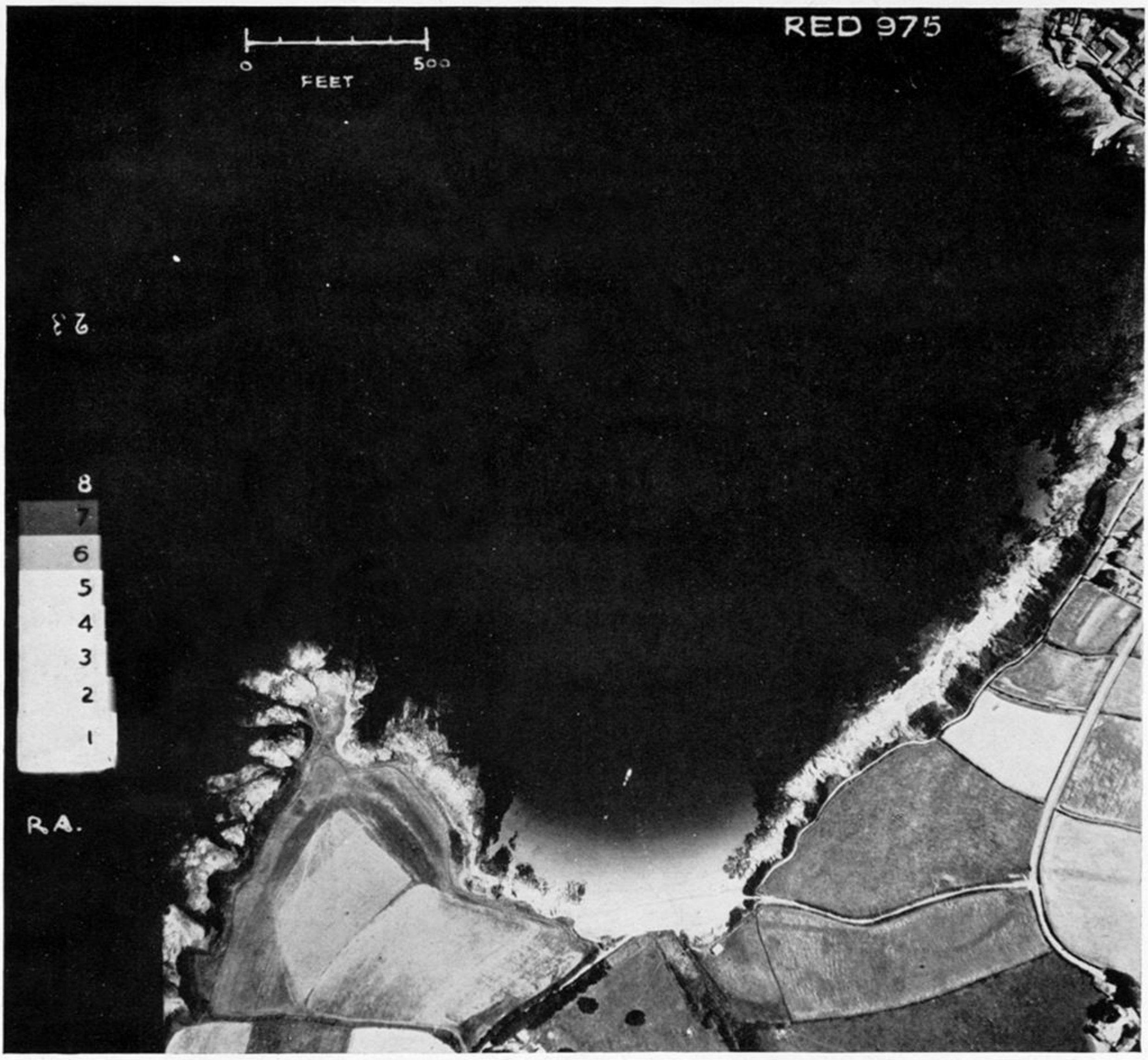
RED 975
0
500
FEET
23
8
7
6
5
4
3
2
1
R.A.

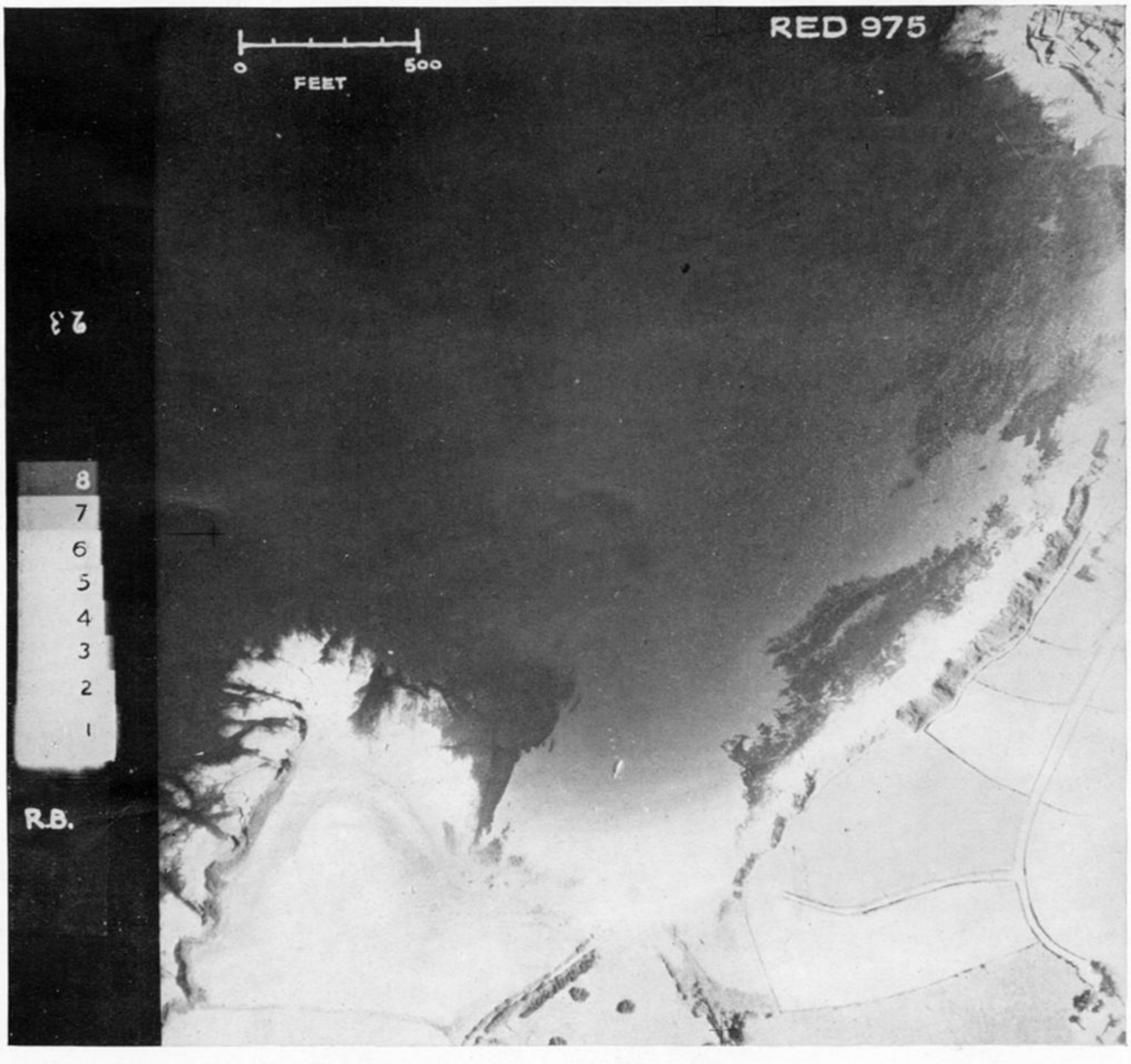
RED 975
0
500
FEET
23
8
7
6
5
4
3
2
1
R.B.

PLATES 11–12. A SANDY CORNISH BEACH (975)

Description. Porthscatho, near Falmouth. 3 August 1945. Taken at 5000 ft. with 8 in. F.24 cameras; 1/250 sec. at *f* 5·6. Sun altitude 46°, slight haze, cloudless sky, calm sea. Contact prints; scale 1/7500.

Comment. These are the photographs on which measurements were made to illustrate the methods of calculating depths from negatives and from prints. The sensitometer wedges have not been removed from these prints, and their step numbers have been shown (tables 5 and 9).

The position of the selected profile is shown by a series of needle holes; on the photographs it passes across the launch from which the water samples were taken.

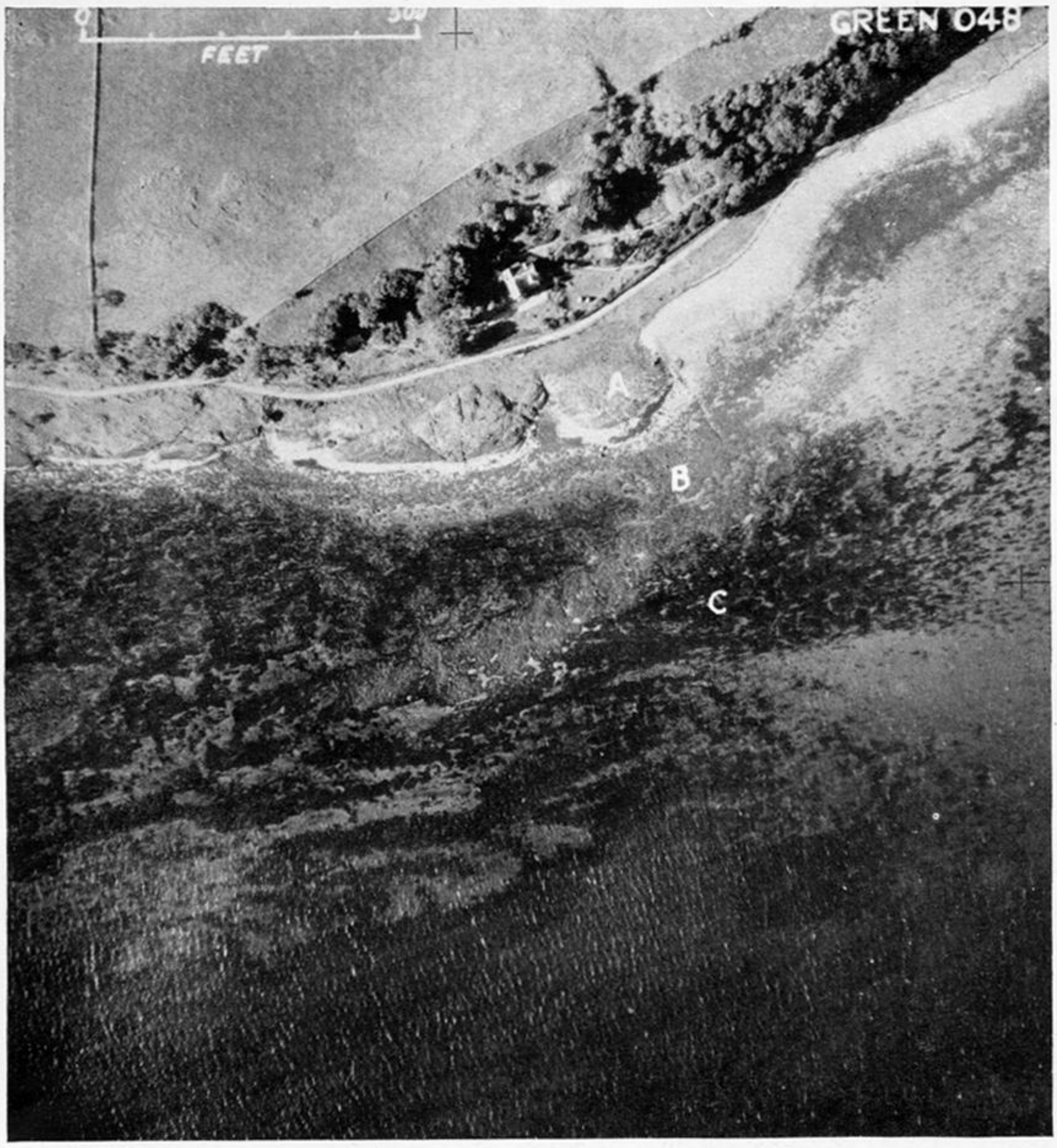

DETECTION OF COMMERCIALLY VALUABLE SEAWEED (048/050)

Description. Lismore Island (west coast of Scotland). 25 September 1945. Taken at 3000 ft. with 8 in. F.24 cameras; 1/250 sec. at *f* 4. Sun altitude 25°, cloudless sky, calm sea. Contact prints, scale 1/7500.

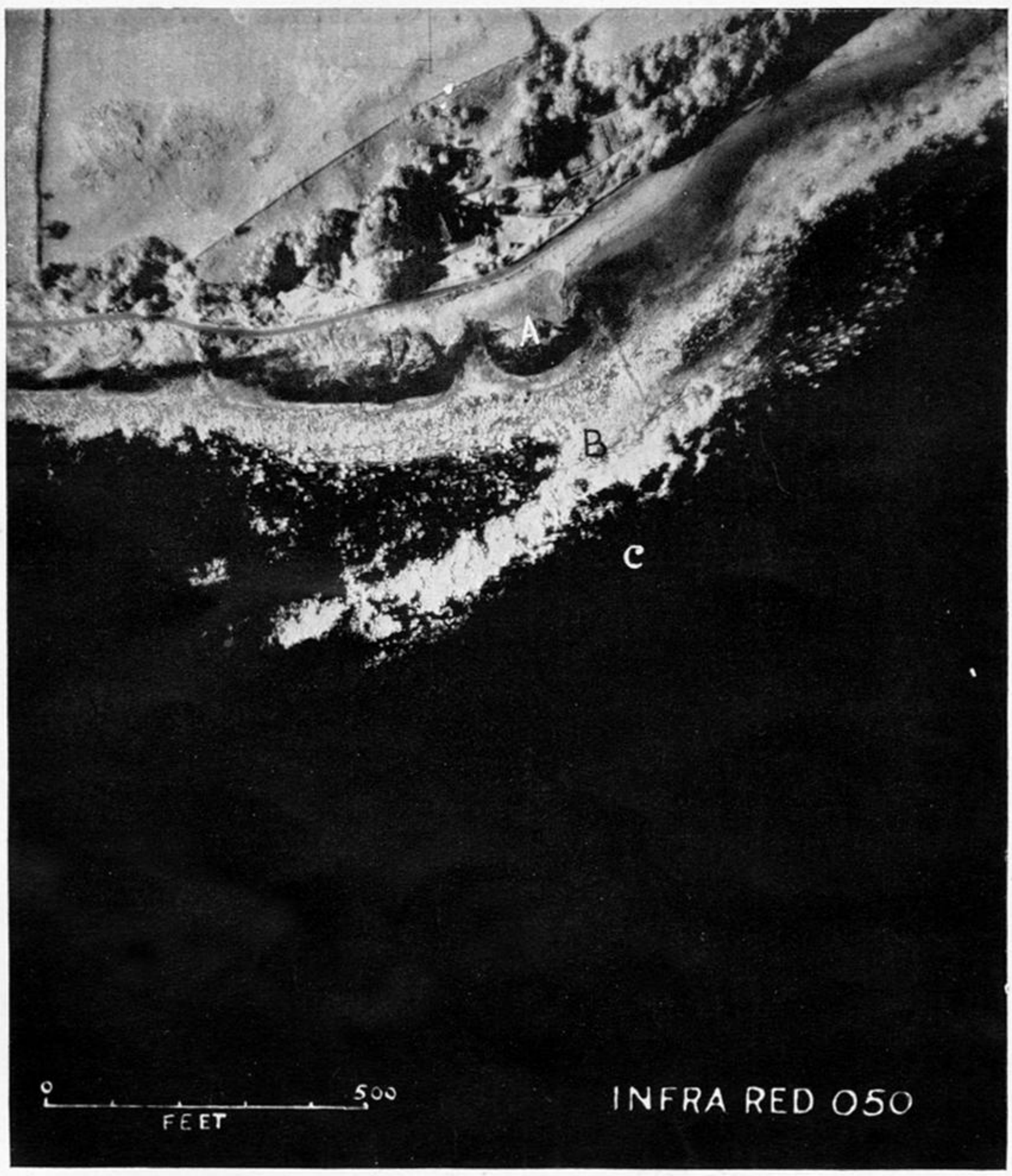

Comment. The green print shows a belt of probable rock weed (*B*) and a belt of bottom weed (*C*). That belt (*B*) is weed and not dark toned or wet bare rock is clear from the infra-red print, on which the weed appears very bright owing to its high reflectivity in deep red light.

Bare rock (*A*) or sand and shingle appear dark on the infra-red print in contrast to the weed. Underwater weed (*C*) is invisible on the infra-red print except for isolated plants covered by a few inches of water; stereoscopic examination of green prints, however, confirms bottom weed at (*C*).

Plates 14–15. A harbour entrance (072)

Description. Penzance, Cornwall. 17 June 1945. Conditions as for plate 13. Sun altitude 38°, low tide. Contact prints from enlarged negatives.

Comment. Rock detail on either side of the harbour approaches is clearly visible on the green print; unfortunately, it is not possible to reproduce the full set of overlapping photographs which show the rock detail at greater depths. (*Contd. on plate* 15.)

(*Contd. from plate* 14.)

The photographs were taken at low water; the position of the waterline is shown on the smaller scale infra-red print.

A bank of sand is visible at the harbour entrance; from a study of its tone on the red print, the shape of this sand bank appears to have altered since the 1943 Admiralty Chart was issued. The value of this type of photograph for the control of harbour works will be apparent.